

# *HIPPARCOS* age-metallicity relation of the solar neighbourhood disc stars

A. Ibukiyama<sup>1</sup> and N. Arimoto<sup>1,2</sup>

<sup>1</sup> Institute of Astronomy (IoA), School of Science, University of Tokyo, 2-21-1 Osawa, Mitaka, Tokyo 181-0015, Japan

<sup>2</sup> National Astronomical Observatory, 2-21-1 Osawa, Mitaka, Tokyo 181-8588, Japan

Received /Accepted 1 July 2002

**Abstract.** We derive age-metallicity relations (AMRs) and orbital parameters for the 1658 solar neighbourhood stars to which accurate distances are measured by the *HIPPARCOS* satellite. The sample stars comprise 1382 thin disc stars, 229 thick disc stars, and 47 halo stars according to their orbital parameters. We find a considerable scatter for thin disc AMR along the one-zone Galactic chemical evolution (GCE) model. Orbits and metallicities of thin disc stars show now clear relation each other. The scatter along the AMR exists even if the stars with the same orbits are selected. We examine simple extension of one-zone GCE models which account for inhomogeneity in the effective yield and inhomogeneous star formation rate in the Galaxy. Both extensions of one-zone GCE model cannot account for the scatter in age -  $[\text{Fe}/\text{H}]$  -  $[\text{Ca}/\text{Fe}]$  relation simultaneously. We conclude, therefore, that the scatter along the thin disc AMR is an essential feature in the formation and evolution of the Galaxy. The AMR for thick disc stars shows that the star formation terminated 8 Gyr ago in thick disc. As already reported by Gratton et al. (2000) and Prochaska et al. (2000), thick disc stars are more Ca-rich than thin disc stars with the same  $[\text{Fe}/\text{H}]$ . We find that thick disc stars show a vertical abundance gradient. These three facts, the AMR, vertical gradient, and  $[\text{Ca}/\text{Fe}]$ - $[\text{Fe}/\text{H}]$  relation, support monolithic collapse and/or accretion of satellite dwarf galaxy as thick disc formation scenario.

**Key words.** Stars: abundances ; distances – Galaxy: abundances ; evolution ; solar neighbourhood ; kinematics and dynamics

## 1. Introduction

The individual ages for solar neighbourhood stars are indispensable in the research of star formation history of the Galaxy. Twarog (1980) first derived the age-metallicity relation (AMR) for the disc in the neighbourhood of the Sun from *ubvy* and  $\text{H}\beta$  photometry of a large sample of field stars. Theoretical isochrones used in the age determination were taken from Ciardullo & Demarque (1977). In the Twarog's AMR, the metallicity increases from  $[\text{Fe}/\text{H}] = -1.0$  at 13 Gyr to  $[\text{Fe}/\text{H}] = -0.03$  at the age of the Sun. The mean metallicity has increased more slowly since then to a present value of  $[\text{Fe}/\text{H}] = +0.01$  for the youngest stars. The dispersion in  $[\text{Fe}/\text{H}]$  is as small as  $\pm 0.1$  dex at any given age. Carlberg et al. (1985) used stellar models of Vandenberg (1983) and a revised metallicity calibration that takes into account a temperature dependence. Both ages and metallicities were estimated in a photometric manner, and the resulting AMR is qualitatively similar to that of Twarog (1980), but  $[\text{Fe}/\text{H}]$  in-

creases more gradually, showing an increase of only 0.3 dex over the past 15 Gyrs (cf. Nissen & Schuster 1991). The metallicity dispersion decreases from  $\pm 0.15$  dex for the oldest stars (13 – 20 Gyrs) to  $\pm 0.05$  dex for younger stars.

Edvardsson et al. (1993) derived elemental abundances of O, Na, Mg, Al, Si, Ca, Ti, Fe, Ni, Y, Zr, Ba, and Nd for 189 nearby long-lived disc dwarfs by using high resolution, high S/N, spectroscopic data. Individual ages were derived photometrically from fits in the  $\log T_{\text{eff}} - \log g$  plane of the isochrones by Vandenberg (1985). The uncertainties in the relative ages are about 25%. Due to metallicity measurements of high precision, Edvardsson et al. (1993) improved greatly the AMR, but ironically the resulting AMR clearly indicated a considerable scatter ( $\sim 0.15$  dex) in the metallicities of disc stars formed at any given time, implying that there is only a very weak correlation between age and metallicity. The scatter seems to be substantially larger than that can be explained by observational errors. If the scatter is real, it would cause a serious difficulty for galactic chemical evolution (GCE) models, because it is easy to fit the average run of the data, but difficult to explain such

Send offprint requests to: A. Ibukiyama

Correspondence to: aibukiya@optik.mtk.nao.ac.jp

a large scatter without breaking some of assumptions that GCE models usually make (Pagel & Tautvaišienė 1995). Edvardsson et al. (1993) suggested that the scatter arises from star formation stimulated from sporadic episodes of gas infall, although it is also possible that a different rate of chemical enrichment, depending on the distance from the Galactic centre, causes a scatter of this kind.

In this article, we derived the ages and orbital parameters for 1658 solar neighbourhood stars, almost ten times more than the previous researches. Hence we succeed in finding out the new features of the Galaxy using stellar ages, chemical components, and orbits. The article is organised as follows. Section 2 derives the ages and the orbital parameters for sample stars. Section 3 shows the features relevant to thin disc stars while Sect. 4 shows those of thick disc. Section 5 discusses observational error in our data, abundance gradient, the abundance distribution functions, the formation of thick disc, and the scatter along the thin disc AMR. Section 6 concludes the present study.

## 2. The Data

### 2.1. The observational data

#### 2.1.1. Absolute magnitudes and colours

Visual magnitudes,  $B - V$  colours, and parallaxes of nearby field stars were all taken from the *HIPPARCOS* catalogue (ESA 1997). The absolute magnitudes,  $M_{V_0}$ , and unreddened colours,  $(B - V)_0$ , were then calculated by applying the reddening corrections given by the model of Arenou et al. (1992). Certain number of stars in the *HIPPARCOS* catalogue suffer from uncertainties in parallaxes, binarities, and variabilities. Thus, the following criteria were introduced in our sample selection: (1)  $\sigma_\pi/\pi < 0.1$ , where  $\pi$  and  $\sigma_\pi$  are the parallax and the dispersion, respectively; (2) no binaries – binaries were excluded if explicitly identified in the *HIPPARCOS* catalogue; (3) non-variables – variables were excluded if assigned in the *HIPPARCOS* catalogue or in the [Fe/H] catalogue of Cayrel de Strobel et al. (2001); (4) no giants – giants were excluded according to their location on the CM diagram; LK bias (Lutz & Kelker 1973) was not corrected because Carretta et al. (1999) has shown recently that the bias is negligible if a strict sample selection ( $\sigma_\pi/\pi < 0.12$ ) is applied (see also Ng & Bertelli 1998).

#### 2.1.2. Metallicities

The stellar metallicities for F, G, and K stars were taken from the latest [Fe/H] catalogue of Cayrel de Strobel et al. (2001) which compiles the [Fe/H] values derived from high S/N and high resolution spectra. We cross-identified the *HIPPARCOS* catalogue and the [Fe/H] catalogue to derive a set of reliable  $M_{V_0}$ ,  $(B - V)_0$ , and [Fe/H] for 429 stars. When several [Fe/H] values were given in the [Fe/H] catalogue, we adopted the newest observation. Since we

wish to use preferentially the CCD data, we excluded the [Fe/H] data before 1985.

Additionally we took *ubvy*-H $\beta$  photometry for F and G stars from the catalogue of Hauck & Mermilliod (1998). We calculated [Fe/H] from these data adopting the calibration by Schuster & Nissen (1989). We define the AMR using spectroscopic metallicity of Cayrel de Strobel et al. (2001) as “spectroscopic AMR” and the AMR using photometric metallicity derived from the data of Hauck & Mermilliod (1998) as “photometric AMR” hereafter.

Abundances of Ca were taken from Boesgaard & Tripicco (1986), Smith & Lambert (1986), Smith & Lambert (1987), Hartmann & Gehren (1988), Abia et al. (1988), Magain (1989), Cayrel de Strobel & Bentolila (1989), Gratton & Sneden (1991), Berthet (1991), Edvardsson et al. (1993), Pilachowski et al. (1993), Smith et al. (1993), Nissen et al. (1994), Beveridge & Sneden (1994), Nissen & Schuster (1997), Tomkin et al. (1997), Carney et al. (1997), Castro et al. (1997), Giridhar et al. (1997), Gonzalez (1998), Feltzing & Gustafsson (1998), King et al. (1998), Jehin et al. (1999), Clementini et al. (1999), Sadakane et al. (1999), Santos et al. (2000), Thorén & Feltzing (2000), Chen et al. (2000), Gonzalez & Laws (2000), and Fulbright (2000). Ca abundances may be less accurate than Fe abundances, for the number of Ca lines used in data reduction is fewer than that of Fe.

#### 2.1.3. The kinematic data

We adopted radial velocities from the *HIPPARCOS* Input Catalogue (Turon et al. 1993), Barbier-Brossat et al. (1994), Duflot et al. (1995), and Malaroda et al. (2001). Proper motions were taken from the *HIPPARCOS* Catalogue. The space motions relative to the Sun,  $(U, V, W)$ , were calculated using Johnson & Soderblom (1987); Edvardsson et al. (1993).

We obtained 4240 sample stars by cross checking *HIPPARCOS* data, [Fe/H] or *ubvy*-H $\beta$  catalogue, and radial velocity catalogue. From 4240 whole sample, 1380 stars of poor parallax data, 1311 binaries, 428 variables, 1252 giants, and 133 stars observed before 1985 were excluded. In total, 1658 stars remained as our sample including 489 stars with spectroscopic [Fe/H] and 1169 stars with photometric [Fe/H]. [Ca/Fe] values were obtained for 277 stars among them.

Figure 1 shows the distances from the Sun of the sample stars. The sample stars are currently locating at the distances from 10 pc to 120 pc with a median value of 40 pc.

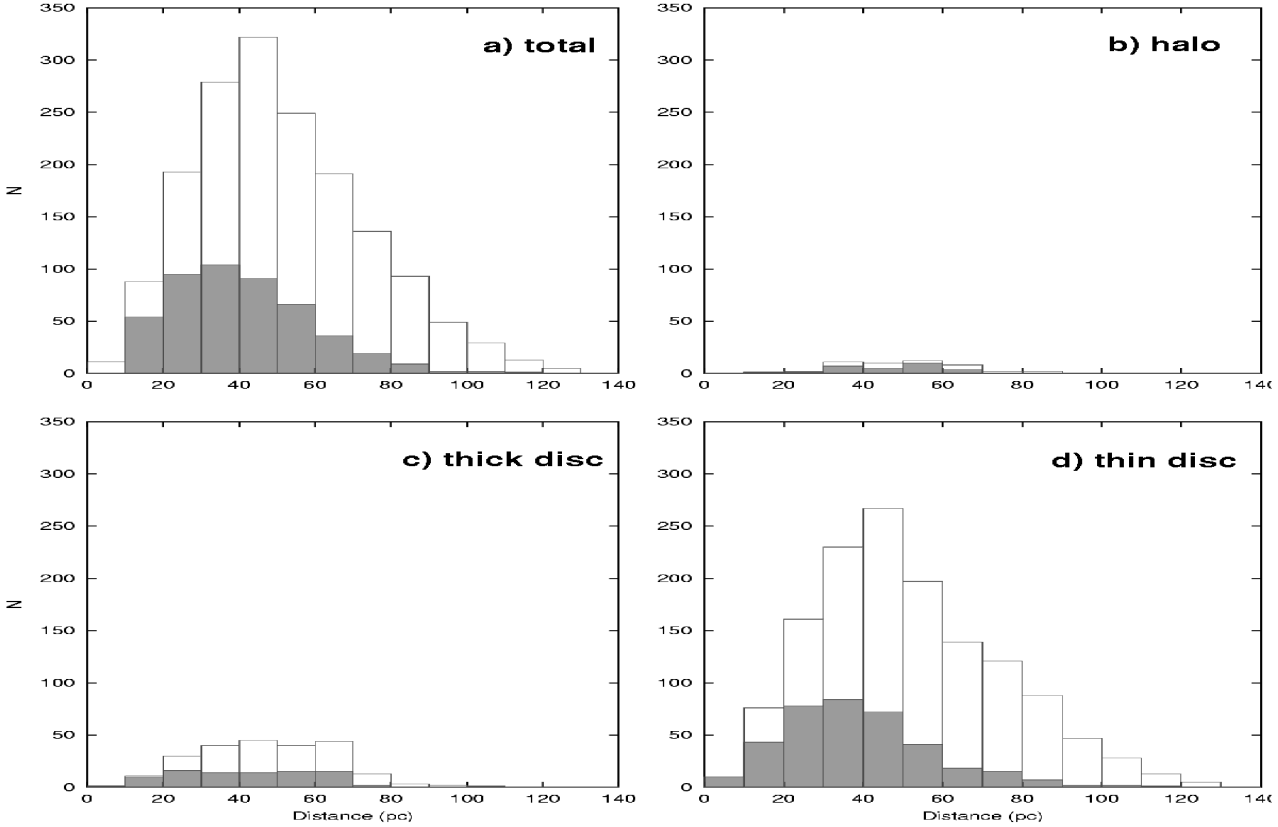
## 2.2. The Analysis

### 2.2.1. Ages

Once  $M_{V_0}$ ,  $(B - V)_0$ , and [Fe/H] were known, it was direct to derive ages of the selected stars by using the isochrone fitting. We adopted Yonsei-Yale isochrones (Yi et al. 2001), which were calculated with new OPAL opac-

**Table 1.** The sample stars.

	thin disc	thick disc	halo	total
photometric [Fe/H]	1010	143	16	1169
spectroscopic [Fe/H] (without [Ca/Fe])	173	28	11	212
spectroscopic [Fe/H] (with [Ca/Fe])	199	58	20	277
total	1382	229	47	1658

**Fig. 1.** The distribution of distances of the sample stars from the sun. **a)** whole 1658 stars. **b)** 47 halo stars. **c)** 229 thick disc stars. **d)** 1382 thin disc stars. Gray boxes show the stars with spectroscopic data while open boxes represent the stars with photometric data.

ities and Kurucz model atmospheres for a set of metallicities  $Z = 0.00001, 0.0001, 0.0004, 0.001, 0.004, 0.007, 0.01, 0.02$  (solar), 0.04, 0.06, 0.08 and ages from  $t = 1.0$  Gyr to 20.0 Gyr with an interval of  $\Delta t = 1.0$  Gyr. The mixing length and helium enrichment rate were fixed to  $\alpha \equiv l/H_p = 1.7$  and  $\Delta Y/\Delta Z = 2$ , respectively, while no convective overshooting was introduced. Since Yonsei-Yale isochrones were calculated for  $Z$  instead of  $[\text{Fe}/\text{H}]$ , we converted  $[\text{Fe}/\text{H}]$  of the selected stars into  $Z$  by using an empirical relation for the solar neighbourhood stars (Clementini et al. 1999):

$$\log(Z/Z_\odot) \simeq [\alpha/\text{H}] \simeq \begin{cases} [\text{Fe}/\text{H}] + 0.4, & [\text{Fe}/\text{H}] \leq -1.0 \\ 0.6[\text{Fe}/\text{H}], & [\text{Fe}/\text{H}] \geq -1.0 \end{cases} \quad (1)$$

where  $Z_\odot = 0.02$ , and  $\alpha$  elements are assumed to dominate  $Z$ . Admittedly, this is rather a crude approximation, but it would not introduce significant effects on the resulting AMR and, we believe, is far better than a sim-

ple assumption of  $\log(Z/Z_\odot) = [\text{Fe}/\text{H}]$ . We also calculated ages of the sample stars with the assumption of  $\log(Z/Z_\odot) = [\text{Fe}/\text{H}]$  to find that the resulting ages are systematically older by  $\sim 0.2$  dex for metal-poor stars ( $[\text{Fe}/\text{H}] \leq -1$ ). The difference becomes smaller toward higher  $[\text{Fe}/\text{H}]$ .

Finally, knowing  $Z$  for the star, we interpolated the isochrones in  $\log Z$  with the two adjacent metallicities and derived a set of the isochrones with  $Z$  and ages from 1.0 to 20.0 Gyr. As illustrated in Fig. 2, the stellar age was derived by interpolating linearly the nearest two grid points of the isochrones on the  $M_{V_0} - (B - V)_0$  diagram. Uncertainties in  $M_{V_0}$ ,  $(B - V)_0$ , and  $Z$  cause errors for resulting ages. Errors in parallax of 10%,  $(B - V)_0$  of 0.02 mag, and metallicity of 0.1 dex result in uncertainties in age of 0.064 dex, 0.073 dex, 0.082 dex, respectively. Thus 0.12 dex age error exists for our sample in average.

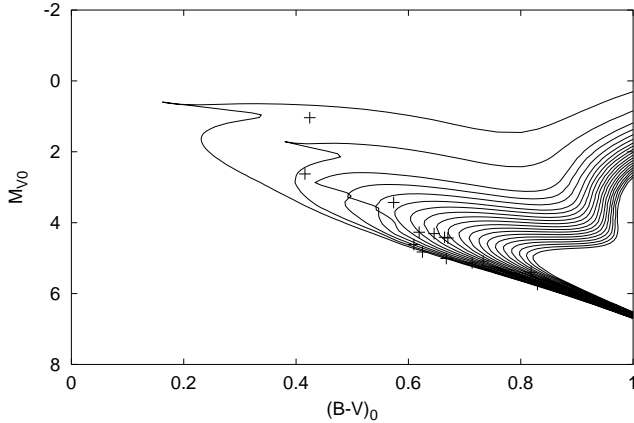


**Fig. 2.** The sample of isochrone fitting. Crosses represent solar metallicity stars ( $0.0 \leq [\text{Fe}/\text{H}] < 0.005$ ) while solid lines represent the isochrones for solar metallicity stars from 1 Gyr (top left) to 20 Gyr (bottom right).

### 2.2.2. The Galactic orbital parameters

We examined kinematics of the sample stars and calculated their orbital parameters in a similar way to Edvardsson et al. (1993) and Nissen & Schuster (1997).

We integrated their orbit backward in time by using a four-component Miyamoto-Nagai potential model including thin disc, thick disc, bulge, and halo (Sofue 1996). Integration was done using 6th order Symplectic formula with a constant time step of  $10^5$  year. We adopted the correction for the solar velocity of  $(U_{\odot}, V_{\odot}, W_{\odot}) = (-10, 232, 6)$   $\text{km s}^{-1}$ . The galactocentric distance and circular velocity of the sun were fixed to be 8.0 kpc and 226.0  $\text{km s}^{-1}$ , respectively (Edvardsson et al. 1993). Energy and angular momentum of the sample stars were conserved within an accuracy of  $10^{-8}$ . We derived apogalactocentric distance projected to the Galactic plane,  $R_a$ , peri-galactocentric distance,  $R_p$ , and maximum deviation from the plane,  $z_{\text{max}}$ . We also derived eccentricity,  $e \equiv (R_p - R_a)/(R_p + R_a)$ , and mean distance,  $R \equiv (R_p + R_a)/2$ . Tables 2 & 3 give the orbital parameters of the sample stars.

We identified the populations of stars by using their rotational velocities,  $V$ , with respect to the Galaxy centre. The stars with  $V \geq -62$   $\text{km s}^{-1}$ ,  $-182$   $\text{km s}^{-1} \leq V < -62$   $\text{km s}^{-1}$ , and  $V < -182$   $\text{km s}^{-1}$  are assigned as thin disc, thick disc, and halo stars, respectively. Following Carney et al. (1989) and Prochaska et al. (2000), stars with  $z_{\text{max}} > 600$  pc are identified to be thick disc component even if their rotational velocities,  $V$ , are larger than 170  $\text{km s}^{-1}$  in addition.

In our 1658 sample stars, we identified 1138 thin disc stars, 229 thick disc stars, and 47 halo stars.

The identified stellar populations are listed in Tables 2 & 3. Figures 3 show the CM diagrams of the whole sample with  $[\text{Fe}/\text{H}]$  measurements before sample selection (4240 stars), the selected 1138 thin disc stars, 229 thick disc stars, and 47 halo stars, respectively.

Thin disc stars rotate, in average, around the Galactic centre every 0.2 Gyr. For example, a 10 Gyr old star has rotated 50 times till now. Figures 4 show the snapshots of the orbit of our sample stars when we integrate their orbit backward to 0.2 Gyr and 2 Gyr. In the top two figures, the majority of stars rotate almost once. In such a short time scale, the orbits did not deviate so much and the similarity preserved. In the bottom figures, in which the orbits were integrated for 2 Gyr, however, the stars rotate for so long times that they are uniformly distributed in the torus because of their random motion. As a result, the sample stars older than 2 Gyr trace the star formation history in the various region in the torus, in spite of the fact that they now exist in the region within 100 pc from the sun. Hereafter, we define this region as the solar torus in which the “solar neighbourhood stars” formed in the past. Our sample stars reflect the star formation history not in the narrow sphere with radius of 100 pc but in the wide torus region of which radius is 6 kpc  $\sim$  9 kpc from the Galactic centre described in Figs 4.

## 3. The Thin Disc

### 3.1. The thin disc AMR

Figure 5 shows the spectroscopic AMR and the photometric AMR of thin disc stars. The line represents the GCE model by Pagel & Tautvaišienė (1995), which includes delayed elements production by type Ia supernovae (SNIa) and low mass type II supernovae (SNII). Thin disc AMR has a considerable scatter. The scatter is larger than that expected from observational errors. Thin disc star seems to appear at the beginning of the Galaxy formation although we are not sure to this feature because such stars have large errors in age determination due to heavy crowding of main sequence isochrones.

For thin disc stars, general trends of the AMR are apparently inconsistent with those previously derived by Twarog (1980), Edvardsson et al. (1993), and Ng & Bertelli (1998). In our data, the mean metallicity is almost constant from 14 Gyr to 1 Gyr and the scatter along the AMR decrease into younger stars while the mean metallicity increases gradually from  $[\text{Fe}/\text{H}] = -0.8$  at 16 Gyr to  $[\text{Fe}/\text{H}] = -0.1$  at the present in the previous researches. Since the Edvardsson et al.’s AMR includes thick disc and halo stars in these previous researches, however, the direct comparison is not appropriate. We carefully examined, therefore, both orbits and the AMR of Edvardsson et al. (1993). Figure 6 shows the AMR by Edvardsson et al. (1993) for thin disc stars according to the criteria given in Sect. 2.2.2. We see that a similar feature is already seen in Edvardsson et al. (1993) if we consider the stars younger than 10 Gyrs. For the stars older than 10 Gyrs, our AMR includes more metal rich stars than that of Edvardsson et al. (1993), and yet it would be difficult to discuss this difference in detail because the age determination of these old stars contains larger error than younger stars and the number of the sample stars of Edvardsson et al. (1993) is

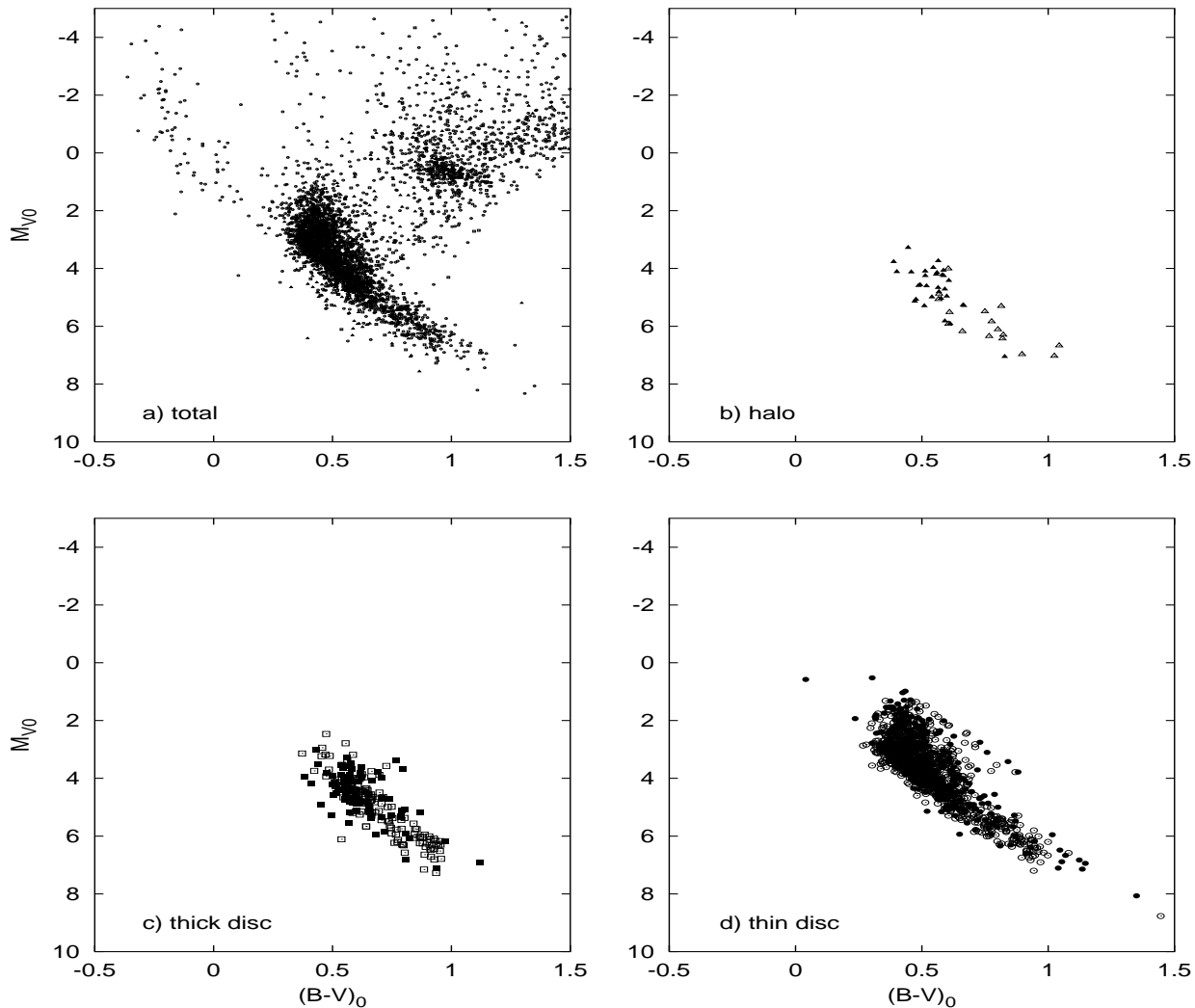


**Fig. 3.** Colour-magnitude diagram for the sample stars. **a)** 4240 stars before sample selection. **b)** **c)**, and **d)** the selected samples. Filled symbols represent the star with spectroscopic data, while open symbols represent stars with photometric data. Circles, squares and triangles represent thin disc, thick disc and halo stars, respectively.

not enough adequate. There are several features that were not clearly seen in Edvardsson et al.’s AMR: a) the upper envelope of the AMR is remarkably flat at a level similar to the solar metallicity ( $[\text{Fe}/\text{H}] \simeq 0.0 - 0.1$ ) for all the time from 14 Gyr to 1 Gyr; and b) although the AMR tends to converge to the point  $[\text{Fe}/\text{H}] \simeq +0.3$  at 1.6 Gyr in the Edvardsson et al. (1993)’s AMR, we found that a fairly large scatter in  $[\text{Fe}/\text{H}]$  still exists even at 1 Gyr.

### 3.2. The abundance pattern of thin disc

Figure 7 shows the  $[\text{Ca}/\text{Fe}] - [\text{Fe}/\text{H}]$  relation for thin disc stars. The line represents the GCE model by Pagel & Tautvaišienė (1995). This model predicts that  $[\text{Ca}/\text{Fe}] \simeq 0.3$  for  $[\text{Fe}/\text{H}] < -1.2$  (only SNI contribute for metal production) and that  $[\text{Ca}/\text{Fe}]$  decrease as  $[\text{Fe}/\text{H}]$  increase because of iron production from SNIa. The model shows good agreement with the averaged value of our data. Namely, our data shows the correlation that the more iron-

rich stars show smaller  $[\text{Ca}/\text{Fe}]$ . The dispersion of  $[\text{Ca}/\text{Fe}]$  along the model line is, however, larger than that expected from uncertainty of observation. The scatters among the age,  $[\text{Fe}/\text{H}]$ , and  $[\text{Ca}/\text{Fe}]$  are discussed in Sect. 5.5.

## 4. The Thick Disc

### 4.1. The thick disc AMR

Figure 8 presents the spectroscopic AMR and the photometric AMR for thick disc. We realise three features, i.e.,

1) Bulk of thick disc stars are older than 5 Gyr. The average age of thick disc stars is 8.2 Gyr. The AMR suggests that the star formation in thick disc seized almost 8.2 Gyr ago.

2) The mean metallicity of thick disc stars is  $\langle [\text{Fe}/\text{H}] \rangle \sim -0.5$  and the spread in  $[\text{Fe}/\text{H}]$  ranges from  $[\text{Fe}/\text{H}] = -1.0$  to solar. This feature is consistent with previous

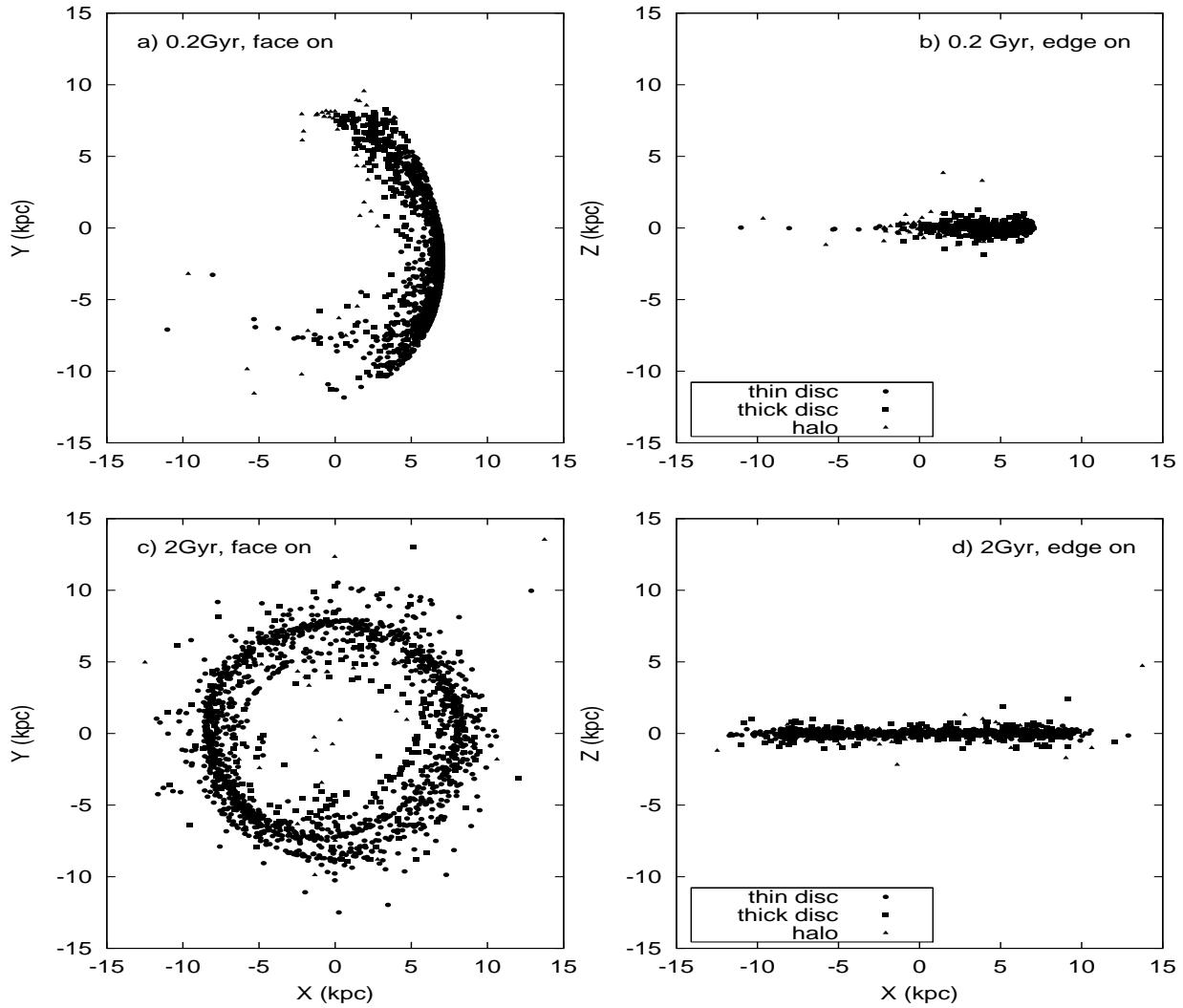


**Fig. 4.** Snapshot of the orbits of our sample stars. **a)** and **b)** the positions of stars of 0.2 Gyr ago. **c)** and **d)** these of 2 Gyr ago. The left panels are face on views and the right panels are edge on views.

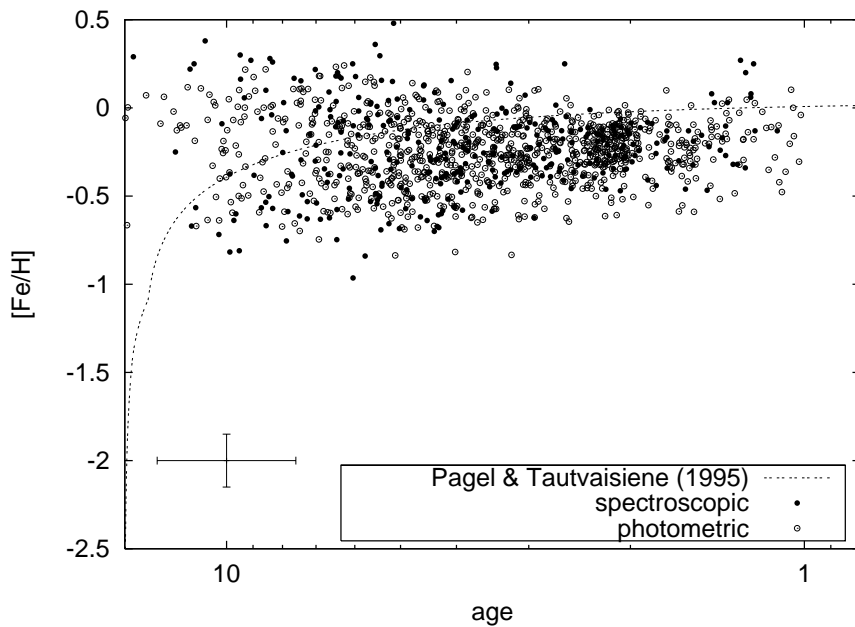


**Fig. 5.** The spectroscopic and photometric AMR for thin disc stars.

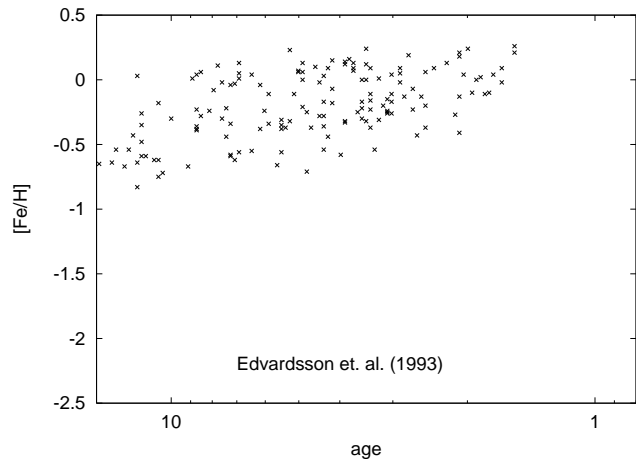


**Fig. 6.** The photometric AMR for thin disc stars by Edvardsson et al. (1993).

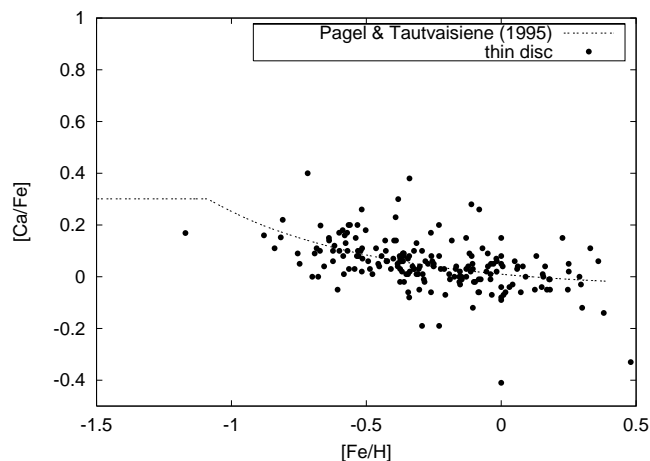


**Fig. 7.** The  $[\text{Ca}/\text{Fe}]$  -  $[\text{Fe}/\text{H}]$  diagram for thin disc stars.

researches (Gilmore & Wyse 1985; Carney et al. 1989; Layden 1995a,b)

3) The scatter along the AMR is larger than that for thin disc.

#### 4.2. The abundance pattern of thick disc

Figure 9 show the  $[\text{Ca}/\text{Fe}]$  -  $[\text{Fe}/\text{H}]$  diagram for thick disc stars. The dotted line in Fig.9 represents the best fit model for the chemical evolution for outer thin disc by Pagel & Tautvaišienė (1995). Clearly, Fig.9 shows that the thick disc stars are more  $\alpha$ -enhanced than the thin disc stars at the same  $[\text{Fe}/\text{H}]$  value.

This trend has been already reported by Gratton et al. (2000) and Prochaska et al. (2000). Prochaska et al. (2000) suggested that  $\alpha$ -enhancement in the thick disc indicates that the thin disc stars formed from gas more polluted by SNIa, which suggests that the thin disc formation significantly delayed ( $> 1$  Gyr) from the thick disc formation. We could not find, however, any clear evidence for delayed thick disc formation from the AMRs of thin

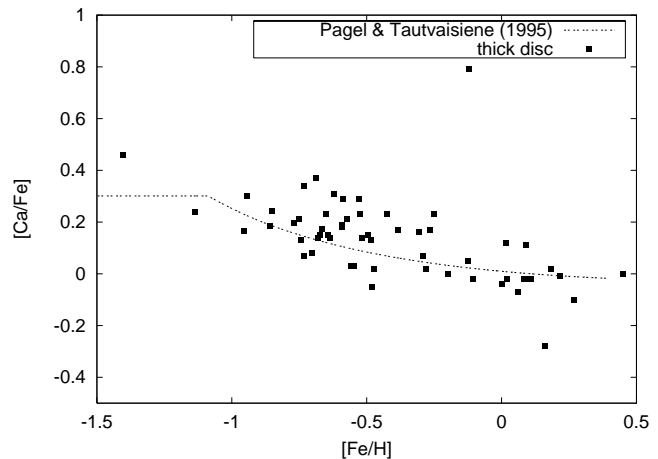


**Fig. 9.** The  $[\text{Ca}/\text{Fe}]$  -  $[\text{Fe}/\text{H}]$  diagram for thick disc stars.

disc and thick disc stars. Interestingly, bulge stars of the Galaxies show the similar trend of  $\alpha$ -enhancement and are believed to be experienced the rapid star formation history (McWilliam & Rich 1994; Rich & McWilliam 2000). The  $\alpha$ -enhancement of thick disc stars, therefore, may be also understood as the result of the rapid star formation.

## 5. Discussion

### 5.1. Uncertainty in the AMR

#### 5.1.1. Inhomogeneity of Spectroscopic $[\text{Fe}/\text{H}]$ data

Unfortunately, our AMR contains large errors in metallicity; typically  $\epsilon_{[\text{Fe}/\text{H}]} = 0.15$  dex due to inhomogeneous data taken from different authors, while  $\epsilon_{[\text{Fe}/\text{H}]} = 0.1$  dex in Edvardsson et al. (1993) due to their homogeneous  $[\text{Fe}/\text{H}]$  data reduced by the same analysis method. Even if stellar spectra were taken with high S/N and high resolution,  $[\text{Fe}/\text{H}]$  estimates by different authors could result in large scatter in  $[\text{Fe}/\text{H}]$ .

Therefore, without examining carefully the details of individual analyses to understand the differences, it would be dangerous to argue too much details of the value of metallicity. We also have to keep in our mind that  $[\text{Fe}/\text{H}]$  determinations are affected by the adopted effective temperatures, gravities and microturbulent velocities, and that a stellar metal abundance can be in error, even if the observations are of excellent quality (Cayrel de Strobel et al. 1997).

However, recent observations are in good agreement for different observers. We have studied the most observed 30 stars in the  $[\text{Fe}/\text{H}]$  catalogue to find the average dispersion in metallicity is 0.13 dex (See. Table 4). Our sample includes extremely metal-deficient stars, in which the dispersion in metallicity is apt to show the larger values. The dispersion in the metallicity for stars with  $[\text{Fe}/\text{H}] > -2.5$  is even smaller. Considering that the our sample includes a very small number of extremely metal-deficient stars, we conclude that the dispersion in the metallicity can be estimated to be 0.11 dex.

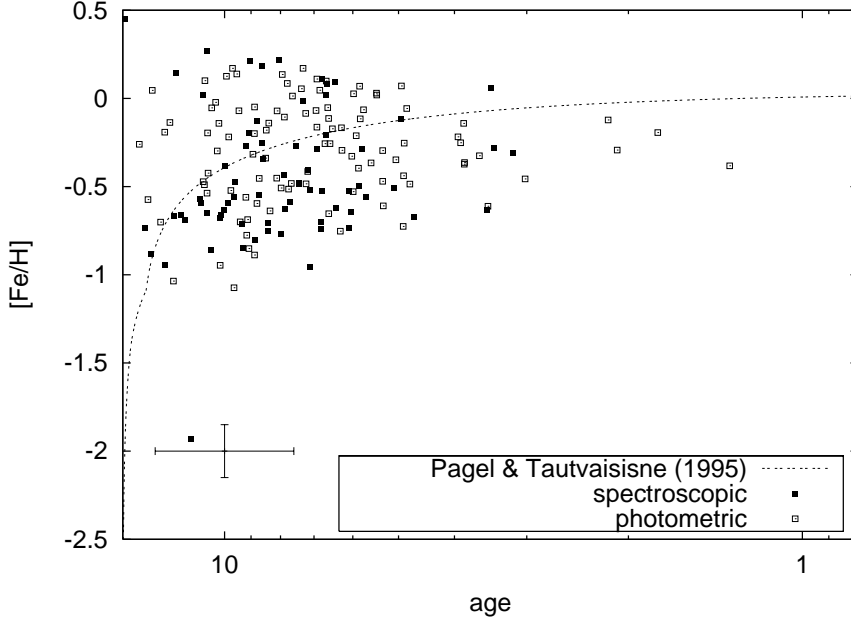


**Fig. 8.** The spectroscopic and photometric AMR for thick disc stars.

**Table 4.** Differences of  $[\text{Fe}/\text{H}]$  values with different observations.

Name	Number of obs.	$[\text{Fe}/\text{H}]_{\text{average}}$	$[\text{Fe}/\text{H}]_{\text{max}}$	$[\text{Fe}/\text{H}]_{\text{min}}$	$\epsilon_{[\text{Fe}/\text{H}]}$
CD -38 245	8	-3.95	-4.42	-3.00	0.39
HD 122563	16	-2.69	-2.93	-2.45	0.10
BD +03 740	11	-2.66	-2.98	-2.3	0.22
HD 140283	26	-2.49	-2.75	-2.21	0.14
BD +2 3375	10	-2.28	-2.65	-1.95	0.19
HD 216143	9	-2.21	-2.26	-2.10	0.05
HD 128279	9	-2.19	-2.50	-1.97	0.16
HD 165195	11	-2.18	-2.26	-1.92	0.09
HD 84937	12	-2.14	-2.43	-1.86	0.17
BD +37 1458	9	-2.02	-2.33	-1.79	0.19
HD 19445	19	-2.00	-2.31	-1.76	0.14
HD 187111	13	-1.78	-2.35	-1.54	0.19
HD 26297	10	-1.77	-1.87	-1.68	0.06
HD 122956	13	-1.75	-1.96	-1.53	0.10
HD 64090	12	-1.68	-1.94	-1.49	0.16
HD 211998	10	-1.53	-1.68	-1.25	0.14
HD 83212	11	-1.46	-1.57	-1.37	0.06
HD 94028	11	-1.44	-1.66	-1.31	0.12
HD 103095	15	-1.34	-1.59	-1.17	0.11
HD 194598	17	-1.14	-1.37	-0.99	0.11
HD 201891	15	-1.01	-1.12	-0.87	0.06
HD 76932	14	-0.92	-1.05	-0.76	0.09
HD 63077	15	-0.89	-1.16	-0.53	0.16
HD 022879	12	-0.86	-0.99	-0.76	0.05
HD 59984	14	-0.82	-1.60	-0.52	0.24
HD 124897	14	-0.54	-0.69	-0.37	0.10
HD 61421	13	-0.02	-0.18	0.05	0.05
HD 9826	8	0.09	-0.03	0.17	0.05
HD 217014	8	0.15	0.05	0.21	0.07
HD 128620	10	0.19	0.10	0.25	0.04



### 5.1.2. Uncertainty in the age

Uncertainties in  $M_{V0}$ ,  $(B - V)_0$  and  $Z$  cause errors for resulting ages. Errors in  $M_{V0}$  and  $(B - V)_0$  are typically 0.2 mag ( $\approx 10\%$  in parallax) and 0.02 mag in our data. Combined with  $Z$  uncertainties, we can determine the expected error in the resulting age. The errors in ages also depend on the initial mass of the stars through their position of colour-magnitude diagram and the nature of the isochrones hereon. We conducted, therefore, Monte Carlo simulations assuming the AMR and the star formation history in the one zone infall model of Pagel & Tautvaišienė (1995). We took the set of stars (the simple stellar population) from 15 Gyr old to the present, with given metallicity from AMR and star formation history of Pagel & Tautvaišienė (1995). The locations on the colour-magnitude diagram are derived from Yi et al. (2001), adding Gaussian errors of  $M_{V0}$ ,  $(B - V)_0$  and  $Z$ . Then we obtained the age by using the same method in Sect. 2.2. Figure 10 shows the resulting AMR with errors of 0.07 in  $Z$  (left) and 0.13 in  $Z$  (right). Notably, the expected spread in age – due only to errors – shown by both panels of Fig. 10 is smaller than the observed dispersion of points in Fig. 5 for stars older than 3 Gyr.

## 5.2. Abundance Gradient

In order to discuss the radial abundance gradient of the Galaxy, it is not appropriate to use the present position of the stars as mean position of the stellar orbit. We used, instead,  $R \equiv (R_p + R_a)/2$ , for the distance from the Galactic centre (Edvardsson et al. 1993). We also employed  $z_{\max}$  for the characteristic distance from the Galactic plane.

### 5.2.1. Thin disc abundance gradient

Figure 11 presents the  $[\text{Fe}/\text{H}]-R$  relation for thin disc stars. Filled symbols represent spectroscopic data while empty symbols represent photometric data. Both spectroscopic and photometric data show no strong correlations between  $R$  and  $[\text{Fe}/\text{H}]$ . The line are the observations derived by Díaz (1989). Figure 12 shows the  $[\text{Fe}/\text{H}]-z_{\max}$  relation for thin disc stars. These data also show no strong correlations.

### 5.2.2. Thick disc abundance gradient

Figure 13 represents the  $[\text{Fe}/\text{H}]-R$  relation for thick disc stars. Filled symbols represent spectroscopic data, while empty ones represent photometric data. Both spectroscopic and photometric data show little correlation between  $R$  and  $[\text{Fe}/\text{H}]$ . Figure 14 shows the  $[\text{Fe}/\text{H}]-z_{\max}$  relation for thick disc stars. Unlike thin disc stars, thick disc stars show the feature that the stars more distant from the Galactic plane tend to be more metal poor. Namely, a vertical abundance gradient is seen in thick disc. Comparing the thin disc stars and thick disc stars with  $100 \text{ pc} < z_{\max} < 600 \text{ pc}$ , the thick disc stars are clearly more

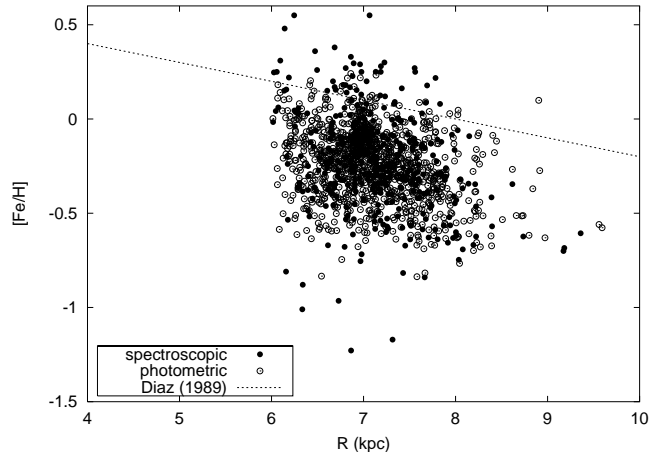


**Fig. 11.** The  $[\text{Fe}/\text{H}]-R$  relation for thin disc stars. Dashed line represents observations of H II regions (Díaz 1989).

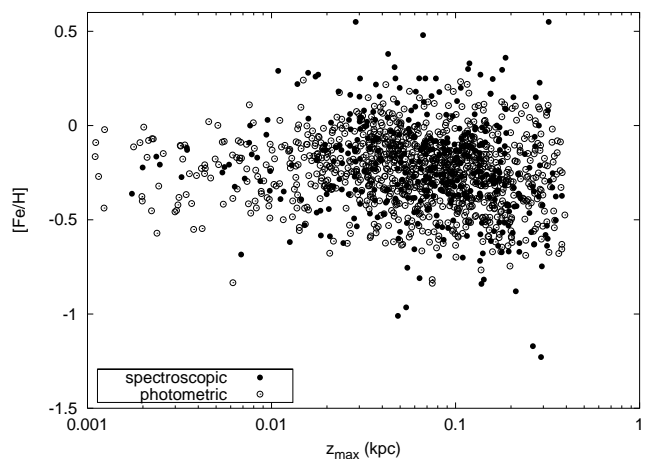


**Fig. 12.** The  $[\text{Fe}/\text{H}]-z_{\max}$  relation for thin disc stars.

metal-deficient than the thin disc stars. This phenomenon is naturally understood if we surmise that these two kinds of stellar groups have different origin: the thick disc stars located at the distance  $z_{\max} > 100 \text{ pc}$  formed intrinsically in the region distant from the Galactic plane while the thin disc stars formed near the Galactic plane and drifted or heated-up vertically to 100 pc away from their original birth place.

## 5.3. The G-dwarf problem

Figure 15 shows the metallicity distribution function for thin disc stars and thick disc stars. Although it is impossible to discuss the property of the abundance distribution because our sample lacks completeness, it is clear that both thin disc and thick disc are deficient in metal-poor stars. Notably, the G-dwarf problem do exist for thick disc stars. Since the metallicity distribution function of metal deficient halo stars can be explained by the simple model (Laird et al. 1988), thick disc presents a striking contrast to halo, instead abundance distribution function

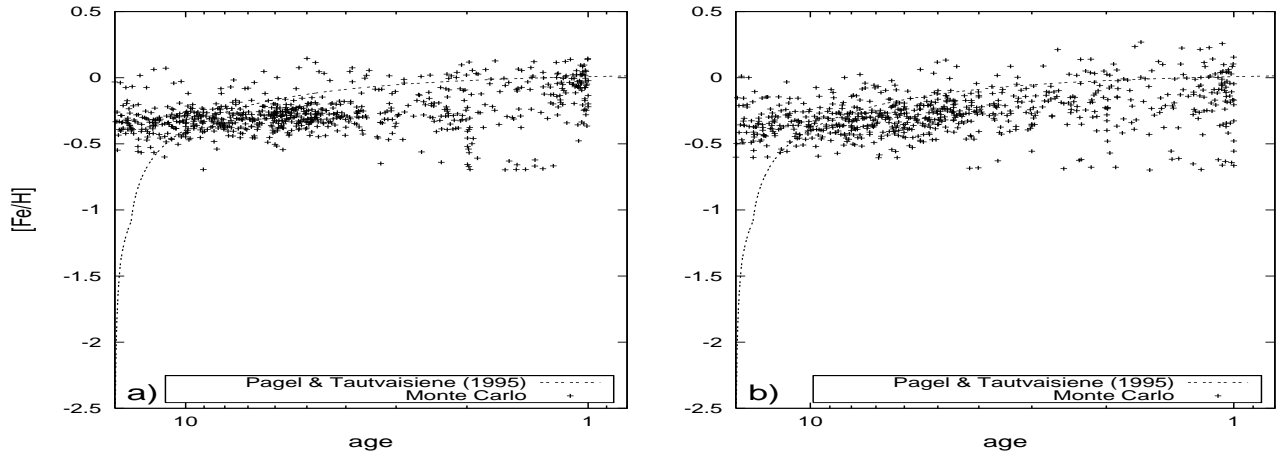


**Fig. 10.** The simulated AMR from one zone infall model by Pagel & Tautvaišienė (1995). **a)** The errors in  $Z$  are set to be 0.07. **b)** these are set to be 0.13. The errors in  $M_{V_0}$  and  $(B - V)_0$  are 0.2 mag and 0.02 mag in both figures.

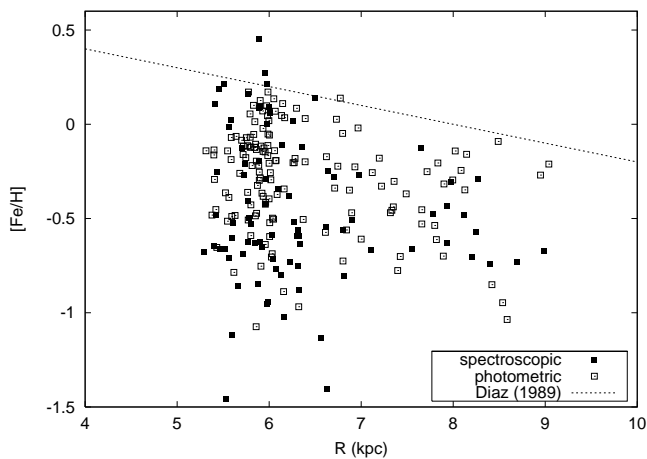


**Fig. 13.** The  $[\text{Fe}/\text{H}]-R$  relation for thick disc stars. Dashed line represents observations of H II regions (Díaz 1989).

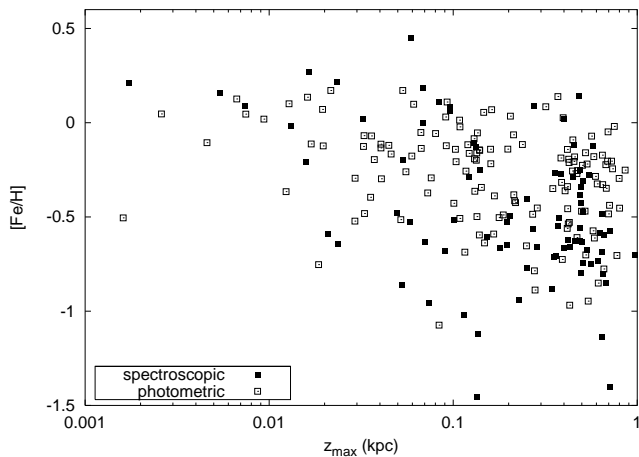


**Fig. 14.** The  $[\text{Fe}/\text{H}]-z_{\text{max}}$  relation for thick disc stars.

for thick disc stars shows rather close feature to that of bulge (McWilliam & Rich 1994).

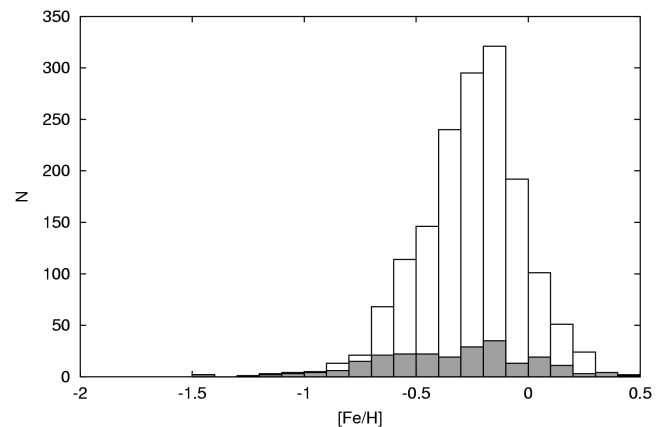


**Fig. 15.** Abundance distribution function for thin disc (open boxes) and thick disc (gray boxes).

#### 5.4. Formation process for thick disc

We here discuss how thick disc formed in the Galaxy. In summary, thick disc shows three important features, i.e. 1) thick disc stars are older than 5 Gyr, 2) thick disc stars show vertical abundance gradient, and 3) thick disc stars have different abundance patterns compared with thin disc counterparts. To date, thick disc formation scenarios, such as monolithic collapse (Larson 1976; Jones & Wyse 1983), dynamical heating (Noguchi 1998), major merger, and accretion of dwarf galaxies (Quinn & Goodman 1986) have been proposed.

Major merger should invoke a strong peak in age-distribution. It is also widely believed that merger will work as reducing vertical abundance gradient. Our research does not, therefore, support the thick disc formation with major merger. If thick disc is formed from heating of thin disc, the star formation history of thick disc should be similar to that of thin disc and the similar star formation history essentially produces the similar  $[\text{Ca}/\text{Fe}]-[\text{Fe}/\text{H}]$  relation. Heating mechanism is, therefore, unlikely

to explain the thick disc formation. The other two theories both account for our result.

### 5.5. Scatter in the AMR for thin disc

In this section, we will try to find the way to explain the scatter along the AMR by simple extension of the one zone model derived by Pagel & Tautvaišienė (1995).

#### 5.5.1. Metallicity-Orbit relation

The solar neighbourhood stars consist of a mixture of stars born at different place with different orbit. This fact may account for the scatter along the thin disc AMR (Edvardsson et al. 1993; Pagel & Tautvaišienė 1995; Prantzos & Boissier 2000). Already seen in Sec. 5.2, the abundance gradient is not significant for thin disc stars. Another relation between orbital elements and metallicity relation may exist for thin disc stars. For example, if we find metallicity-orbit relation that stars with larger eccentricity tend to be more metal deficient, the scatter along the AMR can be attributed to such kind of relation. Therefore, we examined the  $U$ ,  $V$ ,  $W$ ,  $e$  -  $[\text{Fe}/\text{H}]$  relation (Fig. 16). All of these relations, however, show more a scattered feature than a strong correlation. Notably, a large scatter in  $[\text{Fe}/\text{H}]$  is seen even if the stars with the same orbital parameters are selected. The scatter along the AMR cannot, therefore be attributed to the relation of this kind.

#### 5.5.2. Inhomogeneous effective yield and star formation

The effective yield can be different from place to place although the true yield is homogeneous, because the supernova ejecta are inhomogeneous due to axisymmetric explosions of rotating massive stars (Maeda et al. 2001). Even if the explosions are isotropic, the ejecta may stochastically contaminate the surroundings, unless the ISM is distributed uniformly. The scatter can be explained even if the star formation history in the “solar torus” is completely homogeneous. It is also possible that the local inhomogeneity of star formation rate produces the scatter. To examine these scenarios, we prepared 7 models by modifying the parameters in the analytical model of Pagel & Tautvaišienė (1995). Table 5 shows the adopted parameters for each model. Model A is an original infall model taken from Pagel & Tautvaišienė (1995). Model B and C assumed twice and half yield SNII ejecta, respectively. SNIa yield and star formation timescale is changed in model D, E and model F, G in the same manner.

The scatter may arise if relative contributions of SNIa and SNII differ from place to place. The various panels of Fig. 17 show the AMR, age- $[\text{Ca}/\text{Fe}]$  relation, and the  $[\text{Ca}/\text{Fe}]$ - $[\text{Fe}/\text{H}]$  diagram with models A, B, and C. Clearly the difference in the effective yield of SNII produces smaller scatter along the AMR than the observation,

**Table 5.** The parameters for 7 GCE models, originally introduced by Pagel & Tautvaišienė (1995).  $1/\omega$  represent the star formation timescale.

model	$\omega$	$y_{\text{Fe,SNIa}}$	$y_{\text{Fe,SNII}}$	$y_{\text{Ca,SNIa}}$	$y_{\text{Ca,SNII}}$
A	0.3	0.42	0.28	0.18	0.56
B	0.3	0.42	0.56	0.18	1.12
C	0.3	0.42	0.14	0.18	0.28
D	0.3	0.84	0.28	0.36	0.56
E	0.3	0.21	0.28	0.09	0.56
F	0.15	0.42	0.28	0.18	0.56
G	0.6	0.42	0.28	0.18	0.56

while the scatter in the  $[\text{Ca}/\text{Fe}]$ - $[\text{Fe}/\text{H}]$  diagram (right) is too large to explain the observation.

Next, we examined the inhomogeneous effective yield of SNIa. Figures 18 show the models with different effective yields for SNIa. Models A, D, and E reproduce fairly well both the trend of thin disc stars’ AMR and the scatter along it. However, dividing the  $[\text{Fe}/\text{H}]$  relation into two parts (Fig. 19), metal rich stars and metal poor stars, and examining the  $[\text{Ca}/\text{Fe}]$  -  $[\text{Fe}/\text{H}]$  diagram in detail, we found that this model cannot account for the scatters. In Fig. 19 the sample stars are divided into two parts. More iron rich stars than model A are designated in circles while metal poor stars are in triangles. Model D and E predict that iron rich stars (circles) will show smaller  $[\text{Ca}/\text{Fe}]$  than model A on Fig. 19 and that the metal poor stars (triangles) will show larger  $[\text{Ca}/\text{Fe}]$  than model A. In our data, however, both iron rich stars and iron poor stars are distributed along model A and show no clear split of  $[\text{Ca}/\text{Fe}]$  on Fig. 19. Thus, models with different effective yield for SNIa cannot explain this feature on the  $[\text{Ca}/\text{Fe}]$  -  $[\text{Fe}/\text{H}]$  diagram.

Finally, the inhomogeneity of star formation rate is examined. Figures 20 show the models with different star formation rate. The scatter along the age- $[\text{Ca}/\text{Fe}]$  relation is clearly larger than expected from the models.

Comparing these three hypotheses and our data, we conclude that such a simple modification of one-zone model cannot explain the scatter along the AMR, age- $[\text{Ca}/\text{Fe}]$  relation, and  $[\text{Ca}/\text{Fe}]$ - $[\text{Fe}/\text{H}]$  relation simultaneously.

#### 5.5.3. Planet migration

There is a growing evidence that the star formation mechanism may have some influence on the metallicity of the star: in particular, Gonzalez (1997) has recently suggested that stars with planets are systematically more metal-rich than stars without planets, and that this is due to the presence of planets (“planet migration”). This effect can cause the scatter in the AMR. Our data include, however, only 14 discovered planet host stars (Mayor & Queloz 1995; Fischer et al. 1999; Butler et al. 2000; Henry et al. 2000; Korzennik et al. 2000; Marcy et al. 2000; Mazeh et al. 2000; Udry et al. 2000; Vogt et al. 2000; Butler et al. 2001; Fischer et al. 2001; Gonzalez et al. 2001; Tinney et al.

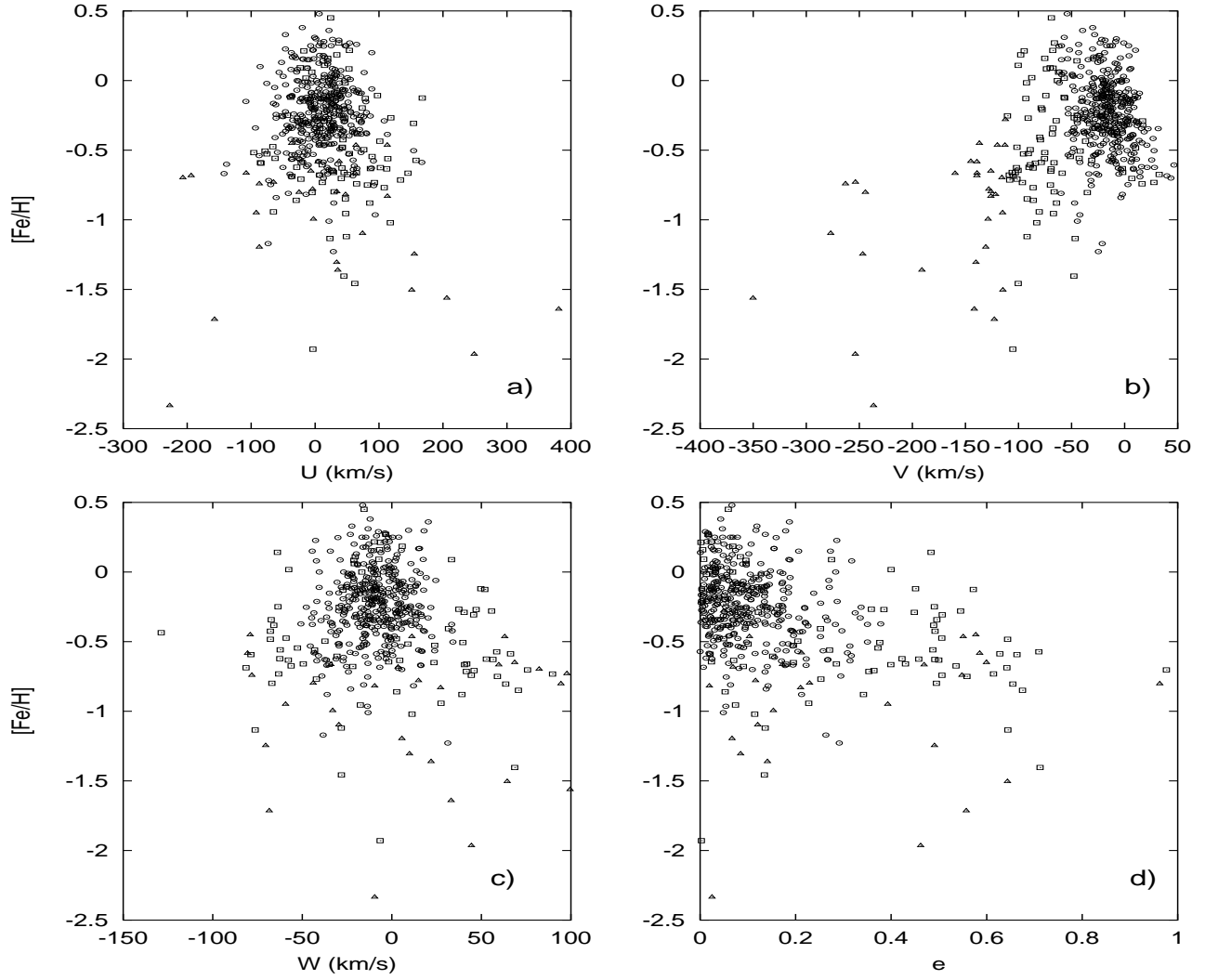


**Fig. 16.** a)  $U$  -  $[Fe/H]$  relation. b)  $V$ - $[Fe/H]$ . c)  $W$ - $[Fe/H]$ . d)  $e$ - $[Fe/H]$ . Circles, squares, and triangles represent thin disc, thick disc, and halo stars, respectively.

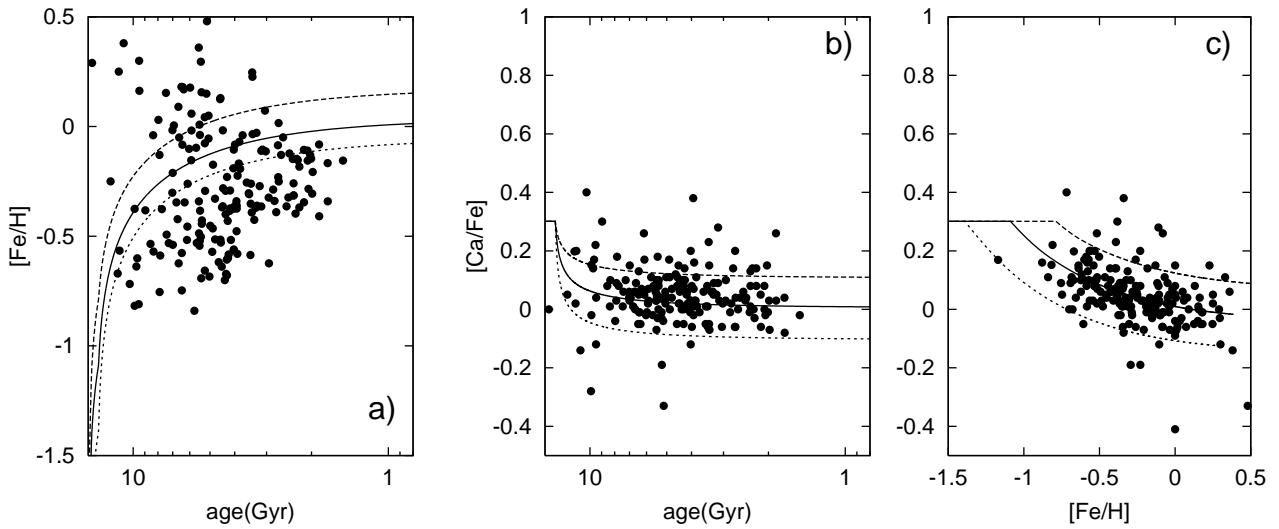


**Fig. 17.** Comparison of a) the AMR, b) age- $[Ca/Fe]$  relation, and c)  $[Ca/Fe]$ - $[Fe/H]$  diagram with models A (solid line), B (long dashed line), and C (short dashed line).

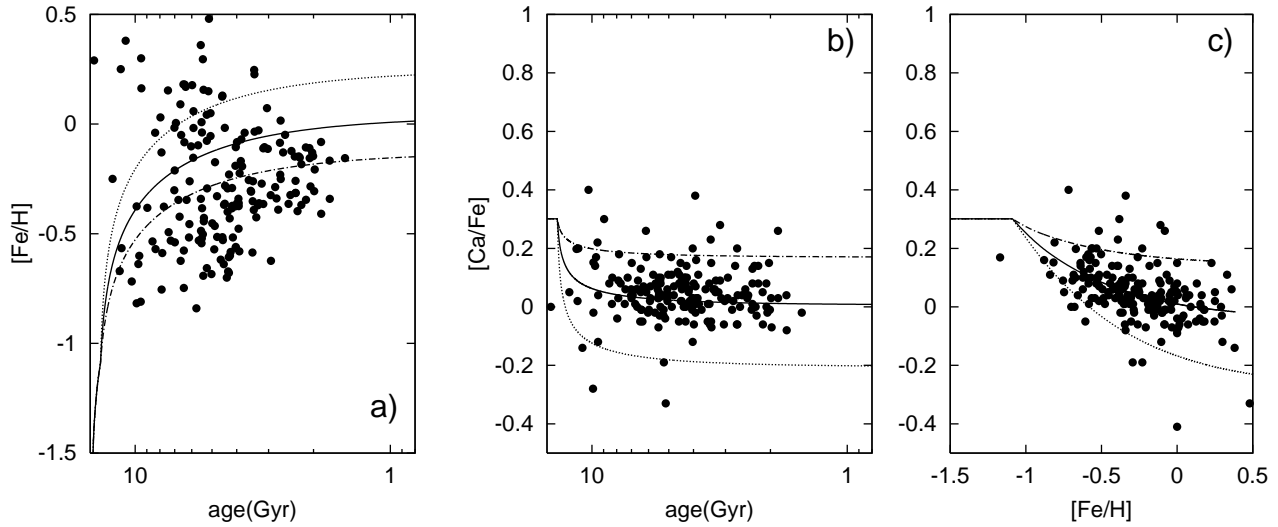


**Fig. 18.** Comparison of a) the AMR, b) age-[Ca/Fe] relation, and c) [Ca/Fe]-[Fe/H] diagram with models A (solid line), D (dotted line), and E (dash-dotted line).

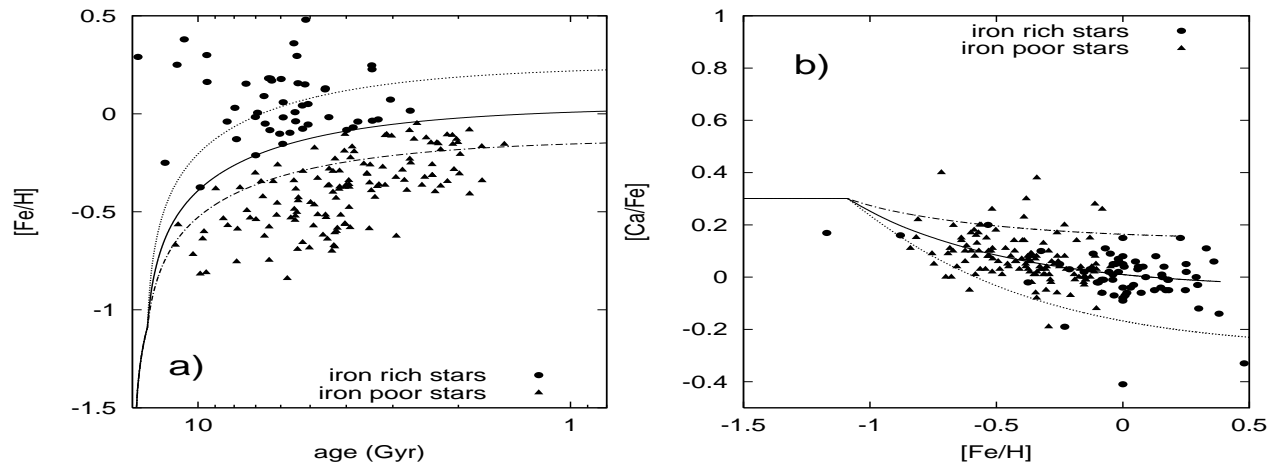


**Fig. 19.** Comparison of a) the AMR and b) the [Ca/Fe] diagram in detail. Circles represent stars more iron rich than the model A, while triangles represent iron poor stars.

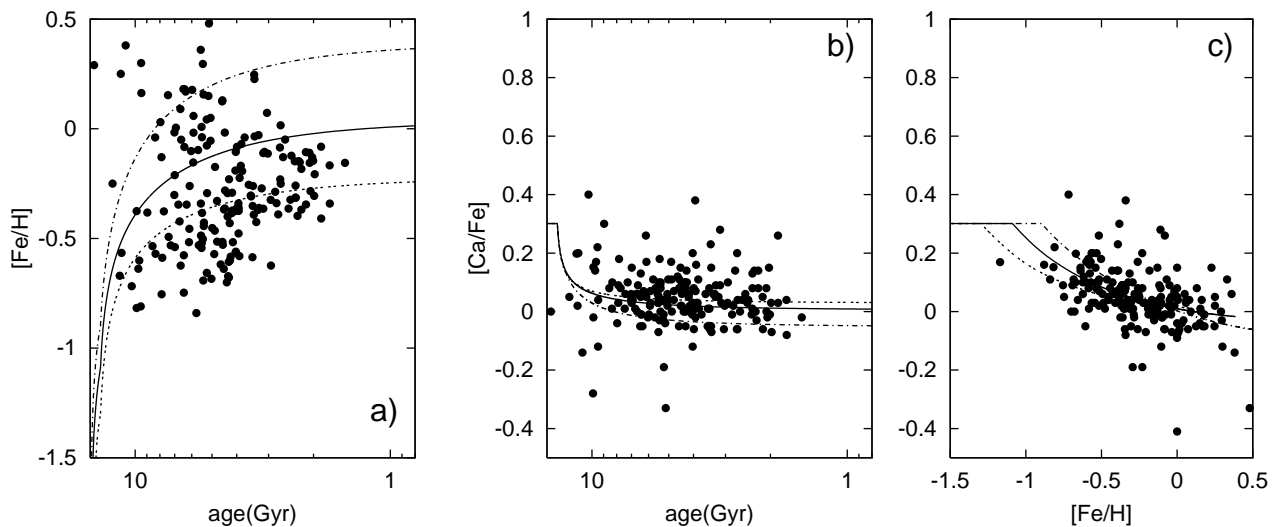


**Fig. 20.** Comparison of a) the AMR, b) age-[Ca/Fe] relation, and c) [Ca/Fe]-[Fe/H] diagram with models A (solid line), F (dash-dotted line), and G (short dashed line).

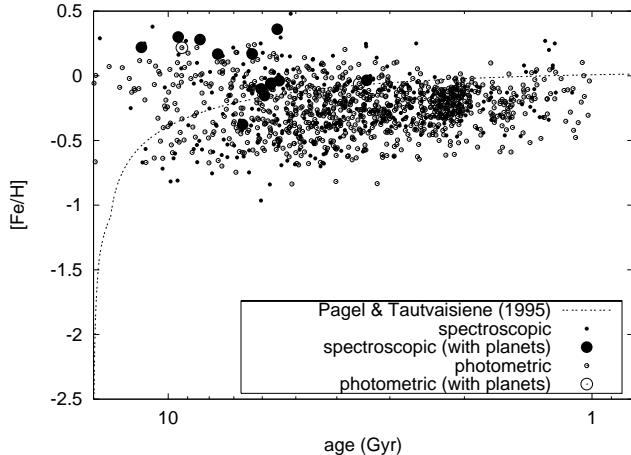


**Fig. 21.** The AMR and planets hosting stars in our sample. Large symbols denote known planets host stars.

2001), and we have scatter in the AMR when we consider only stars without planets. Fig. 21 shows the AMR with known planets host stars and other stars. As already noted by Gonzalez (1997) the planets host stars tend to have larger metallicities than the general trend of the AMR. It should be noted that the Sun also shows this “over-metallicity”. It seems that the idea is reasonable because the “over-metallicity” of 0.1 dex in  $[Fe/H]$  result in the underestimate of the age of  $\sim 1$  Gyr. If we consider that ages and  $[Fe/H]$  of planets host stars are underestimated and overestimated, respectively, the original  $[Fe/H]$  and ages of planets stars shows better fit to the one-zone AMR model. However, it is insufficient or even dangerous to study the general nature of the scatter of the AMR from such small number of stars (less than 1% of the total samples stars) and we cannot conclude yet that the planet migration is the major cause for the scatter along the AMR.

## 6. Summary & Conclusion

The AMR and orbital parameters are newly derived for 1658 solar neighbourhood stars to which accurate distances are measured by the *HIPPARCOS* satellite. The sample stars are divided into 1382 thin disc stars, 229 thick disc stars, and 47 halo stars according to their orbital parameters. Notably, the thin disc AMR shows a considerable scatter along the one-zone GCE model. No clear relation between orbit and metallicity are found. Namely, the scatter along the AMR exists even if the stars with the same orbits are selected. We examined simple extension of one-zone GCE models which account for i) inhomogeneity in the effective yield caused by the spatially localised mixing of inter stellar medium; and ii) inhomogeneous star formation history. We found both extensions of one-zone GCE model cannot account for the scatter in age -  $[Fe/H]$  -  $[Ca/Fe]$  relation simultaneously. In our work, the scatter along the AMR for thin disc stars have been confirmed for far larger samples (1382 stars), which is more than 5 times larger than that used in the previ-

ous work of Edvardsson et al. (1993). We concluded that this scatter, which should be accounted for by any Galaxy models, is one of the most important feature in the formation and evolution of the Galaxy. On the other hand, the AMR for thick disc stars shows that the star formation terminated 8 Gyr ago in thick disc. We reconfirmed the trend that the thick disc stars are more Ca-rich than the disc stars with the same  $[Fe/H]$ , which has been already reported by Gratton et al. (2000) and Prochaska et al. (2000). Thick disc stars show a vertical abundance gradient. These three facts, the AMR, vertical gradient, and  $[Ca/Fe]$ - $[Fe/H]$  relation, support monolithic collapse and/or accretion of satellite dwarf galaxy as thick disc formation scenario.

*Acknowledgements.* We are grateful to the anonymous referee whose suggestions on the early version greatly improved the paper. We thank to Dr. Chiaki Kobayashi for useful discussions. A. I. thanks the Japan Society for Promotion of Science (JSPS) Research Fellowships for Young Scientists.

**Table 2.** The sample stars with spectroscopic [Fe/H] observation.

Name	Sp. type	[Fe/H]	[Ca/Fe]	age (Gyr)	$R$ (kpc)	$e$	$z_{\max}$ (kpc)	population
HD400	F8IV	-0.44	0.08	5.39	8.02	0.11	0.03	thin
HD693	F5V	-0.54	0.03	5.49	7.86	0.09	0.14	thin
HD739	F3/F5V	-0.27	0.05	3.19	8.33	0.05	0.04	thin
HD1581	F9V	-0.29	-0.19	5.23	8.43	0.19	0.50	thin
HD1671	F5III	-0.19		1.56	8.17	0.02	0.08	thin
HD2025	K2V	-0.19			7.63	0.14	0.03	thin
HD2151	G2IV	-0.07		6.28	7.00	0.23	0.29	thin
HD2454	F6V	-0.38	0.05	4.18	7.29	0.12	0.09	thin
HD2615	F5V	-0.68	0.11	5.02	10.24	0.25	0.01	thin
HD2630	F2/F3V	-0.27		2.04	7.59	0.07	0.01	thin
HD3079	F8	-0.38		6.37	6.89	0.27	0.20	thin
HD3158	F3IV-V	-0.26	-0.06	3.45	7.54	0.06	0.34	thin
HD3229	F5IV	-0.46		2.53	7.33	0.11	0.10	thin
HD3268	F7V	-0.34	0.08	5.53	7.69	0.17	0.06	thin
HD3823	G1V	-0.39		7.69	8.38	0.31	0.37	thin
HD4813	F7IV-V	-0.31	0.01	2.35	8.22	0.10	0.07	thin
HD5133	K2V	-0.10		5.35	7.61	0.10	0.15	thin
HD6660	K4V	0.15			7.21	0.13	0.33	thin
HD6920	F8V	-0.28	-0.02	2.06	8.71	0.15	0.04	thin
HD7570	F8V	-0.08	-0.01	5.24	7.60	0.12	0.05	thin
HD8634	F5III	-0.26		1.81	7.56	0.07	0.13	thin
HD8671	F7V	-0.40		4.24	8.50	0.09	0.14	thin
HD8673	F7V	-0.12		4.06	7.61	0.11	0.10	thin
HD9407	G6V	0.03		5.63	8.47	0.19	0.09	thin
HD9430	G5	-0.34	0.38	3.94	8.31	0.32	0.14	thin
HD9562	G2IV	-0.10	-0.02	5.67	7.40	0.08	0.22	thin
HD9919	F0V	-0.47		2.08	8.58	0.09	0.06	thin
HD10307	G2V	-0.02	0.07	5.90	7.32	0.13	0.05	thin
HD10697	G5IV	0.17		7.64	7.52	0.16	0.25	thin
HD10874	F6V	-0.34		2.92	7.92	0.03	0.08	thin
HD11112	G4V	0.20		6.43	7.29	0.28	0.18	thin
HD11505	G0	-0.05	0.09	6.60	7.65	0.24	0.18	thin
HD11592	F5V	-0.52	0.11	4.55	7.83	0.22	0.30	thin
HD12042	F8V	-0.53	0.08	4.53	8.03	0.13	0.02	thin
HD12235	G2IV	0.16	0.00	5.39	6.69	0.20	0.13	thin
HD12363	F5/F6IV/V	-0.22		3.43	7.80	0.04	0.00	thin
HD13421	G0IV	-0.12		2.81	8.31	0.15	0.03	thin
HD13456	F5V	-0.24		2.67	7.47	0.13	0.22	thin
HD13555	F5V	-0.37	0.07	3.93	7.84	0.04	0.11	thin
HD14214	G0.5IV	-0.08	-0.01	6.42	8.83	0.18	0.26	thin
HD14221	F4V	-0.34		2.65	9.05	0.17	0.26	thin
HD14412	G8V	-0.42			9.35	0.14	0.05	thin
HD14802	G2V	-0.14		6.34	7.68	0.05	0.04	thin
HD15096	G5	-1.23			7.50	0.09	0.43	thin
HD15335	G0V	-0.35	0.01	6.77	9.61	0.17	0.10	thin
HD15798	F5V	-0.43	0.06	3.35	8.23	0.13	0.30	thin
HD16141	G5IV	0.10		8.55	7.53	0.32	0.10	thin
HD16176	F5V	-0.20		2.52	6.89	0.17	0.18	thin
HD16220	F8V	-0.39		2.97	7.93	0.02	0.24	thin
HD16397	G0V	-0.60	0.17	9.63	8.78	0.45	0.54	thin
HD16399	F6IV	-0.24		1.93	7.25	0.11	0.02	thin
HD16673	F6V	-0.28	0.06	4.44	8.42	0.09	0.01	thin
HD17051	G3IV	-0.05		3.76	7.71	0.08	0.01	thin
HD17922	F5	0.02		4.22	7.42	0.15	0.05	thin
HD18149	F5V	-0.11		1.92	7.78	0.05	0.07	thin
HD18256	F6V	-0.24		3.85	6.72	0.20	0.05	thin
HD18262	F7IV	-0.02		3.29	7.63	0.06	0.20	thin
HD18803	G8V	0.14		3.22	7.50	0.07	0.00	thin
HD19319	F0IV	-0.44		1.80	8.09	0.09	0.11	thin

Table 2. (continued)

Name	Sp. type	[Fe/H]	[Ca/Fe]	age (Gyr)	$R$ (kpc)	$e$	$z_{\max}$ (kpc)	population
HD20407	G3V	-0.45		3.50	8.89	0.10	0.10	thin
HD20619	G0	-0.21		2.19	7.31	0.10	0.02	thin
HD21197	K5V	0.33	0.11		7.54	0.19	0.19	thin
HD21770	F4III	-0.32		2.75	7.60	0.18	0.04	thin
HD21794	F7V	-0.27		2.12	7.36	0.25	0.18	thin
HD22328	F5	-0.21		2.88	7.15	0.17	0.00	thin
HD22484	F9V	-0.21	0.03	7.00	7.78	0.04	0.42	thin
HD23754	F3/F5V	-0.11	0.02	3.02	7.65	0.15	0.18	thin
HD24341	G1V	-0.50		8.45	11.45	0.46	0.15	thin
HD24421	F5	-0.52	0.10	5.48	8.81	0.18	0.09	thin
HD25169	F6/F7V	-0.56	0.20	4.03	7.96	0.11	0.25	thin
HD25173	F8V	-0.75	0.09	7.88	7.66	0.27	0.09	thin
HD25621	F6IV	-0.30	-0.05	3.52	7.36	0.12	0.26	thin
HD26491	G3V	-0.13	0.03	7.88	7.43	0.12	0.12	thin
HD26794	K3V	-0.09			9.06	0.20	0.13	thin
HD28946	K0	-0.12	0.09		8.14	0.21	0.01	thin
HD29645	G0V	0.01	-0.07	5.49	7.70	0.15	0.23	thin
HD30501	K0V	0.08	0.04		8.65	0.16	0.48	thin
HD30606	F8V	-0.08		2.99	7.84	0.07	0.11	thin
HD30743	F3/F5V	-0.52	0.02	4.14	8.15	0.11	0.21	thin
HD32147	K3V	0.31	-0.04		6.62	0.21	0.08	thin
HD33167	F5V	-0.36		2.66	7.61	0.12	0.00	thin
HD33256	F2V	-0.40	0.07	4.34	8.04	0.01	0.09	thin
HD33608	F5V	-0.03	0.05	3.29	7.61	0.08	0.07	thin
HD33811	G8IV/V	0.26		8.33	7.10	0.22	0.03	thin
HD35984	F6III	-0.47		1.47	7.50	0.07	0.05	thin
HD36066	F8V	-0.22		5.08	7.37	0.17	0.13	thin
HD36130	G0	0.15	-0.04	5.16	6.60	0.23	0.47	thin
HD37124	G4IV-V	-0.38		6.67	6.92	0.19	0.47	thin
HD37495	F5V	-0.11		2.37	7.68	0.07	0.16	thin
HD37655	G0V...	-0.25		6.34	7.91	0.24	0.35	thin
HD38007	G0	-0.30	0.04	7.02	7.85	0.20	0.21	thin
HD39283	A2V	-0.12	-0.09		8.32	0.08	0.05	thin
HD40105	K1V	-0.06		8.70	8.88	0.25	0.42	thin
HD40136	F1V	-0.13		1.22	8.59	0.07	0.09	thin
HD43318	F6V	-0.22	0.03	3.90	8.62	0.18	0.39	thin
HD43834	G5V	0.15		4.09	7.36	0.13	0.06	thin
HD43905	F5III...	0.27		1.29	7.49	0.07	0.03	thin
HD43947	F8V	-0.49	0.06	7.40	7.91	0.09	0.04	thin
HD45391	G0	-0.58	0.16	3.91	7.99	0.01	0.45	thin
HD45701	G3III/IV	0.15	0.01	7.44	7.63	0.10	0.05	thin
HD48565	F8	-0.57		8.71	8.31	0.11	0.27	thin
HD48938	F7V	-0.57	0.10	8.32	9.34	0.15	0.30	thin
HD50223	F5III	-0.29	0.01	4.17	7.89	0.11	0.16	thin
HD52265	G0III-IV	-0.10	-0.02	6.03	7.67	0.14	0.03	thin
HD52298	F5/F6V	-0.84	0.11	5.76	8.49	0.22	0.22	thin
HD53927	G5	-0.32	0.10		7.42	0.09	0.15	thin
HD54717	F5	-0.59	0.08	3.47	8.48	0.06	0.17	thin
HD55575	G0V	-0.38	0.08	7.72	8.59	0.22	0.54	thin
HD56513	G2V	-0.53	0.20		7.48	0.17	0.13	thin
HD58461	F3V	-0.42		3.99	8.43	0.06	0.28	thin
HD58551	F6V	-0.64	0.15	4.50	8.30	0.15	0.26	thin
HD59380	F8V	-0.29	0.10	4.34	8.36	0.04	0.24	thin
HD60532	F6V	-0.34	0.02	2.79	6.87	0.19	0.04	thin
HD61295	F6II	0.25		1.22	7.70	0.06	0.07	thin
HD61902	F5/F6w...	-0.75	0.05	6.44	8.88	0.25	0.46	thin
HD62644	G5IV	0.23	0.15	3.41	7.51	0.19	0.44	thin
HD63333	F5	-0.53	0.08	5.64	8.51	0.07	0.28	thin
HD65486	K3V	-0.24		15.51	8.03	0.13	0.25	thin



**Table 2.** (continued)

Name	Sp. type	[Fe/H]	[Ca/Fe]	age (Gyr)	$R$ (kpc)	$e$	$z_{\max}$ (kpc)	population
HD66011	G0IV	0.25		2.60	8.39	0.05	0.11	thin
HD66573	G0	-0.57	0.20	11.31	8.71	0.16	0.39	thin
HD67228	G2IV	0.18	-0.01	5.98	8.53	0.14	0.12	thin
HD67458	G2V	-0.24		3.82	8.41	0.22	0.21	thin
HD67483	F3V	-0.32		1.56	8.26	0.07	0.01	thin
HD68456	F5V	-0.36	0.08	3.99	7.82	0.10	0.34	thin
HD69830	K0V	0.06	0.04		6.59	0.26	0.05	thin
HD69897	F6V	-0.36	0.09	4.45	7.07	0.14	0.15	thin
HD70110	F9V	-0.02	0.02	4.45	7.60	0.07	0.09	thin
HD71030	F6V	-0.27		3.72	7.11	0.17	0.23	thin
HD72673	K0V	-0.26			8.76	0.21	0.23	thin
HD72769	K1IV:+...	0.27		9.08	8.37	0.14	0.21	thin
HD73524	G1V	0.09		4.36	8.51	0.08	0.28	thin
HD75289	G0Ia0:	-0.04	0.05	5.47	7.73	0.10	0.18	thin
HD75332	F7Vn	-0.15	0.02	5.92	7.85	0.02	0.01	thin
HD75732	G8V	0.29	0.00	14.50	7.68	0.10	0.02	thin
HD76151	G3V	0.07	-0.06	3.04	7.64	0.11	0.06	thin
HD76292	F3III	-0.22		1.46	7.86	0.09	0.01	thin
HD78234	F2V	-0.32		1.31	7.77	0.15	0.03	thin
HD79601	G2V	-0.67	0.20	11.50	7.22	0.11	0.35	thin
HD79765	A3	-0.24		1.40	7.86	0.17	0.27	thin
HD80218	F5	-0.43	0.10	5.38	7.70	0.05	0.32	thin
HD83443	K0V	0.38	-0.14	10.89	7.34	0.13	0.07	thin
HD83951	F3V	0.03	0.05	1.36	7.82	0.05	0.04	thin
HD83962	F3Vn	0.00			8.12	0.03	0.41	thin
HD84737	G2V	0.09	0.00	6.65	8.11	0.07	0.28	thin
HD85091	F8	-0.38	-0.02	9.87	7.24	0.21	0.12	thin
HD87141	F5V	-0.09	-0.06	2.71	8.08	0.05	0.10	thin
HD87838	G0	-0.58	0.13	6.44	8.19	0.25	0.22	thin
HD88725	G1V	-0.72	0.40	10.31	7.66	0.27	0.23	thin
HD88737	F9V	0.02	-0.06	2.69	7.36	0.11	0.03	thin
HD88986	G0V	-0.04	0.01	8.35	7.56	0.07	0.29	thin
HD89449	F6IV	-0.13		3.40	7.39	0.08	0.06	thin
HD89744	F7V	-0.03	-0.07	3.40	7.30	0.10	0.09	thin
HD89948	G8III+...	-0.13	0.15	2.02	7.43	0.08	0.27	thin
HD91280	F6/F7V	-0.12		3.67	8.72	0.08	0.13	thin
HD91345	G0w...	-1.01			6.91	0.16	0.08	thin
HD91347	F8	-0.62	0.06	6.64	9.74	0.24	0.04	thin
HD91752	F3V	-0.48	0.01	3.93	8.18	0.09	0.12	thin
HD93765	F5V	-0.46		1.61	8.60	0.07	0.09	thin
HD94444	F8IV-V	-0.61		7.48	7.56	0.18	0.25	thin
HD94835	G0	0.04	-0.03	5.25	6.56	0.22	0.07	thin
HD95128	G0V	0.01	0.04	6.92	8.17	0.05	0.09	thin
HD95456	F8V	-0.13		4.85	8.38	0.05	0.15	thin
HD97320	G1V-VI	-1.17	0.17		8.04	0.26	0.43	thin
HD98560	F6IV	-0.20		4.03	7.47	0.14	0.06	thin
HD98991	F3IV	-0.16	0.00	2.07	7.25	0.17	0.13	thin
HD99747	F5V	-0.62	0.10	2.94	9.14	0.13	0.33	thin
HD99984	F4V	-0.32	0.03	2.46	8.73	0.08	0.38	thin
HD100219	F7V	-0.15		4.85	7.80	0.04	0.13	thin
HD100446	F8	-0.53	0.08	8.55	6.72	0.21	0.05	thin
HD100563	F5V	-0.10	0.03	3.12	7.57	0.06	0.04	thin
HD101132	F1III	-0.17		1.39	8.20	0.06	0.01	thin
HD101227	G0	-0.40			8.08	0.10	0.06	thin
HD101242	G5	0.03	-0.04	7.96	6.86	0.20	0.06	thin
HD102365	G3/G5V	-0.26	0.17	6.12	7.23	0.20	0.13	thin
HD103026	F8V	-0.30		5.62	6.98	0.19	0.16	thin
HD104731	F6V	-0.26	0.08	2.35	7.91	0.19	0.15	thin
HD105837	G0/G1V	-0.50	0.18	5.43	8.43	0.08	0.49	thin

**Table 2.** (continued)

Name	Sp. type	[Fe/H]	[Ca/Fe]	age (Gyr)	$R$ (kpc)	$e$	$z_{\max}$ (kpc)	population
HD106156	G8V	0.13	0.08	4.55	7.67	0.20	0.17	thin
HD107113	F4V	-0.69	0.09	5.41	8.98	0.17	0.12	thin
HD107213	F8Vs	-0.04	-0.01	3.72	6.82	0.18	0.08	thin
HD108076	G0V	-0.96		6.04	7.37	0.29	0.09	thin
HD108954	F9V	-0.19	0.01	3.81	8.60	0.08	0.26	thin
HD109358	G0V	-0.19	-0.01	4.05	8.15	0.07	0.09	thin
HD110010	G0	0.18	-0.01	6.39	7.49	0.07	0.09	thin
HD112164	G2IV	0.25	-0.05	3.42	6.51	0.23	0.27	thin
HD117361	F0IV	-0.27		1.96	7.86	0.12	0.09	thin
HD117718	F5IV	-0.16		2.23	8.36	0.06	0.00	thin
HD117939	G3V	-0.15		7.17	7.87	0.38	0.32	thin
HD118216	F2IV SB	-0.30		1.65	8.72	0.11	0.13	thin
HD118244	F5V	-0.57	0.17	4.90	8.02	0.15	0.00	thin
HD118646	F3V	-0.13		1.73	7.46	0.07	0.03	thin
HD119288	F3Vp	-0.36	0.06	2.51	6.85	0.21	0.04	thin
HD120559	G5V	-0.88	0.16		6.88	0.18	0.35	thin
HD120690	G5V	0.04		6.46	6.82	0.19	0.03	thin
HD120691	F7/F8V	-0.29		4.31	7.75	0.32	0.26	thin
HD121560	F6V	-0.45	0.04	4.99	7.61	0.08	0.03	thin
HD122066	F6V	-0.06		2.08	7.09	0.17	0.10	thin
HD122742	G8V	-0.01		6.62	7.84	0.07	0.21	thin
HD123710	G5	-0.60	0.10	4.25	8.01	0.08	0.07	thin
HD123999	F9IVw	-0.13		2.13	7.97	0.05	0.19	thin
HD124425	F7Vw	-0.16		2.39	8.87	0.24	0.18	thin
HD124553	F9V	-0.07		5.21	7.80	0.18	0.12	thin
HD124570	F6IV	-0.10	-0.12	4.03	7.27	0.14	0.22	thin
HD124850	F7V	-0.29	-0.01	2.83	7.21	0.16	0.08	thin
HD125111	F2IV	-0.34	-0.06	2.14	7.35	0.10	0.07	thin
HD125406	F5	-0.19		2.28	7.65	0.07	0.04	thin
HD126053	G1V	-0.35		5.20	7.83	0.10	0.41	thin
HD126141	F5V	-0.17	0.04	1.73	7.88	0.06	0.08	thin
HD126614	K0	0.55	-0.28	9.90	6.72	0.23	0.54	thin
HD127334	G5V	0.16	0.04	9.46	8.21	0.12	0.04	thin
HD127486	F6IV-V	-0.10		1.37	7.43	0.09	0.22	thin
HD127739	F2IV	0.08		1.45	7.76	0.07	0.09	thin
HD127986	F8IVw	-0.13		2.23	7.78	0.10	0.12	thin
HD128385	F5	-0.37	0.08	2.23	8.99	0.11	0.15	thin
HD128582	F7V	-0.07		4.28	7.28	0.13	0.17	thin
HD130551	F8V	-0.67	0.10	4.32	8.24	0.15	0.27	thin
HD130817	F2V	-0.40	0.14	2.31	7.31	0.17	0.06	thin
HD130945	F7IVw	-0.05	0.04	2.58	7.83	0.07	0.08	thin
HD131117	G0/G1V	-0.05	0.02	5.06	7.29	0.19	0.20	thin
HD132254	F7V	-0.07	0.11	3.83	7.90	0.12	0.06	thin
HD133484	F6IV	-0.09		2.92	7.57	0.07	0.01	thin
HD134169	G1Vm	-0.82	0.15	9.87	8.22	0.08	0.21	thin
HD134987	G5V	0.36	0.06	5.53	7.06	0.14	0.30	thin
HD136064	F9IV	-0.17	0.00	4.87	7.68	0.23	0.22	thin
HD136351	F8V	-0.13	0.00	2.63	7.58	0.07	0.01	thin
HD136359	F7V	-0.23		2.98	7.69	0.04	0.11	thin
HD136751	F4IVs	0.08		1.24	8.11	0.12	0.05	thin
HD137052	F5IV	-0.25	0.04	2.69	7.48	0.07	0.08	thin
HD137510	G0V	0.12	-0.05	4.56	7.94	0.01	0.10	thin
HD138290	F4Vw	-0.21	-0.07	1.98	8.41	0.06	0.01	thin
HD138776	K0	0.48	-0.33	5.14	6.67	0.20	0.11	thin
HD139211	F6V	-0.20		4.65	7.85	0.09	0.08	thin
HD139457	F8V	-0.54	0.15	6.99	7.91	0.31	0.14	thin
HD139798	F2V	-0.13		1.11	8.40	0.11	0.03	thin
HD142529	F1IV	-0.46		2.21	7.23	0.11	0.03	thin
HD142640	F6V	-0.09		1.84	7.96	0.05	0.22	thin

**Table 2.** (continued)

Name	Sp. type	[Fe/H]	[Ca/Fe]	age (Gyr)	$R$ (kpc)	$e$	$z_{\max}$ (kpc)	population
HD144172	F8	-0.58	0.01	4.23	7.87	0.09	0.03	thin
HD144253	K3/K4V	-0.03			8.10	0.17	0.23	thin
HD144284	F8IV-V	-0.07		2.73	7.71	0.11	0.14	thin
HD144585	G5V	0.30	-0.03	5.43	7.57	0.08	0.28	thin
HD144628	K3V	-0.33			7.97	0.15	0.32	thin
HD145675	K0V	-0.00			8.09	0.11	0.05	thin
HD150012	F5III-IV	-0.08	0.26	1.87	7.32	0.09	0.06	thin
HD150177	F3V	-0.68	0.00	4.29	7.46	0.07	0.22	thin
HD150281	K0	-0.02		16.72	8.36	0.26	0.04	thin
HD151044	F8V	-0.01		2.35	8.19	0.08	0.19	thin
HD151769	F7IV	-0.16	-0.02	1.51	8.22	0.06	0.17	thin
HD152830	F5II	-0.13	0.15	1.59	8.19	0.06	0.14	thin
HD153597	F6Vvar	-0.35	0.01	3.46	8.00	0.03	0.25	thin
HD154153	A4III	-0.32		1.33	8.96	0.12	0.11	thin
HD154345	G8V	-0.15			8.31	0.21	0.38	thin
HD154417	F9V	-0.17	0.03	3.86	7.29	0.10	0.16	thin
HD155078	F5IV	-0.20		1.80	7.89	0.05	0.16	thin
HD155646	F6III	-0.41		2.61	8.86	0.23	0.15	thin
HD156098	F6V	-0.11	0.05	2.14	7.63	0.10	0.19	thin
HD157089	F9V	-0.59	0.18	7.83	8.56	0.48	0.04	thin
HD157347	G5IV	0.05	0.06	5.07	7.71	0.06	0.15	thin
HD157373	F6V	-0.61	-0.05	4.30	10.44	0.24	0.13	thin
HD157466	F8V	-0.56	0.03	4.03	8.83	0.16	0.08	thin
HD157856	F3V	-0.31	0.03	1.99	8.78	0.10	0.11	thin
HD157881	K7V	-0.20			6.71	0.20	0.04	thin
HD157919	F3III	0.20	-0.08	1.26	7.76	0.15	0.08	thin
HD157968	F7V	-0.12		3.44	7.81	0.08	0.19	thin
HD159222	G5V	0.05		4.56	6.81	0.19	0.05	thin
HD159332	F6V	-0.36	-0.02	3.93	6.85	0.18	0.23	thin
HD160032	F3IV	-0.37	0.06	3.30	7.91	0.02	0.15	thin
HD160691	G5V	0.28		8.41	7.95	0.01	0.02	thin
HD160915	F6/F7V	-0.31	0.01	3.51	8.06	0.06	0.13	thin
HD160933	F9V	-0.38	0.04	5.47	7.09	0.24	0.10	thin
HD161023	F0V	-0.41	0.03	1.87	7.37	0.09	0.07	thin
HD161149	F5II	0.55			7.80	0.10	0.04	thin
HD162396	F8V	-0.46	0.05	6.13	7.89	0.04	0.29	thin
HD162917	F4IV-V	-0.15	-0.01	2.01	7.65	0.08	0.21	thin
HD163989	F6IV-Vs	-0.32	0.03	2.94	7.45	0.10	0.17	thin
HD164259	F3V	-0.21		2.05	7.87	0.09	0.20	thin
HD165499	G0V	-0.11		6.47	8.37	0.14	0.10	thin
HD167588	F8V	-0.35	0.07	6.28	7.86	0.16	0.13	thin
HD167665	F8V	-0.31		5.07	7.93	0.05	0.24	thin
HD168009	G2V	-0.02	0.06	7.01	6.51	0.23	0.18	thin
HD168151	F5V	-0.37	0.06	4.17	7.86	0.02	0.55	thin
HD169830	F8V	-0.08	-0.06	3.99	8.29	0.04	0.11	thin
HD171620	F6p	-0.63		6.88	8.83	0.19	0.41	thin
HD173093	F7V	-0.23		2.07	7.22	0.19	0.08	thin
HD174912	F8	-0.64	0.14	9.71	8.63	0.08	0.46	thin
HD175225	G9IVa	-0.01		4.82	8.19	0.06	0.26	thin
HD175317	F5/F6IV/V	-0.15	0.00	2.29	7.07	0.15	0.04	thin
HD176095	F5IV	-0.23	0.20	2.70	7.42	0.10	0.06	thin
HD176377	G0	-0.35		2.05	7.52	0.11	0.02	thin
HD177565	G8V	0.06	0.03	5.90	7.46	0.23	0.12	thin
HD178089	F2V	0.00	0.08		7.66	0.13	0.01	thin
HD178476	F3V	-0.25			7.59	0.10	0.01	thin
HD178596	F0III-IV	0.03		1.43	6.98	0.16	0.02	thin
HD180134	F7V	-0.30		4.43	7.97	0.06	0.09	thin
HD181096	F6IV:	-0.37	0.03	4.04	7.25	0.20	0.23	thin
HD182101	F6V	-0.36	0.09	3.27	8.20	0.05	0.17	thin

Table 2. (continued)

Name	Sp. type	[Fe/H]	[Ca/Fe]	age (Gyr)	$R$ (kpc)	$\epsilon$	$z_{\max}$ (kpc)	population
HD182274	F6V	-0.34	-0.08	1.73	7.34	0.09	0.05	thin
HD182900	F6III	-0.09		1.99	7.77	0.08	0.13	thin
HD184601	G0	-0.81	0.22	9.51	6.68	0.27	0.11	thin
HD184663	F6IV	-0.29		2.29	8.67	0.08	0.10	thin
HD184960	F7V	-0.32		3.86	8.37	0.10	0.08	thin
HD186379	F8V	-0.53	0.10	7.25	7.53	0.15	0.49	thin
HD187098	F3V	-0.38		2.84	7.62	0.11	0.09	thin
HD187637	F5	-0.33	0.04	4.78	8.38	0.12	0.50	thin
HD188376	G3/G5III	-0.13		2.77	8.59	0.09	0.04	thin
HD188815	F6V	-0.66	0.04	5.24	8.81	0.09	0.09	thin
HD188985	F8/G0III:wp	-0.42		3.83	8.40	0.08	0.28	thin
HD189567	G2V	-0.25		7.99	7.54	0.21	0.54	thin
HD190009	F7V	-0.15		2.90	8.51	0.08	0.16	thin
HD190248	G5IV-Vvar	0.25	0.02	11.38	7.88	0.12	0.10	thin
HD191096	F4V	-0.18		1.74	7.78	0.04	0.15	thin
HD192310	K3V	-0.09		10.19	8.10	0.19	0.14	thin
HD192985	F5V:	-0.12	0.04	2.44	7.03	0.14	0.05	thin
HD193307	G2IV-V	-0.42	0.06	6.70	6.98	0.22	0.50	thin
HD195838	G0V	-0.25		5.28	8.01	0.10	0.26	thin
HD196378	F8V	-0.49	0.03	5.52	6.98	0.24	0.06	thin
HD196385	A9V	-0.34		1.27	7.96	0.06	0.06	thin
HD197373	F6IV	-0.31	0.13	2.35	7.66	0.06	0.21	thin
HD197692	F5V	-0.15	-0.03	2.26	8.21	0.10	0.10	thin
HD199623	F5IV-V	-0.46	0.11	4.88	9.13	0.12	0.37	thin
HD199684	F2V	-0.27		2.18	7.95	0.03	0.24	thin
HD199960	G1V	0.18	-0.05	6.47	7.46	0.07	0.04	thin
HD200163	F3V	-0.17		2.76	7.66	0.07	0.06	thin
HD202457	G5V	0.06		9.32	6.84	0.29	0.16	thin
HD202628	G5V	0.00			8.32	0.04	0.24	thin
HD203454	F8V	-0.26		4.18	8.23	0.09	0.13	thin
HD203608	F6V	-0.70	-0.00	4.37	10.23	0.22	0.16	thin
HD204121	F5V	-0.11	0.28	3.15	7.62	0.07	0.41	thin
HD204363	F7V	-0.43	0.14	4.26	8.89	0.14	0.31	thin
HD205156	G3V	-0.67		8.54	9.03	0.46	0.33	thin
HD205289	F5V	-0.39		2.42	8.55	0.08	0.07	thin
HD205294	F5V	-0.51	0.07	4.77	7.49	0.11	0.27	thin
HD205420	F7V	-0.14		2.53	8.47	0.08	0.16	thin
HD205582	G2V-VI	-0.63		7.25	8.50	0.24	0.42	thin
HD206860	G0V	-0.23	0.08	4.29	7.55	0.06	0.05	thin
HD207978	F6IV	-0.62	0.12	4.62	8.91	0.12	0.02	thin
HD209100	K5V	-0.23	-0.19		7.27	0.25	0.11	thin
HD209149	F5III	-0.32		2.74	8.42	0.05	0.27	thin
HD209458	F8	-0.06		5.72	7.63	0.05	0.09	thin
HD210277	G0	0.22		11.56	6.74	0.19	0.02	thin
HD210302	F6V	-0.11		3.18	8.04	0.09	0.04	thin
HD210464	F6/F7V	-0.18		2.62	7.58	0.08	0.05	thin
HD210631	G0	-0.38	0.30	8.96	8.34	0.22	0.24	thin
HD210848	F7II	0.06	-0.41	1.24	7.98	0.07	0.19	thin
HD211575	F3V	-0.15	-0.01	2.37	8.47	0.10	0.08	thin
HD211976	F6V	-0.39	0.23	3.43	8.54	0.07	0.02	thin
HD212487	F5IV:	-0.35		3.22	8.39	0.18	0.05	thin
HD212753	G5	-0.35			7.60	0.17	0.19	thin
HD213042	K4V	0.25	0.05		6.57	0.23	0.12	thin
HD214749	K4/K5V	0.12			8.00	0.03	0.07	thin
HD214759	G8/K0V	0.25		6.05	7.94	0.11	0.05	thin
HD216219	G0IIp	-0.39	0.14	2.75	7.87	0.04	0.02	thin
HD216385	F7IV	-0.37	0.02	4.49	8.18	0.15	0.34	thin
HD216435	G3IV	0.02		5.64	7.54	0.08	0.05	thin
HD216437	G4IV-V	0.22		7.02	8.65	0.08	0.05	thin

**Table 2.** (continued)

Name	Sp. type	[Fe/H]	[Ca/Fe]	age (Gyr)	$R$ (kpc)	$e$	$z_{\max}$ (kpc)	population
HD216756	F5II	-0.34		3.10	7.29	0.10	0.11	thin
HD217014	G5V	0.17	-0.05	6.34	7.33	0.09	0.24	thin
HD217107	G8IV	0.30	-0.12	9.47	7.99	0.03	0.17	thin
HD217877	F8V	-0.30		7.43	7.74	0.12	0.01	thin
HD218209	G6V	-0.52	0.26	6.15	6.99	0.26	0.09	thin
HD218235	F6Vs	-0.00		3.34	7.73	0.12	0.05	thin
HD218261	F7V	-0.19		4.25	7.74	0.08	0.06	thin
HD218470	F5V	-0.26	0.06	3.59	7.97	0.06	0.19	thin
HD218804	F5IV	-0.36	0.09	3.15	7.33	0.21	0.03	thin
HD219571	F1III	-0.30		2.57	8.37	0.07	0.14	thin
HD219693	F5V	-0.28		3.34	7.37	0.09	0.27	thin
HD220729	F4V	-0.11	0.08	2.08	8.65	0.08	0.27	thin
HD221970	F6V	-0.28		2.05	8.29	0.05	0.10	thin
HD222451	F1V	-0.18	0.14	2.23	7.70	0.12	0.03	thin
HD223421	F2IV	-0.35		2.03	9.15	0.13	0.01	thin
HD224022	F8IV	-0.07		5.70	7.77	0.12	0.05	thin
HD224087	G5	-0.25	0.05	12.26	6.98	0.19	0.16	thin
HD224617	F4IV	-0.27		1.37	7.56	0.06	0.11	thin
HD245	G2V	-0.66		11.91	5.70	0.43	0.55	thick
HD3628	G2V	-0.13	0.05	8.77	8.26	0.50	1.00	thick
HD3795	G3/G5V	-0.27		9.18	6.00	0.36	0.70	thick
HD4308	G3V	-0.25		8.60	5.72	0.47	0.27	thick
HD4597	F7/F8V	-0.51		5.09	7.49	0.30	0.63	thick
HD6434	G3IV	-0.59	0.18	10.99	6.87	0.37	0.04	thick
HD11007	F8V	-0.29	0.07	6.93	9.13	0.16	0.66	thick
HD13445	K0V	-0.11	-0.02		6.62	0.38	0.24	thick
HD14056	G5	-0.73	0.34	13.71	6.29	0.43	1.69	thick
HD16784	F8V	-0.71		9.34	6.35	0.55	0.68	thick
HD17820	G5	-0.69	0.37	11.70	5.81	0.43	1.17	thick
HD18907	G8/K0V	-0.12	0.79	4.94	6.80	0.25	0.75	thick
HD20512	G5	0.02	0.12	6.66	6.70	0.21	0.66	thick
HD20794	G8V	-0.13			6.08	0.41	0.25	thick
HD21543	G2V-VI	-0.52	0.23	6.77	5.99	0.38	0.11	thick
HD22309	G0	-0.47	0.02	9.60	8.53	0.24	0.79	thick
HD22879	F9V	-0.77	0.20	7.99	6.48	0.43	0.47	thick
HD27126	F5	-0.25	0.23		7.14	0.22	0.79	thick
HD29528	K0	0.09	0.11	16.30	6.43	0.26	0.48	thick
HD30562	F8V	0.08	-0.02	6.64	6.33	0.31	0.17	thick
HD31128	F3/F5Vw	-1.46			5.85	0.42	0.27	thick
HD37986	G8/K0IV	0.27	-0.10	10.74	6.44	0.26	0.03	thick
HD44594	G4V	0.09	-0.02	6.45	6.37	0.28	0.01	thick
HD45067	F8V	-0.29		5.77	6.45	0.24	0.21	thick
HD45205	G0	-0.88		13.43	6.78	0.32	0.60	thick
HD46341	G0	-0.80		8.87	7.30	0.11	0.97	thick
HD50806	G3/G5V	0.21		9.04	5.86	0.38	0.00	thick
HD51929	G2IV	-0.63	0.14	10.01	6.88	0.40	0.13	thick
HD52711	G4V	-0.21		6.68	6.16	0.30	0.03	thick
HD56274	G5V	-0.63		3.51	8.71	0.24	0.78	thick
HD62301	F8V	-0.68	0.14	10.18	5.58	0.44	0.17	thick
HD63077	G0V	-0.67	0.17	12.24	7.69	0.45	0.71	thick
HD63598	G2V	-0.86	0.18	10.54	6.06	0.35	0.10	thick
HD65583	G8V	-0.61			5.95	0.35	0.29	thick
HD74011	F8	-0.65	0.23	10.73	6.36	0.27	0.33	thick
HD76932	F7/F8IV/V	-0.85	0.24	9.29	6.04	0.36	1.17	thick
HD78558	G3V	-0.38	0.17	9.97	6.59	0.30	0.83	thick
HD88261	G3V	-0.63		7.87	6.15	0.48	0.84	thick
HD88446	Gp	-0.48	-0.05	7.45	5.75	0.41	0.10	thick
HD89707	G1V	-0.28	0.02	3.42	7.20	0.23	0.87	thick
HD96094	G0	-0.55	0.03	8.73	7.14	0.30	0.63	thick

Table 2. (continued)

Name	Sp. type	[Fe/H]	[Ca/Fe]	age (Gyr)	$R$ (kpc)	$e$	$z_{\max}$ (kpc)	population
HD99109	K0	0.45	0.00	14.84	6.35	0.26	0.11	thick
HD103932	K4V	0.16	-0.28		6.21	0.29	0.01	thick
HD108309	G5IV-V	0.22	-0.01	8.04	6.46	0.29	0.04	thick
HD108564	K2V	-0.63			6.10	0.34	0.86	thick
HD110897	G0V	-0.70	0.08	6.81	8.91	0.14	1.37	thick
HD114606	G1V	-0.57	0.21	11.04	8.95	0.45	1.19	thick
HD114762	F9V	-0.75	0.21	8.43	6.67	0.33	0.94	thick
HD118659	G5	-0.56	0.03	9.63	7.34	0.26	0.79	thick
HD125968	G3/G5V	0.11	-0.02	6.78	5.73	0.40	0.16	thick
HD126511	G5	0.06	-0.07	3.45	6.50	0.24	0.17	thick
HD126512	F9V	-0.59	0.19	9.86	6.58	0.42	1.14	thick
HD126681	G3V	-1.13	0.24		6.99	0.15	0.99	thick
HD128429	F5V	-0.31	0.16	3.16	8.70	0.44	0.86	thick
HD131653	G5	-0.43	0.23		6.24	0.31	0.85	thick
HD134088	G0V:	-0.80			6.49	0.24	0.82	thick
HD136352	G2V	-0.27	0.17	7.52	7.57	0.36	0.61	thick
HD136834	K3V	0.00	-0.04		6.47	0.24	0.12	thick
HD142373	F9V	-0.48	0.13	7.43	8.91	0.14	0.93	thick
HD145417	K0V	-1.12			5.95	0.38	0.26	thick
HD148211	F8/G0V	-0.65	0.15	6.05	5.73	0.40	0.05	thick
HD149996	G0	-0.53	0.29	6.08	6.17	0.44	0.37	thick
HD158809	G0	-0.59	0.29	7.70	6.28	0.30	1.05	thick
HD165401	G0V	-0.50	0.15	5.84	6.16	0.39	0.38	thick
HD166913	F6V	-1.40	0.46		7.04	0.18	1.09	thick
HD171999	G5	0.02	-0.02	10.88	5.96	0.34	0.06	thick
HD175518	K0IV-V	0.19	0.02		8.60	5.79	0.39	thick
HD181720	G1V	-0.66		10.14	5.82	0.44	0.35	thick
HD190360	G6IV+...	0.14		12.11	6.98	0.15	0.76	thick
HD192718	F8	-0.56		5.70	6.78	0.41	0.48	thick
HD195987	G9V	-0.66			8.30	0.07	0.62	thick
HD199288	G0V	-0.71		8.41	5.78	0.41	0.67	thick
HD199289	F5V	-0.95	0.17	7.11	6.45	0.28	0.13	thick
HD200580	F9V	-0.52	0.14	7.11	6.79	0.42	0.18	thick
HD200973	F5V	-0.67	0.15	4.70	9.94	0.23	0.80	thick
HD205650	F6V	-1.02			6.64	0.44	0.21	thick
HD208998	G0V	-0.41		7.18	6.14	0.31	0.45	thick
HD210483	G1V	-0.20	0.00	9.07	6.34	0.36	0.10	thick
HD210752	G0	-0.73	0.07	6.10	9.59	0.17	0.89	thick
HD210918	G5V	-0.02		7.33	5.93	0.38	0.02	thick
HD212029	G0	-0.94	0.30	12.67	6.40	0.38	0.42	thick
HD213941	G5V	-0.34		8.56	6.44	0.24	0.82	thick
HD215257	F8	-0.74	0.13	6.82	9.26	0.21	0.76	thick
HD216179	G	-0.62	0.31	6.41	6.03	0.36	0.76	thick
HD218502	F3:w	-1.93	0.19	11.41	5.64	0.42	0.01	thick
HD233832	K0V	-0.44		7.88	8.22	0.31	2.68	thick
HD19445	A4p	-1.72	0.46	9.56	6.83	0.66	1.07	halo
HD25329	K1V...	-1.36	0.31		4.40	0.83	0.57	halo
HD29907	sdG4	-1.64			21.86	0.94	2.39	halo
HD34328	sdG5	-1.56	0.14		8.02	0.68	2.61	halo
HD51754	G0	-0.68		7.13	7.25	0.76	0.13	halo
HD59374	F8V	-0.82	0.30		5.41	0.50	0.04	halo
HD69611	F8	-0.58	0.21	9.44	5.03	0.61	0.47	halo
HD84937	sdF5	-2.33	0.41	14.36	1002.87	1.00	0.05	halo
HD94028	F4V	-1.31	0.19		5.08	0.58	0.20	halo
HD94518	G2V	-0.45		8.24	5.26	0.57	1.22	halo
HD102158	G2V	-0.46		11.16	5.86	0.56	0.23	halo
HD102200	F2V	-1.20			5.62	0.60	0.16	halo
HD108754	G7V	-0.58	0.21	8.39	5.12	0.56	1.11	halo
HD113083	G1V	-0.80		8.58	346.17	1.00	1.78	halo

**Table 2.** (continued)

Name	Sp. type	[Fe/H]	[Ca/Fe]	age (Gyr)	$R$ (kpc)	$e$	$z_{\max}$ (kpc)	population
HD121004	G11V-V	-0.73	0.19	4.19	12.15	0.97	5.05	halo
HD121849	G5V	-0.28			5.51	0.45	0.10	halo
HD134113	F9V	-0.83	0.36	12.20	5.77	0.58	0.42	halo
HD140283	sdF3	-1.96	0.21	11.38	28.14	0.99	4.81	halo
HD148816	F8V	-0.74	0.33	8.36	5.02	0.90	2.88	halo
HD155918	G2V	-0.65		10.68	5.35	0.50	1.15	halo
HD160693	G0V	-0.70		9.07	8.59	0.73	2.07	halo
HD176021	G0/G1III	-0.66	-0.02	12.00	5.71	0.65	0.30	halo
HD184499	G0V	-0.67	0.18	11.73	4.93	0.68	1.34	halo
HD188510	G5Vwe	-1.50			6.55	0.60	1.18	halo
HD193901	F7V	-1.25	0.12		337.19	1.00	0.13	halo
HD194598	F7V-VI	-1.10	0.28	7.66	4.59	0.82	0.41	halo
HD196892	G2w...	-1.00	0.22	6.55	5.25	0.53	0.33	halo
HD198245	sdK0	-0.78		10.43	5.26	0.52	0.25	halo
HD201891	F8V-VI	-0.95	0.18	8.03	5.99	0.54	0.75	halo
HD204155	G5	-0.80	0.29	10.66	5.32	0.51	0.47	halo
HD221830	F9V	-0.46	0.24	10.06	5.69	0.47	1.02	halo

**Table 3.** The sample stars with *ubvy*- $H\beta$  photometry.

Name	Sp. type	[Fe/H]	age (Gyr)	$R$ (kpc)	$e$	$z_{\max}$ (kpc)	population
BD -13 2948	K0	-0.51	4.52	9.70	0.27	0.18	thin
BD -11 220	G0	-0.51	5.62	7.01	0.34	0.35	thin
BD 4 415	K3V	-0.41		7.76	0.45	0.28	thin
BD 7 385	K8	-0.28		7.59	0.09	0.52	thin
BD 9 1627	K2V	-0.08	7.98	7.69	0.33	0.01	thin
BD 13 374	K0	-0.10	12.03	7.30	0.22	0.08	thin
BD 16 71	K3	-0.24		6.96	0.16	0.09	thin
BD 16 5012	K2	-0.28		7.70	0.10	0.17	thin
BD 19 5185	G0	-0.05		8.84	0.25	0.38	thin
BD 20 17	K3	-0.23		7.26	0.21	0.01	thin
BD 20 1828	K0	-0.19	18.33	7.12	0.19	0.15	thin
BD 21 55	K5	-0.25	2.19	7.83	0.05	0.42	thin
BD 21 2442	K0	-0.29		7.44	0.31	0.30	thin
BD 24 4563	G0	0.05	7.03	8.90	0.25	0.28	thin
BD 24 4592	K2	-0.15		6.90	0.30	0.19	thin
BD 25 77	K0	-0.23		7.18	0.19	0.07	thin
BD 29 1539	G5	0.08		6.86	0.17	0.24	thin
BD 30 228	K2	-0.02		7.58	0.20	0.24	thin
BD 30 516	K2	-0.25	6.66	7.18	0.16	0.32	thin
BD 32 1561	K2V	-0.29	8.57	8.67	0.09	0.27	thin
BD 33 4737	K0	-0.04		7.20	0.26	0.34	thin
BD 35 355	K2	-0.34		7.69	0.10	0.44	thin
BD 35 1484	G0	-0.19		6.68	0.24	0.20	thin
BD 43 395	K2	-0.34		8.01	0.25	0.10	thin
BD 43 699	K2	-0.32		7.51	0.09	0.25	thin
BD 45 564	K1	-0.13	12.19	6.84	0.21	0.32	thin
BD 48 3755	G8	-0.54		9.06	0.26	0.18	thin
HD203	F2IV	-0.18	1.27	7.72	0.04	0.01	thin
HD268	F5V	-0.37	3.26	6.84	0.18	0.20	thin
HD276	F5IV-V	-0.33	2.22	7.21	0.11	0.18	thin
HD373	F5	-0.47		7.95	0.05	0.10	thin
HD900	F2V	-0.20	1.70	8.18	0.02	0.14	thin
HD1000	F7V	-0.22	4.26	7.06	0.23	0.17	thin
HD1273	G2V	-0.50	9.53	8.40	0.10	0.02	thin
HD1343	F3V	-0.38	2.14	8.16	0.03	0.05	thin
HD1352	F6V	-0.28	3.02	7.58	0.11	0.11	thin
HD1368	F9V	-0.56		8.71	0.28	0.42	thin
HD1461	G0V	0.15	5.75	7.07	0.15	0.06	thin
HD1683	F6V	-0.31	2.14	8.17	0.12	0.11	thin
HD1779	G5V	-0.40	10.27	7.48	0.34	0.01	thin
HD1887	K0	-0.22		7.24	0.25	0.04	thin
HD1966	F5	-0.43	3.47	7.73	0.04	0.18	thin
HD1980	F6V	-0.37	5.03	8.07	0.07	0.01	thin
HD2381	F2V	-0.24	1.56	8.08	0.04	0.19	thin
HD2477	F5V	-0.44	5.01	7.73	0.04	0.09	thin
HD2629	F0	-0.35	1.15	6.90	0.17	0.11	thin
HD2663	F8	-0.60	5.25	7.76	0.15	0.13	thin
HD2916	F3III/IV	-0.26	2.05	7.66	0.11	0.14	thin
HD3302	F6V	-0.16	3.06	7.58	0.07	0.05	thin
HD3404	G2V	0.13	5.54	7.81	0.08	0.27	thin
HD3410	G0	-0.19	2.13	7.78	0.03	0.04	thin
HD3440	F6V:	-0.48	8.03	7.68	0.14	0.07	thin
HD3581	F3IV/V	-0.17	2.15	8.48	0.12	0.29	thin
HD3689	F5IV-V	-0.38	4.24	7.70	0.23	0.00	thin
HD3726	F6V	-0.59	6.79	7.14	0.15	0.06	thin
HD3735	F7V	-0.51	5.91	6.81	0.21	0.20	thin
HD3861	F5	-0.15	4.15	8.00	0.12	0.14	thin
HD3914	F5	-0.25	2.49	8.58	0.07	0.15	thin
HD4089	F6V	-0.20	2.64	7.99	0.01	0.11	thin



**Table 3.** (continued)

Name	Sp. type	[Fe/H]	age (Gyr)	$R$ (kpc)	$e$	$z_{\max}$ (kpc)	population
HD4247	F0V	-0.40	1.54	8.83	0.10	0.06	thin
HD4304	F7III	-0.10	3.60	7.32	0.13	0.09	thin
HD4309	F8V	-0.12	2.83	6.76	0.19	0.00	thin
HD4975	G1V	-0.11	5.88	7.84	0.04	0.10	thin
HD5057	F6V	-0.20	3.61	8.13	0.11	0.25	thin
HD5065	G0	-0.26	7.29	7.13	0.25	0.59	thin
HD5072	F7IV	-0.47	8.63	8.19	0.03	0.56	thin
HD5388	F6V	-0.39	4.58	7.35	0.21	0.18	thin
HD5494	F7V	-0.27	5.01	8.14	0.13	0.38	thin
HD5508	F7/F8V	-0.66	7.62	9.11	0.13	0.55	thin
HD5728	F5	-0.23	2.15	8.39	0.05	0.06	thin
HD6225	F8	-0.37	2.59	8.04	0.08	0.11	thin
HD6301	F7IV-V	-0.25	3.85	7.56	0.06	0.14	thin
HD6312	G0	-0.40	6.16	6.63	0.23	0.40	thin
HD6402	F6V	-0.25	4.87	7.94	0.08	0.09	thin
HD6493	F3V	-0.32	2.21	8.23	0.06	0.03	thin
HD6594	G2V	-0.12	6.34	8.33	0.06	0.23	thin
HD6656	F2	-0.83	3.21	7.16	0.20	0.01	thin
HD6680	F5IV	-0.15	2.14	7.76	0.10	0.03	thin
HD6706	F7IV	-0.13	1.86	7.89	0.08	0.13	thin
HD6715	G5	-0.19	11.35	6.73	0.21	0.24	thin
HD6946	F8V	-0.45		7.16	0.18	0.07	thin
HD7238	F5Vs	-0.38	2.30	7.52	0.18	0.12	thin
HD7257	F3V	-0.33	3.10	8.44	0.10	0.03	thin
HD7259	F5IV	-0.17	2.55	7.33	0.10	0.11	thin
HD7361	F0III	-0.17		7.89	0.01	0.01	thin
HD7382	F3/F5V	-0.16	1.04	7.74	0.08	0.02	thin
HD7829	F3V	-0.23		8.29	0.10	0.08	thin
HD8076	G2V	-0.03	3.03	8.57	0.07	0.08	thin
HD8100	G0	0.01	8.38	7.86	0.18	0.08	thin
HD8262	G3V	-0.22	3.72	7.16	0.19	0.15	thin
HD8442	F0	-0.24	2.28	7.46	0.08	0.14	thin
HD8723	F2V:	-0.31	2.29	8.21	0.06	0.14	thin
HD8774	F7IV	-0.05	2.31	7.91	0.07	0.02	thin
HD8826	F0	-0.19	2.25	7.51	0.08	0.21	thin
HD8895	F3IV	-0.23	2.26	8.44	0.05	0.09	thin
HD8909	F5	-0.37	5.59	7.55	0.08	0.05	thin
HD8941	F8IV-V	-0.10	4.52	7.66	0.06	0.02	thin
HD8985	F6/F7V	-0.20	3.70	8.03	0.08	0.21	thin
HD8995	F5	-0.42	2.34	6.94	0.15	0.09	thin
HD9061	F3/F5V	-0.33	2.49	7.69	0.05	0.09	thin
HD9172	F0	-0.42	2.59	8.44	0.06	0.30	thin
HD9468	F5V	-0.57	4.01	7.22	0.17	0.12	thin
HD9544	F4V	-0.30	1.71	7.85	0.11	0.13	thin
HD9896	F2V	-0.16	1.45	7.13	0.15	0.20	thin
HD10023	F0	-0.14		7.96	0.10	0.04	thin
HD10126	G8V	0.00	8.62	8.63	0.27	0.14	thin
HD10481	F3/F5IV/V	-0.17	2.12	8.22	0.03	0.05	thin
HD10647	F8V	-0.24	4.63	7.59	0.06	0.01	thin
HD10800	G2V	-0.08	7.08	8.23	0.04	0.01	thin
HD10863	F2V	-0.20	1.06	7.57	0.06	0.05	thin
HD11151	F5V	-0.03	2.02	7.46	0.08	0.14	thin
HD11152	F0	-0.16	1.95	6.72	0.21	0.00	thin
HD11581	F7V	-0.45	5.59	7.62	0.18	0.03	thin
HD11597	F5V	-0.23	2.13	8.01	0.08	0.12	thin
HD12661	K0	0.22	9.28	7.50	0.22	0.07	thin
HD12724	G8V	-0.20	1.65	6.71	0.28	0.15	thin
HD12894	F2V	-0.23	1.58	7.72	0.04	0.11	thin
HD13024	F0	-0.18	1.75	8.00	0.11	0.19	thin

**Table 3.** (continued)

Name	Sp. type	[Fe/H]	age (Gyr)	$R$ (kpc)	$e$	$z_{\max}$ (kpc)	population
HD13133	F5V	-0.69	4.92	8.47	0.10	0.36	thin
HD13201	F5V	-0.43	4.98	7.17	0.12	0.19	thin
HD13228	F8	-0.32	4.16	8.62	0.15	0.00	thin
HD13540	F5	-0.63	2.58	8.94	0.11	0.04	thin
HD13836	G8V	0.01		6.92	0.18	0.01	thin
HD13871	F6IV-V	-0.11	3.16	7.72	0.10	0.08	thin
HD13997	G5	0.10	9.51	6.66	0.20	0.12	thin
HD14294	F5V	-0.39	3.97	8.38	0.07	0.20	thin
HD14414	F8	-0.36	1.70	7.97	0.01	0.01	thin
HD14642	F6/F7V	-0.40	4.47	8.92	0.22	0.28	thin
HD14687	K0	-0.11	11.97	8.36	0.16	0.03	thin
HD14691	F0V	-0.11	1.14	7.49	0.07	0.01	thin
HD14692	F2/F3V	-0.32	1.62	7.87	0.06	0.05	thin
HD14705	F7V	-0.48	4.90	7.80	0.03	0.19	thin
HD15064	G5IV	0.23	6.47	7.88	0.08	0.16	thin
HD15138	F4V	-0.40	2.91	7.70	0.04	0.12	thin
HD15228	F5V	-0.32	3.11	8.68	0.26	0.05	thin
HD15590	G5IV	0.14	4.77	6.61	0.21	0.08	thin
HD15814	F8V	-0.02	6.02	8.50	0.06	0.05	thin
HD15830	G0	-0.01		7.04	0.20	0.00	thin
HD16170	F6V	-0.11	2.85	8.37	0.06	0.16	thin
HD16287	K0	-0.19		7.65	0.08	0.19	thin
HD16417	G1V	0.24	6.26	7.56	0.12	0.02	thin
HD16538	F5V	-0.18	3.67	7.35	0.09	0.15	thin
HD16556	F6V	-0.23	2.90	7.99	0.01	0.11	thin
HD16626	A9III-IV	-0.54	2.16	8.39	0.05	0.08	thin
HD16647	F3V:	-0.25	2.11	8.11	0.03	0.04	thin
HD16739	F9V	0.06	3.96	7.58	0.11	0.07	thin
HD16825	F5V	-0.23	2.71	8.64	0.07	0.08	thin
HD16920	F4IV	-0.22	1.61	8.12	0.02	0.11	thin
HD16933	F5	-0.11	2.23	7.87	0.08	0.17	thin
HD17190	K1IV	-0.10	7.50	7.41	0.09	0.01	thin
HD17206	F5/F6V	-0.13	2.54	7.69	0.07	0.07	thin
HD17390	F3IV/V	-0.04	1.01	7.91	0.02	0.08	thin
HD17438	F2V	-0.42	1.59	8.14	0.05	0.01	thin
HD17865	F8V	-0.59	8.78	6.95	0.28	0.10	thin
HD17926	F6V	-0.28	3.10	8.10	0.05	0.08	thin
HD18404	F5IV	-0.10	2.13	7.69	0.11	0.05	thin
HD18692	F3V	-0.04	2.02	7.70	0.09	0.03	thin
HD18766	F5V	-0.42	2.62	7.72	0.18	0.08	thin
HD18838	G6V	-0.11		7.27	0.18	0.36	thin
HD18894	G0IV-V	0.15	5.56	7.42	0.08	0.10	thin
HD19301	F3V	-0.32	1.63	8.31	0.07	0.14	thin
HD19467	G3V	-0.06	7.92	7.36	0.13	0.17	thin
HD19618	K0IV-V	-0.07	9.74	7.37	0.21	0.39	thin
HD20165	K0	-0.14	1.53	6.52	0.24	0.20	thin
HD20395	F1V	-0.27	2.07	8.41	0.06	0.14	thin
HD20605	G8/K0V	-0.37		8.75	0.13	0.44	thin
HD20717	F5	-0.57	5.56	7.74	0.16	0.06	thin
HD20853	F7V	-0.06	3.78	7.89	0.03	0.06	thin
HD21024	F4III	-0.11	2.27	7.48	0.07	0.03	thin
HD21132	F5/F6V	-0.52	5.04	8.10	0.08	0.02	thin
HD21722	F3V	-0.11	2.11	7.99	0.01	0.10	thin
HD21774	G5	0.11	7.23	7.82	0.11	0.47	thin
HD21899	F7V	-0.07	2.52	7.58	0.11	0.06	thin
HD21962	F5	-0.08	4.58	7.76	0.09	0.11	thin
HD22044	F0	-0.21		7.15	0.14	0.09	thin
HD22418	F5	-0.21	2.54	9.13	0.21	0.01	thin
HD22521	G0	-0.31	7.37	8.25	0.18	0.41	thin

**Table 3.** (continued)

Name	Sp. type	[Fe/H]	age (Gyr)	$R$ (kpc)	$e$	$z_{\max}$ (kpc)	population
HD22594	F3V	-0.44	4.45	7.45	0.09	0.25	thin
HD22596	F3V	-0.50	4.13	7.34	0.09	0.29	thin
HD23140	K2	-0.14		7.58	0.10	0.19	thin
HD23308	F8V	-0.31	5.13	7.87	0.03	0.37	thin
HD23456	G1V	-0.50	4.32	8.83	0.25	0.22	thin
HD23609	F8IV	-0.02	3.88	8.26	0.08	0.02	thin
HD23626	G0	-0.44	2.98	8.15	0.05	0.04	thin
HD23856	F5V	-0.31	4.81	7.35	0.09	0.23	thin
HD24040	G0	0.18	6.92	6.58	0.23	0.10	thin
HD24206	G0	-0.00		6.83	0.17	0.10	thin
HD24301	G0IV	-0.26	5.25	6.57	0.24	0.11	thin
HD24390	F8V	-0.30	6.72	8.77	0.16	0.05	thin
HD24450	F0V	-0.31	2.04	7.77	0.11	0.02	thin
HD24702	G0	0.01	9.56	6.67	0.23	0.21	thin
HD24755	F6V	-0.57	3.44	8.19	0.22	0.09	thin
HD25061	K1V	-0.06	14.97	7.03	0.30	0.03	thin
HD25102	F5V	-0.09	2.09	7.75	0.11	0.02	thin
HD25322	F5V	-0.67	4.38	8.39	0.12	0.27	thin
HD25346	F2IV	-0.12	1.89	7.84	0.02	0.02	thin
HD25570	F2V	-0.29	2.16	7.76	0.11	0.11	thin
HD25682	G5	0.07	13.78	8.10	0.29	0.51	thin
HD25825	G0	0.02	2.04	7.69	0.11	0.06	thin
HD25948	F5V	-0.13	2.89	7.44	0.08	0.02	thin
HD26129	K0	-0.14	15.80	6.68	0.20	0.12	thin
HD26345	F6V	-0.09	1.97	7.68	0.10	0.06	thin
HD26736	G3V	0.03	4.91	7.67	0.12	0.05	thin
HD26737	F5V	-0.10	2.01	7.70	0.11	0.05	thin
HD26749	G2V	-0.33	10.57	7.04	0.23	0.19	thin
HD26756	G5V	-0.01		7.72	0.11	0.03	thin
HD26767	G0	0.10	1.05	7.70	0.11	0.06	thin
HD26784	F8V	-0.14	3.57	7.65	0.11	0.08	thin
HD27149	G5V	0.07	9.15	7.66	0.11	0.06	thin
HD27157	F5	-0.29	2.13	8.01	0.02	0.23	thin
HD27282	G8V	0.05	4.64	7.67	0.12	0.05	thin
HD27291	A5	-0.48	1.32	8.34	0.04	0.10	thin
HD27406	G0V	-0.12	4.40	7.68	0.11	0.06	thin
HD27483	F6V...	-0.06	2.99	7.69	0.10	0.05	thin
HD27524	F5V	-0.20	2.31	7.64	0.11	0.07	thin
HD27534	F6V	-0.15	2.31	7.61	0.11	0.08	thin
HD27561	F5V	-0.15	2.10	7.63	0.11	0.07	thin
HD27685	G4V	0.02	1.39	7.71	0.10	0.18	thin
HD27731	F5	-0.07	2.05	7.69	0.10	0.06	thin
HD27771	K1V	-0.12	15.41	7.69	0.11	0.05	thin
HD27808	F8V	-0.18	3.40	7.67	0.10	0.07	thin
HD27848	F6V	-0.13	2.33	7.64	0.12	0.05	thin
HD27859	G2V	-0.03	4.78	7.67	0.12	0.06	thin
HD27911	F0	-0.38	3.15	7.06	0.15	0.07	thin
HD28005	G0	0.22	8.56	7.67	0.14	0.18	thin
HD28033	F8V	-0.10	4.42	7.71	0.11	0.06	thin
HD28068	G1V	0.03	4.31	7.76	0.12	0.05	thin
HD28069	F5	-0.18	2.32	7.71	0.08	0.07	thin
HD28099	G8V	0.07	4.71	7.65	0.11	0.06	thin
HD28205	F8V	-0.18	3.83	7.68	0.11	0.05	thin
HD28237	F8	-0.13	4.48	7.64	0.11	0.08	thin
HD28246	F6V	-0.11	2.25	7.99	0.02	0.00	thin
HD28258	K0V	-0.09	13.01	7.67	0.12	0.05	thin
HD28344	G2V	-0.05	5.07	7.65	0.11	0.06	thin
HD28394	F7V	-0.19	4.24	7.69	0.10	0.06	thin
HD28454	F8V	-0.26	3.35	7.33	0.17	0.05	thin

**Table 3.** (continued)

Name	Sp. type	[Fe/H]	age (Gyr)	$R$ (kpc)	$\epsilon$	$z_{\max}$ (kpc)	population
HD28483	F6V	-0.11	2.36	7.71	0.10	0.07	thin
HD28608	F5	-0.15	2.11	7.69	0.10	0.06	thin
HD28620	F5	-0.62	3.05	8.33	0.06	0.07	thin
HD28635	F9V	-0.10	2.18	7.66	0.12	0.04	thin
HD28736	F5V	-0.07	2.02	7.64	0.11	0.06	thin
HD28911	F5V	-0.16	2.12	7.68	0.09	0.07	thin
HD29137	G5V	0.17	8.98	7.41	0.34	0.04	thin
HD29169	F5IV	0.05	1.26	7.66	0.12	0.05	thin
HD29225	F5V	-0.09	2.11	7.72	0.09	0.07	thin
HD29310	G1V	0.03	3.81	7.80	0.11	0.02	thin
HD29419	F5	0.03	1.22	7.65	0.11	0.06	thin
HD29461	G5	0.01	6.54	7.62	0.11	0.08	thin
HD29497	F5	-0.42	2.52	7.97	0.00	0.23	thin
HD29587	G2V	-0.53	7.06	7.69	0.41	0.25	thin
HD29666	K3V-VI	-0.19	6.92	7.07	0.33	0.58	thin
HD29859	F7IV-V	-0.25	2.79	8.06	0.01	0.05	thin
HD29883	K5III	-0.19	6.17	7.48	0.07	0.12	thin
HD30568	F8V	-0.15	3.51	7.72	0.08	0.25	thin
HD30589	F8	-0.09	4.70	7.65	0.11	0.08	thin
HD30676	F8	-0.01	3.93	7.64	0.09	0.10	thin
HD30738	F8	-0.15	4.21	7.65	0.12	0.07	thin
HD30913	F2	-0.18	2.19	7.76	0.11	0.13	thin
HD30974	G0	-0.37	9.88	7.20	0.25	0.19	thin
HD31362	F0	-0.28		8.28	0.07	0.03	thin
HD31423	F5	-0.23	2.73	8.33	0.04	0.35	thin
HD31452	G5	0.00	14.82	6.52	0.23	0.04	thin
HD31460	G0V	-0.49	7.18	6.97	0.30	0.24	thin
HD31746	F3V	-0.29	2.27	7.43	0.08	0.03	thin
HD31975	F8V	-0.25	5.00	7.71	0.08	0.29	thin
HD32070	G5	-0.22	3.76	6.81	0.19	0.16	thin
HD32237	G5	-0.46		6.97	0.23	0.08	thin
HD32348	F2	-0.44	1.45	9.19	0.14	0.24	thin
HD32715	F3V:	-0.18	2.49	7.62	0.06	0.16	thin
HD32820	F8V	-0.04	3.46	7.77	0.07	0.07	thin
HD32850	K0V	-0.17		7.03	0.15	0.19	thin
HD33093	G2V	-0.12	5.00	6.80	0.19	0.06	thin
HD33262	F7V	-0.34	3.17	8.39	0.05	0.06	thin
HD33636	G0	-0.26	3.13	7.32	0.10	0.18	thin
HD33924	F5	-0.11	2.15	7.88	0.07	0.09	thin
HD34180	F0IV	-0.31	2.99	8.27	0.03	0.05	thin
HD34554	F5V	-0.62	3.76	8.62	0.11	0.11	thin
HD34937	F2	-0.29	1.73	7.99	0.22	0.31	thin
HD35072	F7III-IV	-0.10	3.09	7.36	0.15	0.18	thin
HD35386	F6V	-0.39	4.13	7.22	0.13	0.15	thin
HD35643	F2V	-0.23	1.95	7.80	0.11	0.11	thin
HD35689	F3V	-0.56	3.57	7.54	0.08	0.12	thin
HD35783	F6V	-0.40	4.90	7.12	0.26	0.03	thin
HD35863	F0	-0.50	2.30	7.82	0.15	0.08	thin
HD36756	F5	-0.51	4.53	9.24	0.14	0.23	thin
HD36909	F5	-0.34	5.97	7.85	0.05	0.03	thin
HD37070	F5	-0.07	1.35	7.57	0.10	0.06	thin
HD37487	F0	-0.11	2.00	7.63	0.08	0.05	thin
HD37574	F8	-0.15	3.21	8.24	0.07	0.06	thin
HD37605	K0	0.07	10.71	7.21	0.20	0.05	thin
HD37634	G5	-0.63		9.95	0.23	0.57	thin
HD38141	F5	-0.09	2.15	7.70	0.10	0.07	thin
HD38382	F8/G0V	-0.10	5.18	7.57	0.08	0.11	thin
HD38858	G4V	-0.24	3.19	7.34	0.09	0.06	thin
HD39091	G3IV	-0.03	5.42	7.16	0.27	0.08	thin

**Table 3.** (continued)

Name	Sp. type	[Fe/H]	age (Gyr)	$R$ (kpc)	$e$	$z_{\max}$ (kpc)	population
HD39192	G0V	-0.45	6.74	8.56	0.09	0.15	thin
HD39427	G6V	-0.31	4.38	7.80	0.15	0.08	thin
HD39655	F2V	-0.22		7.43	0.08	0.08	thin
HD39962	F2V	-0.48	3.32	8.43	0.12	0.19	thin
HD40125	F3IV/V	-0.10	2.14	7.93	0.07	0.01	thin
HD40421	F0	-0.11	2.16	7.54	0.07	0.10	thin
HD40787	F5	-0.23	2.99	8.27	0.10	0.15	thin
HD40811	F3V	-0.41	1.83	7.33	0.21	0.18	thin
HD40832	F4V	-0.22	3.25	6.74	0.21	0.02	thin
HD40930	F8	-0.63	3.60	8.78	0.09	0.07	thin
HD41019	G0V	-0.42	7.41	7.46	0.08	0.11	thin
HD41304	F6V	-0.28	4.69	6.84	0.18	0.01	thin
HD41323	G3/G5V	-0.41		8.72	0.22	0.12	thin
HD41340	F5V	-0.49	4.40	9.11	0.25	0.26	thin
HD41853	K2V	-0.17		7.20	0.19	0.13	thin
HD42012	K0	-0.10	11.73	6.92	0.18	0.08	thin
HD42548	F0	-0.28	3.03	8.73	0.12	0.15	thin
HD42618	G4V	-0.14		8.21	0.22	0.21	thin
HD42683	F8V	-0.31	3.08	6.85	0.19	0.22	thin
HD42807	G8V	-0.11		7.45	0.09	0.01	thin
HD43382	F6V	-0.49	4.45	8.32	0.08	0.27	thin
HD43856	F6V	-0.40	5.17	8.64	0.23	0.05	thin
HD44447	F8V	-0.43	7.80	7.83	0.03	0.02	thin
HD45184	G2V	-0.02	4.11	8.50	0.08	0.15	thin
HD45194	F7V	-0.37	2.41	7.29	0.13	0.09	thin
HD45289	G5V	0.00	9.30	8.31	0.32	0.07	thin
HD45504	F5	-0.36	5.63	7.56	0.09	0.15	thin
HD45580	G0	-0.26	9.52	7.78	0.09	0.45	thin
HD45983	F2/F3V	-0.39	1.88	7.60	0.05	0.17	thin
HD46569	F8V	-0.15	3.33	7.57	0.06	0.22	thin
HD46588	F8V	-0.26	4.27	7.59	0.13	0.01	thin
HD46781	F5	-0.20	1.96	7.56	0.08	0.10	thin
HD47252	G8/K0V	-0.39		9.13	0.22	0.10	thin
HD47415	F8IV	-0.37	5.92	8.61	0.07	0.22	thin
HD47703	F8III	-0.41	2.22	8.47	0.23	0.23	thin
HD48737	F5IV	-0.06	1.89	7.63	0.06	0.08	thin
HD49095	F7V	-0.36	3.91	7.35	0.11	0.43	thin
HD49565	F8	-0.47	3.27	11.22	0.30	0.09	thin
HD50571	F7III-IV	-0.13	2.35	7.51	0.07	0.02	thin
HD50692	G0V	-0.27	4.63	8.49	0.09	0.01	thin
HD52552	F5	-0.50	2.88	8.82	0.10	0.29	thin
HD52619	F3/F5V	-0.20	2.41	7.95	0.05	0.09	thin
HD54351	G0	-0.11	4.00	6.68	0.22	0.49	thin
HD54718	G0	-0.59	7.94	8.55	0.07	0.22	thin
HD56617	F3V	-0.07	1.81	7.75	0.08	0.19	thin
HD56737	F3V	-0.56	4.04	8.34	0.04	0.29	thin
HD57006	F8V	-0.25	2.23	7.31	0.10	0.20	thin
HD57517	F5	-0.10	5.01	7.83	0.10	0.04	thin
HD57678	K0	0.10	1.73	9.86	0.35	0.45	thin
HD58192	F7V	-0.36	2.12	7.89	0.01	0.07	thin
HD58805	F3V	-0.54	3.43	8.12	0.04	0.06	thin
HD58971	G5	0.03		7.42	0.16	0.42	thin
HD59106	G0	-0.18	4.18	7.59	0.06	0.12	thin
HD60063	F0	-0.41		8.56	0.14	0.07	thin
HD60406	F5	-0.23	3.02	8.02	0.15	0.09	thin
HD60803	G0V	-0.05	3.03	8.58	0.07	0.12	thin
HD60912	F5	-0.22	3.45	7.86	0.06	0.25	thin
HD61859	F7V	-0.15	2.78	8.48	0.06	0.21	thin
HD61997	F5	-0.16	3.07	7.64	0.11	0.16	thin

**Table 3.** (continued)

Name	Sp. type	[Fe/H]	age (Gyr)	$R$ (kpc)	$e$	$z_{\max}$ (kpc)	population
HD62196	F0	-0.77		8.94	0.11	0.20	thin
HD62549	G1V	-0.09	7.11	7.78	0.25	0.43	thin
HD62613	G8V	-0.13		8.63	0.07	0.39	thin
HD63332	F6V	-0.26	4.07	8.55	0.07	0.01	thin
HD64184	G5V	-0.09	6.70	9.30	0.22	0.56	thin
HD64685	F2IV	-0.07	1.45	7.45	0.07	0.06	thin
HD64913	F8	-0.59	9.77	7.25	0.32	0.30	thin
HD65301	F2:V:	-0.09	2.82	8.15	0.14	0.13	thin
HD65430	K0V	-0.11	5.65	6.94	0.24	0.10	thin
HD65523	G5	-0.11		7.85	0.11	0.19	thin
HD66138	F5	-0.20	2.26	7.64	0.08	0.11	thin
HD66553	G5	-0.02	12.35	6.90	0.18	0.23	thin
HD66653	G5V	0.10	4.34	7.71	0.13	0.06	thin
HD66751	F8	-0.67	11.29	8.62	0.12	0.24	thin
HD67827	G0	-0.03	5.25	7.84	0.08	0.03	thin
HD68168	G0	0.13	6.15	7.04	0.14	0.12	thin
HD69548	F4V	-0.24	2.40	8.17	0.08	0.05	thin
HD70937	F2V	-0.10	2.12	8.87	0.16	0.09	thin
HD70954	F2	-0.65	3.68	8.44	0.05	0.12	thin
HD70958	F3V	-0.48	4.92	6.92	0.23	0.07	thin
HD71089	F0	-0.36	4.05	6.84	0.33	0.06	thin
HD71148	G5V	-0.15	6.65	7.13	0.16	0.19	thin
HD71196	F2/F3V	-0.23	1.93	8.50	0.06	0.08	thin
HD71433	F4III	-0.16	1.41	7.83	0.03	0.17	thin
HD72291	F5V	-0.46	2.42	8.37	0.05	0.17	thin
HD72528	F7V	-0.22	3.99	7.61	0.07	0.22	thin
HD73121	G1V	-0.10	6.37	7.22	0.11	0.24	thin
HD73393	G3V	-0.01	4.99	6.79	0.29	0.11	thin
HD73744	G0V	-0.37	5.93	6.84	0.18	0.26	thin
HD74243	F7V	-0.19	2.80	7.45	0.07	0.01	thin
HD74425	F8	-0.55	3.75	7.13	0.15	0.00	thin
HD74546	F2	-0.36	4.66	8.60	0.09	0.24	thin
HD74868	G3IV	-0.03	5.66	7.73	0.10	0.06	thin
HD75487	F5IV-V	-0.10	2.69	8.34	0.04	0.18	thin
HD75528	G2IV	0.03	5.72	8.14	0.12	0.22	thin
HD75576	G0	-0.15	7.14	7.61	0.07	0.41	thin
HD75596	F8	-0.59	1.55	7.62	0.16	0.32	thin
HD75786	F3V	-0.37	2.49	7.24	0.11	0.04	thin
HD76493	F5	-0.26	3.10	7.78	0.05	0.11	thin
HD76653	F6V	-0.14	2.52	8.39	0.07	0.02	thin
HD76735	F2	-0.29	2.03	8.28	0.06	0.05	thin
HD77065	G5	-0.27		6.85	0.23	0.32	thin
HD77084	F5IV/V	-0.14	2.49	7.50	0.08	0.06	thin
HD77408	F6IV	-0.42	5.73	8.77	0.33	0.29	thin
HD77462	F7V	-0.39	5.04	8.66	0.30	0.16	thin
HD78274	F5	-0.34	3.57	7.03	0.21	0.07	thin
HD78366	F9V	-0.11	3.84	7.80	0.07	0.12	thin
HD78661	F2p	-0.53		8.22	0.06	0.15	thin
HD79929	F6V	-0.38	3.62	8.11	0.02	0.20	thin
HD80654	F8V	-0.18	5.02	7.88	0.05	0.12	thin
HD80719	F6V	-0.17	3.45	7.93	0.11	0.03	thin
HD81044	K1V	-0.07		8.57	0.33	0.43	thin
HD81408	K1/K2V	-0.40		8.03	0.48	0.22	thin
HD81440	F5	-0.31	2.44	8.07	0.16	0.24	thin
HD81790	F3Vs	-0.24	2.03	8.00	0.06	0.04	thin
HD82106	K3V	-0.13		7.87	0.09	0.06	thin
HD83108	F5V	-0.07	1.96	7.77	0.04	0.07	thin
HD83170	F2V	-0.32	3.47	7.39	0.09	0.06	thin
HD83273	G0III	-0.02	2.65	7.75	0.11	0.07	thin

**Table 3.** (continued)

Name	Sp. type	[Fe/H]	age (Gyr)	$R$ (kpc)	$e$	$z_{\max}$ (kpc)	population
HD83509	F7V	-0.63	5.18	8.43	0.05	0.12	thin
HD83683	F8	-0.37	3.75	8.02	0.10	0.16	thin
HD84709	F3V	-0.23	2.12	7.36	0.09	0.07	thin
HD85217	F6V...	-0.21	3.87	7.51	0.09	0.08	thin
HD85249	F7V	-0.01	2.18	8.58	0.08	0.05	thin
HD85380	F8V	-0.12	5.00	7.58	0.11	0.19	thin
HD85683	F8V	-0.07	3.97	7.84	0.08	0.19	thin
HD86050	F7V	-0.59	6.68	7.33	0.31	0.18	thin
HD86140	K2V	-0.27	4.29	9.91	0.28	0.37	thin
HD86146	F6Vs	-0.14	3.47	8.05	0.01	0.12	thin
HD86460	G0IV	-0.28	3.29	7.56	0.14	0.36	thin
HD87096	F6IV	-0.28	4.21	7.77	0.10	0.07	thin
HD87209	F6V	-0.52	4.50	8.75	0.13	0.05	thin
HD87301	F4V	-0.11	2.06	7.53	0.07	0.17	thin
HD87810	F3V	-0.05	1.72	8.48	0.10	0.24	thin
HD87827	F0V	-0.11	1.16	7.77	0.05	0.00	thin
HD88201	G0V	-0.17	3.35	7.85	0.08	0.09	thin
HD88215	F2/F3IV/V	-0.18	1.36	7.31	0.09	0.02	thin
HD88371	G2V	-0.23	10.20	8.62	0.38	0.15	thin
HD88697	F8	-0.11	2.54	7.78	0.10	0.08	thin
HD88742	G0V	-0.12	3.45	6.94	0.18	0.03	thin
HD88864	F8V	0.20	3.83	7.01	0.19	0.15	thin
HD89090	F8/G0V	-0.37	5.88	7.28	0.19	0.02	thin
HD89322	F2	-0.14	1.25	7.53	0.06	0.11	thin
HD89389	F9V	-0.15	7.19	8.26	0.05	0.22	thin
HD89507	F2	-0.21	2.32	7.47	0.07	0.01	thin
HD89569	F6V	-0.21	4.13	7.60	0.11	0.01	thin
HD89747	F3IV	-0.16	2.04	7.41	0.08	0.10	thin
HD89777	G8V	-0.03	1.30	7.71	0.38	0.20	thin
HD89813	G5	-0.08		7.47	0.14	0.22	thin
HD90089	F2V	-0.38	2.06	8.40	0.05	0.05	thin
HD90387	F3/F5V	-0.12	1.65	7.90	0.08	0.07	thin
HD90494	F8	-0.22	2.12	6.81	0.18	0.25	thin
HD90520	G3V	0.17	5.64	7.59	0.09	0.18	thin
HD90589	F2IV	-0.12	1.45	8.43	0.06	0.06	thin
HD90663	K0	-0.24	2.28	9.14	0.13	0.54	thin
HD90711	K0V	0.11	11.08	6.55	0.24	0.32	thin
HD90812	K1V	-0.26		8.43	0.24	0.04	thin
HD91135	F7V	-0.03	1.36	7.68	0.07	0.04	thin
HD91248	F2	-0.32	2.39	8.13	0.11	0.03	thin
HD91480	F1V	-0.18	1.28	8.40	0.08	0.00	thin
HD91706	F6V	-0.14	2.25	7.83	0.07	0.05	thin
HD91856	G5	-0.07	10.78	6.95	0.22	0.20	thin
HD92547	F8	-0.48	6.11	8.58	0.07	0.02	thin
HD92577	F2/F3V	-0.29	1.53	8.60	0.08	0.05	thin
HD92719	G2/G3V	-0.20	1.46	8.77	0.15	0.06	thin
HD93135	F0	-0.53	2.89	7.79	0.12	0.07	thin
HD93372	F6V	-0.11	3.36	7.40	0.08	0.02	thin
HD93626	G0V	-0.23		7.33	0.11	0.01	thin
HD93751	F5IV/V	-0.04	2.09	7.64	0.12	0.04	thin
HD93860	F5	-0.46	2.24	8.57	0.12	0.15	thin
HD93932	G3V	-0.21	8.23	6.64	0.24	0.16	thin
HD94012	F8	-0.61	2.21	6.84	0.19	0.04	thin
HD94162	F5	-0.49	4.86	7.55	0.09	0.10	thin
HD94270	G2V	-0.03	3.75	7.15	0.13	0.06	thin
HD94461	F2V	-0.57	3.41	8.63	0.08	0.04	thin
HD94729	F0	-0.18	2.17	7.76	0.10	0.03	thin
HD94864	F5	-0.12	2.24	7.66	0.06	0.10	thin
HD94906	F0V	-0.50	1.98	7.92	0.01	0.22	thin

**Table 3.** (continued)

Name	Sp. type	[Fe/H]	age (Gyr)	$R$ (kpc)	$e$	$z_{\max}$ (kpc)	population
HD95216	F5V	-0.29	3.03	7.84	0.13	0.07	thin
HD95363	F7V	-0.36	4.72	8.29	0.04	0.17	thin
HD95366	K2	-0.06		7.09	0.29	0.22	thin
HD95532	F7/F8V	-0.39	5.14	8.32	0.04	0.40	thin
HD95547	F8Vm	-0.68	4.67	9.16	0.13	0.52	thin
HD95980	G5	-0.07	6.37	7.75	0.21	0.03	thin
HD96418	F8IV	-0.22	4.61	8.02	0.00	0.09	thin
HD96574	F9V	-0.16	5.72	8.02	0.26	0.15	thin
HD96700	G1/G2V	-0.31	8.67	7.17	0.16	0.29	thin
HD96937	G5	0.10	8.92	7.81	0.09	0.02	thin
HD97227	F2	-0.51	6.13	7.81	0.06	0.22	thin
HD97343	G8/K0V	0.05	2.58	7.14	0.19	0.51	thin
HD97358	F2	-0.44	2.37	8.04	0.07	0.23	thin
HD97840	F3V	-0.20	1.49	7.98	0.11	0.05	thin
HD97957	F7V	-0.32	4.02	8.25	0.13	0.10	thin
HD97998	G5V	-0.43		6.98	0.15	0.39	thin
HD98220	F7V	-0.28	4.18	7.52	0.19	0.43	thin
HD98221	F3V	-0.25	2.21	8.41	0.05	0.03	thin
HD98388	F8V	-0.09	3.51	7.79	0.07	0.00	thin
HD98823	F5	-0.15	1.37	7.87	0.05	0.20	thin
HD99373	F6IV	-0.27	2.92	8.34	0.05	0.24	thin
HD99404	G5	0.00	1.05	7.10	0.29	0.01	thin
HD99453	F7V	-0.09	3.89	7.98	0.08	0.17	thin
HD99507	F5	-0.39	2.54	8.60	0.07	0.01	thin
HD99904	F5	-0.26	2.51	7.93	0.04	0.04	thin
HD100004	F6V	-0.46	2.33	7.32	0.27	0.01	thin
HD100043	F2V	-0.11	1.85	8.13	0.08	0.03	thin
HD100604	F2V	-0.28	1.61	7.94	0.07	0.23	thin
HD100953	F5V	-0.15	1.96	7.65	0.08	0.14	thin
HD101093	F9V	-0.28	2.07	8.20	0.16	0.06	thin
HD101563	G2III/IV	0.02	5.26	8.91	0.21	0.22	thin
HD101612	F5/F6V	-0.59	4.77	8.76	0.16	0.23	thin
HD101614	G0V	-0.40	8.75	7.83	0.15	0.05	thin
HD101620	F5	-0.27	2.77	8.08	0.10	0.06	thin
HD101688	F2IV-V	-0.29	2.04	7.56	0.06	0.29	thin
HD101730	F5	-0.36	2.92	7.58	0.06	0.00	thin
HD101805	G1V	-0.10	3.60	8.63	0.08	0.10	thin
HD101941	F5V	-0.54	4.08	8.32	0.20	0.02	thin
HD102028	F6V	-0.12	4.74	8.03	0.10	0.08	thin
HD102136	G8/K0V	-0.07		8.65	0.12	0.08	thin
HD102165	F7V	0.09	3.55	7.52	0.08	0.08	thin
HD102184	F5V	-0.53	3.05	6.81	0.22	0.05	thin
HD102438	G5V	-0.17		7.39	0.08	0.10	thin
HD102555	F2	-0.10	1.67	7.62	0.09	0.17	thin
HD102713	F5IV	-0.29	1.44	7.79	0.08	0.12	thin
HD102843	K0	0.12		7.20	0.31	0.07	thin
HD103021	F6V	-0.51	4.07	8.70	0.08	0.17	thin
HD103072	K2	-0.27		7.34	0.13	0.03	thin
HD103110	F7V	-0.30	3.00	8.14	0.09	0.10	thin
HD103459	G5	0.18	6.88	6.98	0.34	0.17	thin
HD103589	F2IV/V	-0.17	1.55	7.23	0.11	0.01	thin
HD103613	F5	-0.23	2.85	7.84	0.04	0.18	thin
HD103676	F2	-0.02	1.18	7.82	0.08	0.09	thin
HD103746	F3IV-V	0.01	1.57	7.60	0.08	0.08	thin
HD103799	F6V	-0.49	5.51	7.49	0.10	0.31	thin
HD103975	G0V	-0.25	4.60	7.91	0.02	0.14	thin
HD104056	G5	-0.45	7.85	8.18	0.23	0.53	thin
HD104243	G5	-0.00		6.87	0.18	0.04	thin
HD104304	K0IV	0.12	11.68	7.80	0.10	0.12	thin



**Table 3.** (continued)

Name	Sp. type	[Fe/H]	age (Gyr)	$R$ (kpc)	$e$	$z_{\max}$ (kpc)	population
HD104755	F5	-0.33	2.76	6.94	0.16	0.07	thin
HD104868	F6V	-0.35	2.08	8.01	0.09	0.16	thin
HD104904	F6V	-0.46	1.83	8.82	0.10	0.26	thin
HD104982	G5V	-0.14	2.01	7.98	0.22	0.54	thin
HD104988	G8V	-0.04		7.31	0.23	0.10	thin
HD104999	F2	-0.18	2.87	7.04	0.14	0.18	thin
HD105087	K0	-0.41		8.15	0.34	0.43	thin
HD105274	F5V	-0.56	3.99	8.33	0.13	0.02	thin
HD105320	F8V	-0.40	5.19	8.69	0.09	0.36	thin
HD105491	F5IV/V	-0.25	1.58	7.72	0.16	0.22	thin
HD105559	F8V	-0.44	6.50	7.58	0.07	0.02	thin
HD105577	F6V	-0.15	4.65	7.75	0.03	0.03	thin
HD105584	F2	-0.54		7.68	0.15	0.06	thin
HD105698	F9V	-0.39	4.18	8.55	0.07	0.19	thin
HD105736	F3V	-0.17	2.07	7.76	0.15	0.03	thin
HD105881	F5	-0.23	2.30	8.53	0.07	0.04	thin
HD105901	G0	-0.01	3.03	7.02	0.18	0.27	thin
HD105926	F5	-0.18	3.35	7.79	0.07	0.24	thin
HD105946	F2	-0.38	2.37	7.75	0.15	0.01	thin
HD106103	F5V	-0.29	2.17	8.04	0.02	0.08	thin
HD106152	F5	-0.08	4.93	8.01	0.07	0.03	thin
HD106589	G5V	-0.12		9.39	0.29	0.14	thin
HD106691	F5IV	-0.24	2.10	8.09	0.03	0.10	thin
HD106811	F8	0.03	7.55	8.78	0.29	0.34	thin
HD106888	F8	-0.09	2.09	7.52	0.07	0.00	thin
HD106906	F5V	-0.18	3.38	7.71	0.04	0.01	thin
HD106946	F2V	-0.18	1.22	8.05	0.03	0.07	thin
HD106949	F8	-0.15	4.91	7.40	0.17	0.07	thin
HD107038	G0	-0.49	5.45	7.78	0.04	0.23	thin
HD107067	F8...	-0.24		8.11	0.03	0.05	thin
HD107086	F8V	-0.13	2.25	8.50	0.07	0.13	thin
HD107087	G0V	-0.11	5.69	7.49	0.09	0.13	thin
HD107145	F8V	-0.14	2.14	7.75	0.09	0.14	thin
HD107469	K0V	0.09	7.36	8.49	0.17	0.31	thin
HD107685	F5...	-0.32	3.26	8.05	0.02	0.08	thin
HD107877	F5V	-0.28	1.84	8.08	0.02	0.05	thin
HD107888	K5	-0.32		7.79	0.08	0.13	thin
HD108134	G0p	-0.50	9.17	8.23	0.16	0.37	thin
HD108203	F6V	-0.26	2.29	8.07	0.02	0.15	thin
HD108226	F6V	-0.24	2.41	8.04	0.02	0.04	thin
HD108435	F5V	-0.61	3.13	9.04	0.12	0.35	thin
HD108682	K0V	-0.34		8.28	0.24	0.47	thin
HD108713	F9V	-0.29	3.35	7.83	0.12	0.06	thin
HD108807	F7V	-0.21	2.38	7.62	0.05	0.05	thin
HD108846	F8	-0.30	3.28	6.95	0.16	0.49	thin
HD108956	F8V	-0.51	4.78	8.48	0.07	0.45	thin
HD108976	F6V	-0.27	1.58	8.07	0.02	0.08	thin
HD109029	F0	-0.18	2.71	7.37	0.14	0.12	thin
HD109031	F0IV	-0.12	1.97	7.69	0.06	0.07	thin
HD109083	F3V	-0.22	2.19	8.13	0.08	0.13	thin
HD109085	F2V	-0.09	1.56	7.62	0.08	0.03	thin
HD109304	G0	-0.52	6.50	8.33	0.09	0.14	thin
HD109492	G4IV	0.11	2.89	7.21	0.16	0.15	thin
HD109590	sdF2	-0.47	3.68	6.93	0.17	0.31	thin
HD109602	F7V	-0.33	5.14	6.99	0.29	0.56	thin
HD110025	F3V	-0.24	3.45	7.65	0.10	0.07	thin
HD110134	F5V	-0.32	3.68	7.80	0.05	0.11	thin
HD110313	F8	0.01	3.14	7.09	0.27	0.06	thin
HD110314	G2V	0.02	8.32	8.47	0.22	0.14	thin

**Table 3.** (continued)

Name	Sp. type	[Fe/H]	age (Gyr)	$R$ (kpc)	$e$	$z_{\max}$ (kpc)	population
HD110477	F6IV	-0.18	2.27	7.20	0.19	0.13	thin
HD110524	F4V	-0.29	2.10	7.59	0.07	0.05	thin
HD110619	G5V	-0.39		7.53	0.21	0.38	thin
HD110833	K3V	-0.20		7.55	0.07	0.21	thin
HD110949	F8V	-0.30	2.22	8.40	0.05	0.29	thin
HD111238	F8V	-0.34	4.51	7.82	0.04	0.02	thin
HD111347	F7V	-0.30	4.40	8.03	0.05	0.04	thin
HD111456	F5V	-0.31	3.02	8.25	0.08	0.02	thin
HD111564	G0V	-0.09	6.16	7.54	0.30	0.01	thin
HD111718	F6III	-0.23	3.45	7.66	0.11	0.01	thin
HD111997	F8V	-0.20	3.92	7.63	0.06	0.14	thin
HD111998	F5V	-0.08	2.52	7.63	0.10	0.00	thin
HD112039	F5/F6V	-0.49	3.64	8.27	0.06	0.08	thin
HD112887	F4V	-0.44	3.04	8.34	0.07	0.01	thin
HD112974	F7V	-0.13	4.19	8.68	0.09	0.10	thin
HD113037	F5V	-0.27	3.09	8.04	0.02	0.04	thin
HD113283	G5IV-V	-0.09	5.80	8.03	0.06	0.07	thin
HD113302	F8V	-0.27	4.99	7.71	0.08	0.13	thin
HD113893	G0	-0.13		7.04	0.18	0.16	thin
HD114136	F5V	-0.32	4.09	8.92	0.17	0.39	thin
HD114172	G0V	-0.54		8.94	0.20	0.52	thin
HD114675	F5V	-0.26	2.48	8.03	0.07	0.21	thin
HD114838	F5	-0.21	6.07	7.48	0.07	0.06	thin
HD114905	F7V	-0.37	4.24	8.66	0.20	0.05	thin
HD114989	F7V	-0.15	3.29	7.92	0.07	0.06	thin
HD115149	F5V	-0.14	2.26	7.43	0.08	0.03	thin
HD115272	F8V	-0.19	3.67	7.75	0.04	0.03	thin
HD115427	F5V	-0.37	2.86	7.07	0.16	0.19	thin
HD115667	G0V	-0.36	1.08	7.02	0.28	0.09	thin
HD115740	F5V	-0.48	1.09	8.47	0.14	0.17	thin
HD115782	F8IV	-0.38	2.67	9.14	0.17	0.18	thin
HD115981	F2V	-0.32	2.29	8.02	0.06	0.21	thin
HD116012	K2V	-0.18		8.06	0.22	0.06	thin
HD116156	F8V	-0.33	1.71	8.49	0.08	0.03	thin
HD116234	G0V	-0.15	4.47	7.49	0.07	0.00	thin
HD116568	F3V	-0.31	2.19	8.52	0.12	0.14	thin
HD117104	F3/F5V	-0.35	2.53	8.54	0.10	0.13	thin
HD117105	G1V	-0.33	6.35	8.12	0.08	0.55	thin
HD117126	G5	-0.08	9.45	7.68	0.30	0.59	thin
HD117264	F5	-0.34	3.85	8.41	0.05	0.06	thin
HD117854	G0V	-0.53	9.83	9.42	0.31	0.47	thin
HD117858	G0	-0.64	10.79	7.00	0.31	0.18	thin
HD118186	G0V	-0.27	5.80	8.55	0.07	0.12	thin
HD118245	F2	-0.55	2.93	7.34	0.09	0.01	thin
HD118330	F8	-0.36	5.29	6.90	0.17	0.28	thin
HD118475	G2/G3IV/V	0.09	4.31	8.39	0.17	0.44	thin
HD119054	F5	-0.27	5.96	8.33	0.06	0.06	thin
HD119070	G5V	-0.04		7.12	0.13	0.18	thin
HD119550	G2V	-0.10	4.15	6.77	0.27	0.34	thin
HD119629	F8V	-0.29	4.26	8.11	0.10	0.20	thin
HD119638	G2V	-0.31	3.51	7.48	0.12	0.02	thin
HD119756	F3V	-0.12	2.02	7.67	0.11	0.07	thin
HD119932	K0	-0.23		7.25	0.21	0.12	thin
HD119992	F7IV-V	-0.29	3.65	7.62	0.20	0.30	thin
HD119993	F5	-0.19	2.07	7.28	0.15	0.08	thin
HD120005	F5	-0.09	4.03	6.76	0.20	0.12	thin
HD120066	G0V	-0.06	8.15	6.81	0.25	0.12	thin
HD120250	F3/F5V	-0.23	2.30	8.14	0.12	0.11	thin
HD120510	F8V	-0.15	3.75	7.66	0.10	0.08	thin

**Table 3.** (continued)

Name	Sp. type	[Fe/H]	age (Gyr)	$R$ (kpc)	$e$	$z_{\max}$ (kpc)	population
HD120530	F5	-0.23	2.03	7.94	0.01	0.01	thin
HD120544	F6IV/V	-0.10	1.42	8.35	0.06	0.02	thin
HD120623	F0/F2IV	-0.32	1.30	8.04	0.07	0.09	thin
HD120672	F6V	-0.14	2.74	7.16	0.12	0.16	thin
HD120915	F5	-0.01	3.56	8.22	0.06	0.22	thin
HD121105	F5	-0.27	3.74	7.25	0.11	0.22	thin
HD121249	K0	-0.10		8.26	0.25	0.09	thin
HD121256	F5	-0.21	3.84	8.21	0.06	0.08	thin
HD121496	F5	-0.15	3.13	8.19	0.07	0.26	thin
HD121746	F5IV	-0.19	2.38	7.79	0.12	0.15	thin
HD121825	G0	-0.39	10.02	8.52	0.06	0.34	thin
HD121852	F7V	-0.17	4.27	7.59	0.05	0.09	thin
HD122797	F4V	-0.31	2.55	8.27	0.03	0.16	thin
HD122862	G1V	-0.25	6.73	8.21	0.06	0.55	thin
HD123058	F3/F5V	-0.22	1.86	7.84	0.04	0.04	thin
HD123265	K0	0.06	12.83	7.23	0.26	0.38	thin
HD123333	K2V	-0.37		9.84	0.24	0.31	thin
HD123340	F8	-0.52	5.05	8.60	0.17	0.43	thin
HD123651	G1V	-0.49	6.08	7.89	0.07	0.21	thin
HD123760	G5V	-0.02	8.84	6.75	0.19	0.00	thin
HD123845	F7V	-0.39	4.08	8.09	0.08	0.03	thin
HD123944	F0	-0.34	1.70	7.84	0.03	0.03	thin
HD124115	F7V	-0.01	3.18	7.92	0.07	0.03	thin
HD124292	G0	-0.04	2.57	7.01	0.19	0.28	thin
HD124580	F9V	-0.22	3.82	8.29	0.07	0.11	thin
HD126583	G5	0.02		6.86	0.17	0.21	thin
HD126766	F5V	-0.27	2.07	8.03	0.03	0.05	thin
HD126943	F1IV	-0.21	1.60	7.54	0.06	0.03	thin
HD127740	F5III	-0.23	2.27	8.13	0.06	0.17	thin
HD127821	F4IV	-0.31	2.29	7.63	0.06	0.14	thin
HD127825	F7V	-0.34	6.12	7.18	0.17	0.14	thin
HD128311	K0	-0.23		8.14	0.07	0.23	thin
HD128332	F7V	-0.30	4.58	8.16	0.17	0.12	thin
HD128369	F5	-0.59	5.00	8.68	0.19	0.05	thin
HD128608	F0	-0.20	2.88	7.27	0.10	0.04	thin
HD128617	F3IV	-0.07	2.79	7.20	0.17	0.07	thin
HD128917	F4V	-0.08	3.11	8.12	0.07	0.06	thin
HD128931	F6V	-0.32	2.41	7.17	0.13	0.22	thin
HD129417	F3V	-0.02	1.92	7.44	0.12	0.00	thin
HD129502	F2III	-0.10	1.71	7.79	0.10	0.10	thin
HD129747	G2V	-0.05	9.31	7.79	0.25	0.09	thin
HD130265	G3V	-0.27	3.24	9.60	0.24	0.13	thin
HD130307	G8V	-0.23	6.00	7.49	0.07	0.24	thin
HD130989	F6V	-0.36	3.43	7.29	0.16	0.00	thin
HD131271	F6V	-0.54	5.17	8.31	0.05	0.24	thin
HD131424	F3V	-0.10	1.11	7.78	0.08	0.02	thin
HD132051	K0	-0.13	8.32	8.08	0.19	0.18	thin
HD132142	K1V	-0.23		7.18	0.35	0.34	thin
HD132301	F5V	-0.20	3.22	7.55	0.11	0.02	thin
HD132832	F5	-0.43	3.00	7.11	0.13	0.02	thin
HD133002	F9V	-0.30	2.49	8.18	0.25	0.03	thin
HD133564	F8	-0.55	1.86	8.89	0.26	0.01	thin
HD133644	F7V	-0.29	4.78	7.91	0.07	0.03	thin
HD134044	F8V	-0.17	4.51	8.08	0.01	0.06	thin
HD134060	G3IV	0.04	5.69	7.08	0.16	0.15	thin
HD134792	F6III	-0.23	3.01	8.38	0.08	0.21	thin
HD136257	F9V	-0.31	4.30	7.82	0.19	0.14	thin
HD136654	F5	-0.10	4.00	7.71	0.14	0.03	thin
HD136927	F6IV	-0.29	5.14	7.87	0.11	0.20	thin

**Table 3.** (continued)

Name	Sp. type	[Fe/H]	age (Gyr)	$R$ (kpc)	$e$	$z_{\max}$ (kpc)	population
HD138525	F6III	-0.19	2.42	7.32	0.09	0.39	thin
HD139389	F5V:	-0.41	2.49	8.22	0.06	0.16	thin
HD139590	G0V	-0.13	3.86	6.70	0.21	0.12	thin
HD139664	F5IV-V	-0.27	2.20	7.59	0.06	0.04	thin
HD140812	F5V	-0.49	3.68	9.18	0.15	0.22	thin
HD141247	F9V	-0.19	5.59	7.10	0.13	0.23	thin
HD141465	F3V	-0.31		8.34	0.06	0.05	thin
HD142108	F5	-0.31	2.08	8.59	0.07	0.08	thin
HD142217	F5V	-0.53	2.57	7.50	0.07	0.10	thin
HD142254	F0V	-0.30	1.58	7.97	0.04	0.08	thin
HD142542	F3/F5V	-0.19	2.72	8.43	0.11	0.05	thin
HD143463	F6V	-0.38	3.92	7.91	0.06	0.23	thin
HD143790	F5IV/V	-0.20	1.94	7.68	0.11	0.16	thin
HD144492	F4V	-0.42	2.25	8.67	0.08	0.23	thin
HD144579	G8V	-0.59		6.60	0.23	0.14	thin
HD144880	F7V	-0.50	4.59	6.56	0.23	0.58	thin
HD145059	G2/G3V	0.10	3.85	7.52	0.18	0.18	thin
HD145100	F3V	-0.17	2.06	7.58	0.07	0.03	thin
HD145158	F8V	-0.23	3.24	7.69	0.04	0.11	thin
HD145184	F0	-0.63	3.12	8.92	0.12	0.08	thin
HD145809	G3V	-0.37	7.02	7.78	0.06	0.33	thin
HD146775	G5V	-0.02	2.10	7.49	0.08	0.51	thin
HD147644	F9V	-0.35	5.81	6.57	0.25	0.08	thin
HD148433	F0	-0.52	2.07	7.17	0.12	0.13	thin
HD148729	G0	0.10	3.25	7.21	0.14	0.34	thin
HD148967	F5	-0.31	1.72	8.63	0.10	0.19	thin
HD149463	F8	-0.17	2.03	7.53	0.07	0.02	thin
HD149504	F5	-0.27	3.26	7.47	0.12	0.19	thin
HD149612	G3V	-0.47		7.38	0.10	0.06	thin
HD149890	F8V	-0.40	6.91	7.16	0.30	0.13	thin
HD150258	F8	-0.31	2.38	7.22	0.12	0.07	thin
HD150344	F5V	-0.14		7.71	0.04	0.09	thin
HD150466	F5V	-0.33		8.62	0.07	0.03	thin
HD150618	F2	-0.42	1.11	8.16	0.06	0.07	thin
HD150682	F2III	-0.26	2.90	7.85	0.04	0.04	thin
HD150749	F5	-0.32	2.25	7.50	0.08	0.23	thin
HD150937	F3V	-0.17	1.95	7.75	0.09	0.03	thin
HD151258	F8	-0.65	2.56	7.73	0.05	0.27	thin
HD151632	F5	-0.39	1.63	7.60	0.06	0.01	thin
HD151798	G3V	-0.17		7.37	0.09	0.00	thin
HD151900	F1III-IV	-0.55	1.63	8.33	0.13	0.15	thin
HD152377	G0	-0.21	2.21	8.09	0.08	0.14	thin
HD152792	G0V	-0.37	6.61	8.64	0.26	0.18	thin
HD153229	F3IV/V	-0.07		8.03	0.00	0.00	thin
HD153240	F6V	-0.32	2.26	7.59	0.06	0.03	thin
HD153363	F3V	-0.21	2.12	8.20	0.10	0.02	thin
HD153631	G2V	-0.04		8.16	0.31	0.12	thin
HD153897	F5V	-0.25	2.32	7.41	0.08	0.15	thin
HD153950	G2IV-V	-0.17	5.53	7.74	0.12	0.45	thin
HD154578	F7V	-0.43	3.07	8.77	0.26	0.30	thin
HD154931	G0	-0.04	5.21	6.74	0.20	0.15	thin
HD155105	G3V	-0.24	10.04	7.22	0.11	0.14	thin
HD155467	F7V	-0.28	2.35	9.12	0.12	0.14	thin
HD155513	F5	-0.34	1.58	7.95	0.07	0.08	thin
HD155967	F6V	-0.29	2.28	8.05	0.01	0.01	thin
HD157060	F8V	-0.07	4.63	9.19	0.13	0.03	thin
HD157427	F0	-0.13	2.04	7.64	0.09	0.03	thin
HD157950	F3V	-0.25	1.70	7.86	0.04	0.16	thin
HD158630	G2V	-0.28	3.51	7.08	0.21	0.17	thin

**Table 3.** (continued)

Name	Sp. type	[Fe/H]	age (Gyr)	$R$ (kpc)	$e$	$z_{\max}$ (kpc)	population
HD158633	K0V	-0.43		6.76	0.19	0.12	thin
HD159517	F4V	-0.15	1.78	8.07	0.13	0.09	thin
HD159868	G5V	0.04	6.87	6.59	0.23	0.43	thin
HD160043	F5V	-0.44	3.37	7.04	0.14	0.17	thin
HD160346	K3V	-0.23		8.32	0.09	0.20	thin
HD160482	F5V	-0.27	3.92	6.79	0.19	0.01	thin
HD160487	F5	-0.44	2.52	7.39	0.21	0.10	thin
HD161239	G2IIb	0.10	2.93	7.55	0.08	0.20	thin
HD161731	F8	-0.34		7.67	0.27	0.05	thin
HD161767	F8	-0.33	3.00	8.68	0.17	0.31	thin
HD162521	F8V	-0.18	2.20	7.72	0.13	0.21	thin
HD162826	F8V:	-0.06	3.98	8.27	0.04	0.11	thin
HD163840	G2V	0.11	7.42	7.60	0.08	0.01	thin
HD164396	F8	-0.41	3.54	8.20	0.14	0.16	thin
HD165069	F5V	-0.44	3.81	7.11	0.31	0.06	thin
HD165271	G5IV	-0.08	6.58	8.28	0.25	0.27	thin
HD165281	F5V	-0.21	5.23	7.57	0.21	0.03	thin
HD165567	F7V	-0.17	4.21	8.38	0.05	0.02	thin
HD165696	F8V	-0.12	3.19	7.68	0.10	0.10	thin
HD166073	F2	-0.29	1.93	8.27	0.05	0.13	thin
HD166620	K2V	-0.16	4.39	7.32	0.13	0.07	thin
HD167081	F8	0.11	7.48	7.02	0.14	0.22	thin
HD167954	F7V	-0.00	3.13	7.28	0.14	0.03	thin
HD168871	G2V	-0.10	6.43	7.56	0.11	0.16	thin
HD169359	G0	-0.36	7.84	8.69	0.10	0.40	thin
HD170291	F5	-0.35	3.05	7.82	0.13	0.01	thin
HD170579	F5	-0.32	2.19	7.42	0.29	0.18	thin
HD170773	F5V	-0.25	2.34	8.08	0.03	0.10	thin
HD171242	G0	-0.44	9.37	8.03	0.36	0.02	thin
HD171317	F5V	-0.57	3.44	8.42	0.09	0.00	thin
HD171665	G5V	-0.19	7.28	7.34	0.10	0.34	thin
HD171706	F9V	-0.28	5.76	7.39	0.18	0.42	thin
HD171990	G2V	-0.06	4.84	8.76	0.15	0.09	thin
HD172051	G5V	-0.32	1.54	8.32	0.15	0.02	thin
HD172085	F8	0.04		6.71	0.21	0.04	thin
HD172103	F1IV-V	-0.29	1.27	7.63	0.05	0.25	thin
HD172914	F2V	-0.84	5.11	8.40	0.19	0.12	thin
HD173282	F5/F6V	-0.05	1.92	8.14	0.04	0.05	thin
HD173494	F6V	-0.10		7.71	0.06	0.08	thin
HD173883	F9V	-0.75	6.92	7.39	0.23	0.33	thin
HD174153	G0V	-0.28	4.73	7.53	0.23	0.25	thin
HD174160	F8V	-0.23		8.28	0.04	0.03	thin
HD174433	F5	-0.43	8.19	9.06	0.19	0.15	thin
HD174930	F5V	-0.82	4.02	8.51	0.11	0.11	thin
HD175607	G8V	-0.67	14.87	8.55	0.34	0.11	thin
HD176441	F5	-0.39	4.60	8.26	0.15	0.19	thin
HD176464	F8V	-0.44	5.19	8.71	0.12	0.00	thin
HD176796	G0	-0.56	4.21	8.47	0.20	0.00	thin
HD176894	F0	-0.16	2.12	7.99	0.01	0.03	thin
HD176903	F5V	-0.11	1.45	8.52	0.10	0.03	thin
HD177459	F5	-0.26	3.43	7.39	0.19	0.20	thin
HD177552	F1V	-0.30	1.02	7.68	0.07	0.14	thin
HD178619	F5IV-V	-0.45	2.72	7.86	0.14	0.00	thin
HD179422	F5V	-0.16		7.49	0.07	0.07	thin
HD179949	F8V	-0.06	3.54	7.82	0.06	0.05	thin
HD180285	F2	-0.42	4.01	8.08	0.02	0.05	thin
HD180556	F8	0.06	4.68	7.73	0.08	0.05	thin
HD180709	F7V	-0.35	2.15	8.74	0.09	0.13	thin
HD180867	F6V	-0.43	3.64	7.87	0.07	0.14	thin

**Table 3.** (continued)

Name	Sp. type	[Fe/H]	age (Gyr)	$R$ (kpc)	$e$	$z_{\max}$ (kpc)	population
HD181144	F8IV-V	-0.30	4.99	8.05	0.03	0.11	thin
HD181428	G1V	-0.13	5.32	8.84	0.14	0.43	thin
HD181544	G1V	-0.16	5.16	9.11	0.15	0.51	thin
HD182488	G8V	0.03	10.53	7.80	0.04	0.04	thin
HD182901	F5III	-0.13	2.15	7.72	0.11	0.15	thin
HD182926	F5V	-0.33	2.64	7.99	0.04	0.03	thin
HD183028	F5V	-0.24	2.52	8.17	0.05	0.05	thin
HD183127	F6IV	-0.26	2.25	8.33	0.04	0.14	thin
HD183216	G2V	0.06	3.11	6.90	0.19	0.08	thin
HD183255	K3V	-0.45		7.48	0.33	0.30	thin
HD183312	F3V	-0.19	1.53	8.28	0.04	0.26	thin
HD183473	G5	-0.07	2.99	7.87	0.24	0.00	thin
HD184151	F5V	-0.49	2.70	9.15	0.13	0.01	thin
HD184400	F5	-0.09	2.34	9.03	0.51	0.55	thin
HD184592	G5	-0.04	6.25	7.54	0.18	0.46	thin
HD184985	F7V	-0.10	3.63	7.26	0.10	0.19	thin
HD185112	K1V	-0.14		6.73	0.20	0.13	thin
HD185124	F3IV	-0.03	2.11	7.53	0.10	0.03	thin
HD185785	F8	-0.47	5.77	7.33	0.20	0.17	thin
HD186142	G5	-0.22		8.89	0.15	0.07	thin
HD186395	F0	0.07		7.88	0.04	0.07	thin
HD186651	G0V	-0.17	5.05	7.76	0.15	0.04	thin
HD186760	G0V	-0.13	4.49	7.85	0.03	0.33	thin
HD188166	F5	-0.19	4.47	9.22	0.13	0.31	thin
HD188427	K2	-0.30		8.62	0.28	0.20	thin
HD188449	F3V	-0.61	2.11	7.95	0.06	0.08	thin
HD188642	F3V	-0.34	2.23	7.62	0.10	0.01	thin
HD188994	F6Vm	-0.23	1.54	7.22	0.23	0.04	thin
HD189245	F7V	-0.29	3.22	7.40	0.08	0.08	thin
HD189247	F5IV	-0.15	2.19	7.03	0.16	0.03	thin
HD189566	G3IV/V	-0.21	9.64	6.83	0.30	0.55	thin
HD189712	F5	-0.62	3.77	8.93	0.16	0.06	thin
HD189899	F8IV-V	-0.30	4.62	6.99	0.15	0.34	thin
HD189931	G1V	-0.07	3.07	6.82	0.20	0.08	thin
HD190404	K1V	-0.39		7.41	0.33	0.42	thin
HD190422	F8V	-0.22		8.32	0.07	0.03	thin
HD190498	F8	-0.09	2.70	7.17	0.13	0.14	thin
HD190617	G2V	-0.55	4.87	7.52	0.15	0.43	thin
HD190983	F5V	-0.55	4.27	8.76	0.09	0.22	thin
HD191838	F2	-0.18	2.20	8.42	0.05	0.21	thin
HD192021	F6V	-0.51	4.89	9.64	0.18	0.29	thin
HD192145	F8Vws	-0.44	5.73	8.31	0.07	0.16	thin
HD192486	F2V	-0.28	1.12	8.62	0.07	0.15	thin
HD192490	F5	-0.21	2.07	9.16	0.14	0.18	thin
HD192869	F6IV	-0.42	2.76	7.36	0.09	0.05	thin
HD192886	F5V	-0.16	2.23	7.73	0.11	0.00	thin
HD193468	F5	-0.40	4.17	8.48	0.06	0.07	thin
HD193622	F2	-0.19	2.17	7.76	0.09	0.04	thin
HD193664	G3V	-0.25	5.55	8.11	0.09	0.18	thin
HD194012	F8V	-0.33	3.76	8.34	0.04	0.03	thin
HD194640	G6/G8V	0.00	4.53	6.85	0.17	0.02	thin
HD196081	F5V	-0.38	2.41	8.36	0.09	0.01	thin
HD196482	F5	-0.41	4.34	8.68	0.08	0.01	thin
HD196531	G0V	-0.40	5.75	8.21	0.09	0.09	thin
HD196789	F8	-0.30	4.07	8.77	0.16	0.20	thin
HD197037	G0	-0.30	2.13	8.53	0.14	0.09	thin
HD197214	G3/G5V	-0.43	6.86	7.41	0.08	0.19	thin
HD197649	F3/F5V	-0.09	1.72	7.67	0.05	0.03	thin
HD198075	G1V	-0.31		8.17	0.02	0.21	thin

**Table 3.** (continued)

Name	Sp. type	[Fe/H]	age (Gyr)	$R$ (kpc)	$e$	$z_{\max}$ (kpc)	population
HD198585	G0	-0.62	2.93	9.33	0.14	0.30	thin
HD198802	G1V	-0.02	4.25	8.54	0.06	0.04	thin
HD199190	G5IV	0.11	6.32	7.86	0.26	0.23	thin
HD199260	F7V	-0.26	3.46	7.90	0.02	0.08	thin
HD199373	F5V	-0.41	4.67	6.79	0.19	0.08	thin
HD200334	G3IV	0.04	4.28	7.67	0.08	0.07	thin
HD200433	F5	-0.33	2.31	8.63	0.09	0.08	thin
HD200655	G5IV	-0.04	2.27	7.79	0.15	0.05	thin
HD200877	F7IV	-0.42	4.90	7.39	0.08	0.10	thin
HD201154	F5	-0.31	3.13	6.65	0.21	0.02	thin
HD201352	F2IV/V	-0.26	1.99	6.88	0.19	0.03	thin
HD201490	F7V	-0.36	5.68	8.38	0.08	0.27	thin
HD201647	F5IV	-0.10	2.32	7.20	0.12	0.06	thin
HD201772	F5V	-0.28	3.09	7.69	0.14	0.17	thin
HD201835	F5	-0.56	5.36	10.66	0.26	0.10	thin
HD202926	F6V	-0.40	3.30	8.37	0.08	0.02	thin
HD203142	F2/F3V	-0.22	1.65	7.30	0.10	0.02	thin
HD204263	F0	-0.13	2.09	6.96	0.17	0.11	thin
HD204712	G0	-0.57	6.31	7.13	0.20	0.17	thin
HD204889	F5	-0.22	3.04	7.86	0.07	0.18	thin
HD204904	F4IV	-0.27	2.51	8.10	0.04	0.00	thin
HD205027	G2V	-0.51	10.43	7.45	0.41	0.10	thin
HD205067	G2/G3V	0.02	7.45	7.56	0.13	0.08	thin
HD205306	F7V	-0.21	3.95	7.58	0.06	0.13	thin
HD205656	G5	0.05	9.91	7.11	0.32	0.14	thin
HD205855	K0V	0.01	3.87	8.02	0.30	0.45	thin
HD205905	G2V	0.05	1.35	7.72	0.11	0.15	thin
HD206172	G0	-0.24		6.95	0.18	0.08	thin
HD206395	G0IV	0.06	3.71	7.84	0.10	0.00	thin
HD206507	F5V	-0.27	3.28	8.77	0.09	0.23	thin
HD206868	F3V	-0.27	2.32	7.72	0.08	0.02	thin
HD206913	F5	-0.43	5.22	7.71	0.14	0.10	thin
HD206963	F5	-0.32	2.21	8.63	0.08	0.13	thin
HD207061	F6V	-0.19	3.69	7.22	0.12	0.17	thin
HD207190	F6V	-0.60	6.61	8.08	0.05	0.30	thin
HD207692	F6V	-0.40	3.70	7.31	0.23	0.00	thin
HD207795	K2	-0.06	4.86	7.25	0.17	0.18	thin
HD207958	F3IV	-0.24	2.04	7.86	0.11	0.04	thin
HD208215	F5V	-0.26	3.55	7.98	0.16	0.11	thin
HD208323	F5IV-Vn	-0.20	1.60	7.69	0.07	0.13	thin
HD208362	F0	-0.52	1.40	9.16	0.13	0.12	thin
HD208502	F5	-0.09	2.43	7.97	0.09	0.01	thin
HD208703	F5IV	-0.27	2.01	7.51	0.08	0.14	thin
HD208808	F5V	-0.30	3.18	8.26	0.06	0.01	thin
HD208812	F8IV-V	-0.46	3.85	7.51	0.07	0.01	thin
HD208880	G0	0.02		8.03	0.09	0.01	thin
HD209320	F8	-0.29	6.95	7.09	0.13	0.28	thin
HD209837	F6V	-0.70	7.47	9.12	0.16	0.15	thin
HD209858	F8V	-0.42	6.46	7.72	0.11	0.44	thin
HD209875	F8	-0.33	6.15	8.54	0.28	0.11	thin
HD210457	F8	-0.42	5.25	7.50	0.07	0.01	thin
HD210460	G0V	-0.45	2.38	8.44	0.06	0.44	thin
HD210737	F5/F6V	-0.68	4.97	7.65	0.10	0.03	thin
HD210763	F7V	-0.19	1.39	8.05	0.10	0.10	thin
HD210923	G0	-0.34	5.54	8.25	0.03	0.26	thin
HD210942	G0	0.06	4.95	7.80	0.08	0.15	thin
HD210985	F8	-0.67	8.01	9.30	0.19	0.48	thin
HD211094	F5	0.02	2.54	6.94	0.16	0.07	thin
HD211476	G2V	-0.21	6.18	7.80	0.34	0.50	thin

**Table 3.** (continued)

Name	Sp. type	[Fe/H]	age (Gyr)	$R$ (kpc)	$e$	$z_{\max}$ (kpc)	population
HD212858	F8	-0.51	9.42	9.73	0.24	0.18	thin
HD213429	F7V	-0.16	5.40	7.57	0.06	0.01	thin
HD213646	K2	-0.19	19.89	8.90	0.32	0.12	thin
HD213845	F7V	-0.13	2.33	7.56	0.06	0.07	thin
HD213928	F7/F8V	-0.56	5.98	7.87	0.11	0.15	thin
HD213996	K0	-0.03		7.69	0.32	0.14	thin
HD214094	F6V	-0.26	4.45	8.08	0.22	0.18	thin
HD214308	F5IV	-0.24	2.67	6.95	0.17	0.05	thin
HD214557	F8	-0.17	5.89	7.45	0.20	0.13	thin
HD214686	G0	-0.11	4.32	7.74	0.13	0.23	thin
HD215152	K0	-0.18		7.45	0.13	0.15	thin
HD215243	G8IV	-0.24	4.83	7.57	0.10	0.15	thin
HD215456	F9V	-0.03	7.03	7.78	0.10	0.08	thin
HD215588	F5	-0.31	1.67	8.17	0.10	0.11	thin
HD215657	G3IV-V	-0.12	2.19	8.35	0.07	0.01	thin
HD215724	F6V	-0.06	2.78	7.78	0.15	0.07	thin
HD215775	K0	-0.10	6.32	8.55	0.19	0.08	thin
HD216106	G0	-0.42	3.04	7.17	0.20	0.32	thin
HD216384	F5	-0.23	2.18	8.10	0.01	0.11	thin
HD216625	F8	-0.14	4.27	8.15	0.11	0.14	thin
HD216631	F8	-0.59	1.65	7.24	0.20	0.17	thin
HD216854	F5	-0.20	2.00	7.14	0.12	0.21	thin
HD217577	G2V	-0.26	10.14	7.37	0.13	0.35	thin
HD218079	F0	-0.18	1.63	8.05	0.09	0.16	thin
HD218099	F5IV	-0.18	2.68	9.39	0.16	0.04	thin
HD218201	G5	-0.31		7.93	0.16	0.30	thin
HD218483	K1V	-0.09	5.13	6.94	0.15	0.02	thin
HD218693	K3V	-0.17	15.82	6.93	0.19	0.05	thin
HD218805	F5	-0.36	4.54	8.73	0.17	0.08	thin
HD219077	G5IV	0.11	7.66	6.67	0.28	0.42	thin
HD219396	G0	-0.13	9.98	6.70	0.20	0.02	thin
HD219487	F5V	-0.30	2.21	8.17	0.03	0.04	thin
HD219497	F6IV	-0.58	5.93	10.69	0.25	0.25	thin
HD219538	K2V	-0.21	5.07	8.21	0.10	0.05	thin
HD219612	F0	-0.44	2.05	8.55	0.15	0.11	thin
HD219983	F2	-0.35	5.15	6.85	0.21	0.16	thin
HD220121	F0	-0.51	2.16	8.16	0.05	0.17	thin
HD220460	FVw	-0.57	2.82	7.99	0.21	0.17	thin
HD221239	K0	-0.25	4.07	7.15	0.12	0.03	thin
HD221354	K2V	0.01	10.46	6.73	0.28	0.12	thin
HD221356	F8V	-0.42	3.52	7.22	0.11	0.01	thin
HD221477	F8V	-0.64	10.30	8.12	0.02	0.28	thin
HD221584	F7V	-0.60	6.17	7.68	0.10	0.44	thin
HD221638	F6V	-0.43	4.82	8.59	0.07	0.12	thin
HD221757	F8	-0.36	6.99	8.99	0.14	0.11	thin
HD221950	F6V	-0.62	4.86	9.80	0.19	0.24	thin
HD221974	K1III	-0.11		7.25	0.30	0.00	thin
HD222249	F5IV	-0.17	2.04	7.16	0.12	0.01	thin
HD223171	G2V	0.04	7.44	8.54	0.31	0.05	thin
HD223238	G2V	-0.06	7.12	7.00	0.23	0.03	thin
HD223241	G0	-0.15	6.09	7.61	0.24	0.40	thin
HD223323	F2IV-V	-0.62	4.01	8.41	0.16	0.22	thin
HD223346	F5III-IV	-0.42	3.53	7.57	0.07	0.25	thin
HD223633	F5IV-V	-0.35	3.09	7.20	0.14	0.09	thin
HD223848	G0	-0.37	4.55	8.63	0.15	0.08	thin
HD224393	G3V	-0.45		7.51	0.12	0.00	thin
HD224529	F5V	-0.26	3.51	7.88	0.01	0.11	thin
HD224619	G8V	-0.14	3.92	6.74	0.21	0.38	thin
HD224808	K0	-0.26		7.29	0.19	0.10	thin



**Table 3.** (continued)

Name	Sp. type	[Fe/H]	age (Gyr)	$R$ (kpc)	$\epsilon$	$z_{\max}$ (kpc)	population
HD224839	F8V	-0.33	9.27	7.51	0.07	0.07	thin
HD225045	F6/F7V	-0.05	2.46	8.52	0.10	0.09	thin
HD225233	F2V	-0.20	2.65	7.63	0.06	0.13	thin
HD231825	G5	-0.00		7.26	0.19	0.08	thin
HD275458	K0	-0.19	10.13	7.13	0.16	0.34	thin
HD284414	K2V	-0.20		7.51	0.12	0.10	thin
HD285690	K3V	-0.18		7.63	0.12	0.08	thin
CD -80 328	G0	-1.67		21.68	0.85	25.81	thick
CD -32 3010	G2	-1.04	12.26	9.15	0.54	1.92	thick
BD -14 363	G5V	-0.95	10.18	9.40	0.29	0.84	thick
BD -14 4454		-0.50		6.46	0.50	0.32	thick
BD -5 3063	K0V	-0.59		6.20	0.35	0.27	thick
BD 6 4665	K3	-0.19		5.81	0.38	0.71	thick
BD 7 2634	G0	-0.70		6.20	0.30	1.21	thick
BD 8 2658	K0V	-0.30		7.72	0.25	1.88	thick
BD 10 2122	K5	-0.36		6.03	0.39	0.74	thick
BD 12 1631		-0.09	16.33	9.39	0.19	0.66	thick
BD 14 1947		-0.37		7.97	0.13	1.57	thick
BD 17 44	K1	-0.35		7.43	0.42	0.61	thick
BD 18 92	K3	-0.12	2.17	6.22	0.33	0.17	thick
BD 19 48	K3	-0.18		6.70	0.23	0.75	thick
BD 19 1739	K0	-0.14		6.39	0.26	0.25	thick
BD 22 301	K1	-0.14		5.57	0.45	0.32	thick
BD 22 4454	G5	-0.20		6.55	0.30	1.13	thick
BD 22 4567	K3V	-0.24	18.79	8.81	0.30	1.14	thick
BD 24 4460	K0V	-0.51		6.89	0.47	0.00	thick
BD 30 1801		-0.50		6.50	0.35	0.24	thick
BD 34 5002	G5	-0.06	5.75	5.98	0.34	0.39	thick
BD 41 379	G0	0.13	9.92	6.36	0.36	0.01	thick
BD 41 727	K2	-0.05	10.52	6.26	0.28	0.24	thick
BD 42 2163	K1V	-0.28		6.07	0.50	1.07	thick
BD 44 619	G8	-0.26	14.05	6.09	0.31	0.10	thick
BD 47 1276	K0	-0.36	3.84	5.85	0.42	0.27	thick
HD1832	F8	-0.05	6.63	6.48	0.24	0.12	thick
HD2070	G3IV	-0.11	6.60	6.19	0.34	0.08	thick
HD3403	G8/K0V	-0.14	8.38	6.52	0.27	0.32	thick
HD3765	K2V	-0.16		6.11	0.33	0.24	thick
HD7817	F8V	-0.35	5.05	8.90	0.13	0.97	thick
HD8638	G6Vw...	-0.32	3.62	6.08	0.32	1.03	thick
HD9670	F8V	-0.40	5.86	6.50	0.24	0.06	thick
HD10015	K0IV-V	-0.02	10.36	6.40	0.28	0.19	thick
HD10145	G5V	0.03	5.46	6.94	0.38	0.16	thick
HD10785	G1/G2V	-0.16	6.92	5.70	0.42	0.22	thick
HD11397	G6IV/V	-0.79	17.37	5.91	0.37	0.51	thick
HD12387	G3V	-0.22	9.84	6.04	0.33	0.92	thick
HD15029	F5	-0.47	5.33	7.45	0.25	0.81	thick
HD16623	F7Vw...	-0.51	7.75	5.92	0.36	0.10	thick
HD16714	G5V	-0.22	3.94	6.32	0.32	0.28	thick
HD18702	K0V	0.05	13.34	6.44	0.41	0.01	thick
HD19034	G5	-0.38	1.34	6.37	0.26	0.37	thick
HD21727	G5	0.07	5.84	6.55	0.26	0.28	thick
HD22380	G5	-0.05	8.87	7.26	0.15	1.04	thick
HD23314	G5	-0.37	5.58	6.40	0.25	0.02	thick
HD24156	G0	-0.42	10.68	6.39	0.29	0.39	thick
HD24202	G2V...	-1.07	9.63	6.29	0.39	0.16	thick
HD25314	F5V	-0.61	5.31	7.61	0.05	0.69	thick
HD26421	G0	-0.44	4.90	7.94	0.15	1.04	thick
HD27485	G0	-0.20	8.88	6.93	0.36	0.24	thick
HD29029	F7V	-0.85	9.08	9.17	0.48	1.04	thick

**Table 3.** (continued)

Name	Sp. type	[Fe/H]	age (Gyr)	$R$ (kpc)	$e$	$z_{\max}$ (kpc)	population
HD31501	G8V	-0.19	1.78	6.44	0.30	0.73	thick
HD36283	G5V	-0.25	4.89	6.18	0.30	0.82	thick
HD37739	F5	-0.49	4.78	6.21	0.39	0.50	thick
HD38014	K1V	-0.14	12.43	5.72	0.40	0.13	thick
HD38510	F5/F6V	-0.78	9.15	7.90	0.53	1.16	thick
HD40040	G0	-0.30	10.29	6.35	0.33	0.07	thick
HD42160	G2V	-0.15		6.42	0.25	0.25	thick
HD42988	F5V	-0.46	3.02	8.03	0.06	0.61	thick
HD43062	K0	-0.06	4.84	6.49	0.28	0.14	thick
HD43147	G9V	-0.22		7.21	0.13	1.01	thick
HD53505	G0	-0.57	13.57	7.08	0.15	0.89	thick
HD54690	G5	-0.07	9.44	5.95	0.44	0.07	thick
HD57901	G5	-0.11		6.48	0.23	0.03	thick
HD60298	G2V	-0.14	10.23	8.77	0.46	0.67	thick
HD64207	F9V	-0.64	8.34	6.42	0.25	0.26	thick
HD65371	K0	-0.02		7.46	0.08	1.07	thick
HD72614	K2V	-0.13		6.31	0.36	0.08	thick
HD72680	K0	0.14	9.53	7.33	0.32	0.63	thick
HD73569	F0V	-0.29	2.09	5.73	0.40	0.14	thick
HD75530	G8V	-0.48	7.23	5.68	0.44	1.17	thick
HD75880	G0	0.14	7.95	6.55	0.32	0.03	thick
HD78670	G0/G1V	-0.37	3.85	6.59	0.28	0.13	thick
HD80509	F5	-0.61	3.50	8.56	0.07	0.83	thick
HD83789	G0	0.11	6.92	6.66	0.30	0.16	thick
HD97507	G3V	-0.54	10.72	8.55	0.31	0.68	thick
HD97783	G1/G2V	-0.70	9.40	8.36	0.34	1.97	thick
HD102800	K0	-0.12		6.12	0.31	0.22	thick
HD105304	K0	-0.21	16.90	6.48	0.28	0.18	thick
HD106510	F8V	-0.53	5.99	8.42	0.05	0.61	thick
HD106869	G1V	0.02	5.45	6.50	0.24	0.02	thick
HD107582	G2V	-0.65	6.60	5.68	0.41	0.48	thick
HD108024	F8	-0.41	7.18	6.39	0.29	0.38	thick
HD109839	F5	-0.25	3.90	8.35	0.06	1.18	thick
HD110537	G0	0.01	7.63	6.29	0.27	0.19	thick
HD111777	G3V	-0.89	8.87	6.57	0.46	0.52	thick
HD113101	G8V	0.03		6.63	0.38	0.37	thick
HD114174	G5IV	0.05	6.84	6.65	0.32	0.00	thick
HD115031	G2/G3V	-0.09	7.24	6.10	0.32	0.23	thick
HD115231	G5	-0.11	7.88	6.30	0.33	0.01	thick
HD117987	K2V	-0.21		8.57	0.36	0.75	thick
HD124605	G0	-0.75	6.30	6.39	0.26	0.03	thick
HD125291	F8V	-0.48	7.66	5.70	0.40	0.06	thick
HD129642	K3V	-0.12		6.29	0.35	0.04	thick
HD131250	G5V	-0.12	5.82	6.32	0.31	0.43	thick
HD132996	G3V	-0.17	6.51	7.06	0.14	0.98	thick
HD133621	G0	-0.47	10.89	6.32	0.28	0.00	thick
HD143291	K0V	-0.34		6.65	0.38	0.26	thick
HD145598	G5V+...	-0.97		6.77	0.18	0.70	thick
HD146800	K3V	-0.39		5.90	0.38	0.32	thick
HD148587	G0V	-0.45	8.12	5.64	0.42	0.55	thick
HD149105	G0V	-0.29	6.26	6.51	0.31	0.05	thick
HD149606	K2V	-0.18		6.17	0.30	0.11	thick
HD151504	G8V	0.09	7.79	6.76	0.32	0.56	thick
HD153075	G0V	-0.51	7.98	6.17	0.41	0.21	thick
HD154160	G5IV:	0.10	6.67	6.46	0.24	0.11	thick
HD159656	G4IV-V	0.03	5.98	7.30	0.10	0.61	thick
HD161612	G6/G8V	0.17	7.32	6.21	0.29	0.10	thick
HD180841	F8	-0.56	9.18	7.43	0.08	0.63	thick
HD183877	K0+...	-0.14	3.86	5.90	0.37	0.19	thick

**Table 3.** (continued)

Name	Sp. type	[Fe/H]	age (Gyr)	$R$ (kpc)	$e$	$z_{\max}$ (kpc)	population
HD184855	G0	-0.32	8.93	8.69	0.29	0.61	thick
HD187645	G5	-0.26	6.57	6.48	0.36	0.21	thick
HD190649	G5V	-0.49	10.83	5.93	0.38	0.35	thick
HD191069	G5V	-0.07	8.11	5.93	0.36	0.98	thick
HD196800	G1/G2V	0.07	4.94	6.40	0.31	0.04	thick
HD197484	G2V	-0.52	9.75	6.50	0.26	0.05	thick
HD197666	G0	-0.73	4.91	7.39	0.13	0.61	thick
HD198188	G3V	-0.17	6.28	6.45	0.38	0.08	thick
HD198273	G2V	-0.70	12.90	8.06	0.34	0.87	thick
HD203448	G1/G2V	-0.21	5.92	10.00	0.33	0.64	thick
HD204670	G3/G5V	-0.30	5.33	8.70	0.19	1.18	thick
HD204814	G8V	-0.12		6.23	0.38	0.08	thick
HD212231	G2V	-0.34	8.49	7.26	0.22	0.68	thick
HD212708	G5V	0.17	9.69	6.48	0.27	0.04	thick
HD214385	G3V	-0.45	8.71	8.29	0.13	1.15	thick
HD216436	G3/G5V	-0.20	10.70	6.30	0.37	0.07	thick
HD217276	G2V	-0.26	6.70	7.76	0.13	0.68	thick
HD219953	K1V	-0.43		6.21	0.40	0.19	thick
HD220197	F8V	-0.60	8.79	6.44	0.42	0.26	thick
HD222935	K2V	-0.16		8.92	0.35	0.85	thick
HD224233	G0	-0.18	8.47	7.80	0.15	0.87	thick
HD224383	G2V	-0.07	6.94	6.22	0.38	0.06	thick
HD224543	G0	0.06	7.36	6.21	0.31	0.26	thick
HD224817	G2V	-0.69	9.12	6.49	0.40	0.21	thick
HD243814		-0.19	12.69	6.56	0.30	0.23	thick
HD250047	K2	-0.13		6.42	0.31	0.06	thick
HD251383	K2V	-0.33	6.02	7.77	0.33	1.06	thick
HD257886	K2V	-0.23	15.11	7.50	0.19	0.79	thick
HD263175	K3V	-0.27		9.91	0.21	0.70	thick
HD275241	K0	0.10	10.82	6.28	0.29	0.02	thick
HD283668	K3V	-0.47		7.96	0.23	0.82	thick
HD316899	K0V	-0.20		6.50	0.46	1.26	thick
BD -1 306	G1V	-0.95	6.23	6.02	0.92	6.98	halo
BD -1 2457	K8	0.05		5.26	0.53	1.68	halo
BD 9 5076	K2	-0.12	2.58	6.30	0.65	0.03	halo
BD 11 4725	G3	-0.82		86.51	1.00	2.98	halo
BD 33 1694	K5	-0.16	1.71	5.76	0.52	0.85	halo
BD 41 3306	K0V	-0.29		5.54	0.55	1.26	halo
BD 66 268	G0	-1.94		8.89	0.50	1.21	halo
HD104006	K1V	-0.48		4.38	0.88	0.35	halo
HD155185	K0V	-0.30		5.90	0.60	1.32	halo
HD161848	K1V	-0.16		5.42	0.51	0.63	halo
HD170357	G1V	-0.51	10.87	5.67	0.47	1.48	halo
HD177095	G6V	-0.60		5.64	0.72	0.28	halo
HD212038	K0V	-0.51		5.04	0.59	0.40	halo
HD217231	G0	-0.73	6.79	5.23	0.57	0.44	halo
HD278543	K2	-0.36		4.65	0.78	0.23	halo
HD281540	K5	-0.49		5.88	0.70	0.58	halo

## References

- Abia, C., Rebolo, R., Beckman, J. E., & Crivellari, L. 1988, *A&A*, 206, 100
- Arenou, F., Grenon, M., & Gómez, A. 1992, *A&A*, 258, 104
- Barbier-Brossat, M., Petit, M., & Figon, P. 1994, *A&AS*, 108, 603
- Berthet, S. 1991, *A&A*, 251, 171
- Beveridge, C. E. & Sneden, C. 1994, *AJ*, 108, 285
- Boesgaard, A. M. & Tripicco, M. J. 1986, *ApJ*, 303, 724
- Butler, R. P., Tinney, C. G., Marcy, G. W., et al. 2001, *ApJ*, 555, 410
- Butler, R. P., Vogt, S. S., Marcy, G. W., et al. 2000, *ApJ*, 545, 504
- Carlberg, R. G., Dawson, P. C., Hsu, T., & Vandenberg, D. A. 1985, *ApJ*, 294, 674
- Carney, B. W., Latham, D. W., & Laird, J. B. 1989, *AJ*, 97, 423
- Carney, B. W., Wright, J. S., Sneden, C., et al. 1997, *AJ*, 114, 363
- Carretta, E., Gratton, R., Clementini, G., & Pecci, F. F. 1999, in *Harmonizing Cosmic Distance Scales in a Post-HIPPARCOS era*, ed. D. Egret & A. Heck, *ASP Conf. Ser.* 167, 255
- Castro, S., Rich, R. M., Grenon, M., Barbuy, B., & McCarthy, J. K. 1997, *AJ*, 114, 376
- Cayrel de Strobel, G. & Bentolila, C. 1989, *A&A*, 211, 324
- Cayrel de Strobel, G., Crifo, F., Lebgreton, Y., & Soubiran, C. 1997, *A&AS*, 124, 299
- Cayrel de Strobel, G., Soubiran, C., & Ralite, N. 2001, *A&A*, 373, 159
- Chen, Y. Q., Nissen, P. E., Zhao, G., Zhang, H. W., & Benoni, T. 2000, *A&AS*, 141, 491
- Ciardullo, R. & Demarque, P. 1977, *Yale Trans.*, 33
- Clementini, G., Gratton, R. G., Carretta, E., & Sneden, C. 1999, *MNRAS*, 302, 22
- Díaz, A. I. 1989, in *Evolutionary phenomena in the galaxies* (Cambridge Univ. Press), 377
- Duflot, M., Figon, P., & Meyssonier, N. 1995, *A&AS*, 114, 269
- Edvardsson, B., Andersen, J., Gustafsson, B., et al. 1993, *A&A*, 275, 101
- ESA. 1997, *The Hipparcos and Tycho Catalogues* (SP-1200)
- Feltzing, S. & Gustafsson, B. 1998, *A&AS*, 129, 237
- Fischer, D. A., Marcy, G. W., Butler, R. P., Vogt, S. S., & Apps, K. 1999, *PASP*, 111, 50
- Fischer, D. A., Marcy, G. W., Butler, R. P., et al. 2001, *ApJ*, 551, 1107
- Fulbright, J. P. 2000, *AJ*, 120, 1841
- Gilmore, G. & Wyse, R. F. G. 1985, *AJ*, 90, 2015
- Giridhar, S., Ferro, A. A., & Parrao, L. 1997, *PASP*, 109, 1077
- Gonzalez, G. 1997, *MNRAS*, 285, 403
- . 1998, *A&A*, 334, 221
- Gonzalez, G. & Laws, C. 2000, *AJ*, 119, 390
- Gonzalez, G., Laws, C., Tyagi, S., & Reddy, B. E. 2001, *AJ*, 121, 432
- Gratton, R. G., Carretta, E., Matteucci, F., & Sneden, C. 2000, *A&A*, 358, 671
- Gratton, R. G. & Sneden, C. 1991, *A&A*, 241, 501
- Hartmann, K. & Gehren, T. 1988, *A&A*, 199, 269
- Hauck, B. & Mermilliod, M. 1998, *A&AS*, 129, 431
- Henry, G. W., Marcy, G. W., Butler, R. P., & Vogt, S. S. 2000, *ApJ Letters*, 529, 41
- Jehin, E., Magain, P., Neuforge, C., et al. 1999, *A&A*, 341, 241
- Johnson, D. R. H. & Soderblom, D. R. 1987, *AJ*, 93, 864
- Jones, B. J. T. & Wyse, R. F. G. 1983, *A&A*, 120, 165
- King, J. R., Stephens, A., Goesgaard, A. M., & Deliyannis, C. P. 1998, *AJ*, 115, 666
- Korzennik, S. G., Brown, T. M., Fischer, D. A., Nisenson, P., & Noyes, R. W. 2000, *ApJ Letters*, 533, 147
- Laird, J. B., Carney, B. W., Rupen, M. P., & Latham, D. W. 1988, *AJ*, 96, 1908
- Larson, R. 1976, *MNRAS*, 176, 31
- Layden, A. C. 1995a, *AJ*, 110, 2288
- . 1995b, *AJ*, 110, 2312
- Lutz, T. E. & Kelker, D. H. 1973, *PASP*, 85, 573
- Maeda, K., Nakamura, T., Nomoto, K., et al. 2001, *ApJ*, 565, 405
- Magain, P. 1989, *A&A*, 209, 211
- Malaroda, S., Levato, H., & Galliani, S. 2001, *Complejo Astronomico El Leoncito*
- Marcy, G. W., Butler, R. P., & Vogt, S. S. 2000, *ApJ Letters*, 536, 43
- Mayor, M. & Queloz, D. 1995, *Nat*, 378, 355
- Mazeh, T., Naef, D., Torres, G., et al. 2000, *ApJ Letters*, 532, 55
- McWilliam, A. & Rich, R. M. 1994, *ApJS*, 91, 749
- Ng, Y. K. & Bertelli, G. 1998, *A&A*, 329, 943
- Nissen, P. E., Gustafsson, B., Edvardsson, B., & Gilmore, G. 1994, *A&A*, 285, 440
- Nissen, P. E. & Schuster, W. J. 1991, *A&A*, 251, 457
- . 1997, *A&A*, 326, 751
- Noguchi, M. 1998, *Nature*, 392, 253
- Pagel, B. E. J. & Tautvaisienė, G. 1995, *MNRAS*, 276, 505
- Pilachowski, C. A., Sneden, C., & Booth, J. 1993, *ApJ*, 407, 699
- Prantzos, N. & Boissier, S. 2000, *MNRAS*, 313, 338
- Prochaska, J. X., Naumov, S. O., Carney, B. W., McWilliam, A., & Wolfe, A. M. 2000, *AJ*, 120, 2513
- Quinn, P. & Goodman, J. 1986, *ApJ*, 309, 472
- Rich, R. M. & McWilliam, A. 2000, in *Proceedings of the SPIE, Vol. 4005, Discoveries and Research Prospects form 8- to 10-Meter-Class Telescopes*, ed. J. Bergeron, 150
- Sadakane, K., Honda, S., Kawanomoto, S., Takeda, Y., & Takada-Hidai, M. 1999, *PASJ*, 51, 505
- Santos, N. C., Israelian, G., & Mayor, M. 2000, *A&A*, 363, 228
- Schuster, W. J. & Nissen, P. E. 1989, *A&A*, 221, 65

- Smith, V. V., Coleman, H., & Lambert, D. L. 1993, *ApJ*, 417, 287
- Smith, W. W. & Lambert, D. L. 1986, *ApJ*, 303, 226
- . 1987, *MNRAS*, 226, 563
- Sofue, Y. 1996, *ApJ*, 458, 120
- Thorén, P. & Feltzing, S. 2000, *A&A*, 363, 692
- Tinney, C. G., Butler, R. P., Marcy, G. W., et al. 2001, *ApJ*, 551, 507
- Tomkin, J., Edvardsson, B., Lambert, D. L., & Gustafsson, B. 1997, *A&A*, 327, 587
- Turon, C., Egret, D., Gomez, A., et al. 1993, *Bull. Inf. CDS*, 43, 5
- Twarog, B. A. 1980, *ApJ*, 242, 242
- Udry, S., Mayor, M., Naef, D., et al. 2000, *A&A*, 356, 590
- VandenBerg, D. A. 1983, *ApJS*, 51, 29
- . 1985, *ApJS*, 58, 711
- Vogt, S. S., Marcy, G. W., Butler, R. P., & Apps, K. 2000, *ApJ*, 536, 902
- Yi, S., Demarque, P., Kim, Y.-C., et al. 2001, *ApJS*, 136, 417